isvr Institute of Sound and Vibration Research

Comparison of Two Locally Active Models of the Cochlea

R.H. Pierzycki and S.J. Elliott

ISVR Technical Memorandum No 938

July 2004

University of Southampton

SCIENTIFIC PUBLICATIONS BY THE ISVR

Technical Reports are published to promote timely dissemination of research results by ISVR personnel. This medium permits more detailed presentation than is usually acceptable for scientific journals. Responsibility for both the content and any opinions expressed rests entirely with the author(s).

Technical Memoranda are produced to enable the early or preliminary release of information by ISVR personnel where such release is deemed to the appropriate. Information contained in these memoranda may be incomplete, or form part of a continuing programme; this should be borne in mind when using or quoting from these documents.

Contract Reports are produced to record the results of scientific work carried out for sponsors, under contract. The ISVR treats these reports as confidential to sponsors and does not make them available for general circulation. Individual sponsors may, however, authorize subsequent release of the material.

UNIVERSITY OF SOUTHAMPTON

INSTITUTE OF SOUND AND VIBRATION RESEARCH

SIGNAL PROCESSING & CONTROL GROUP

Comparison of Two Locally Active Models of the Cochlea

by

R H Pierzycki and S J Elliott

ISVR Technical Memorandum N° 938

July 2004

Authorised for issue by
Prof S J Elliott
Group Chairman

Acknowledgements

This project was conducted under the European Doctorate in Sound and Vibration Studies programme, which is financed by the European Commission under the Marie Curie Training Site scheme.

I wish to signify my indebtedness to Professor Stephen Elliott for his priceless suggestions and support throughout. I would like to thank to all the staff of the ISVR, particularly to Oliver Baumann for inexhaustible willingness to serve with his experience. I am also very grateful to Mrs. Joyce Shotter for her kind support.

This work would not have been possible without the succour of Mary and Laura and all my friends from Cathsoc.

Contents

List of Figures

Following figures were adapted from

Fig.1.	*www.zdrowie.med.pl/bad_w_chor/pojecia.html*
Fig.2.	*http://flash.lakeheadu.ca/~mwesner/Sensory%20Systems/Audition/11_008.jpg*
Fig.3.	*http://earlab.bu.edu/physiology/Mechanics.aspx*
Fig.4.	*www.boystownhospital.org/BasicClinic/neuro/cel/Inside_Cochlea.asp*
Fig.5.	*www.vimm.it/cochlea/cochleapages/anatomy/index.htm*
Fig.6.	*www.vimm.it/cochlea/cochleapages/theory/hydro/hydro.htm*
Fig.7.	Gelfand, *Hearing. An Introduction to Psychological and Physiological Acoustics*, Third Edition, Marcel Dekker Inc., (1998), Fig.4.12, p.133.
Fig.9	*www.vimm.it/cochlea/cochleapages/theory/index.htm*, section Nonlinear Undamping
Fig.10	Dallos, [3] Fig.1.7, p.16.
Fig.34	Lineton, [18]., Fig.4.2, p.54.
Fig.85	Elliott and Harte [8]), Fig.E.1, p.54.

Abstract

Cochlear models, which refer primarily to the study of mechanics within the cochlear partition (micromechanics) and interactions between the cochlear fluids and cochlear partition (macromechanics), though incorporating widely accepted techniques, show a large diversity in modelling approaches. Furthermore, there is a tendency for expanding the number of parameters to which the model may occur sensitive. The lack of uniform mechanical parameters effects greatly the model's response. Finally, in the absence of stability examinations, the cochlear models solved in the frequency domain may provide false conjectures and/or conclusions.

An attempt to generalise two locally active models of the cochlea is presented along with stability considerations. Each of the models was considered independently to examine its inherent assumptions and a generalised model was then presented, used to represent either of the individual models. Furthermore, the equations of motion of the generalised models were used to define a negative feedback system, so that the stability could be examined. Additionally, the stability and phase behaviour of two other models was investigated on the basis of one of the generalised models. Finally, the positive feedback system with a nonlinear network component was derived to define a quasi-linear model of the basilar membrane input-output function.

LIST OF ABBREVIATIONS

CF	characteristic frequency
CP	cochlear partition
DC	Deiters' cells
DOF	degree of freedom
G	Geisler
IHC	inner hair cell
NK	Neely&Kim
OC	organ of Corti
OHC	outer hair cell
RL	reticular lamina
SC	stereocilia
SV	scala vestibuli
TM	tectorial membrane

LIST OF SYMBOLS (SI)

S. Neely & T. Kim (1986) (NK)

P_d	pressure difference across BM $[N \cdot m^{-2}]$
P_a	pressure source in OHC $[N \cdot m^{-2}]$
ξ_p	average z displacement of CP over width of CP $[m]$
ξ_b	maximum z displacement of BM over width of BM $[m]$
ξ_c	shear displacement between TM and RL $[m]$
ξ_t	component of ξ_c due to TM displacement $[m]$
Z_p	impedance of the CP $[N \cdot s \cdot m^{-3}]$
Z_1	impedance associated with ξ_b $[N \cdot s \cdot m^{-3}]$
Z_2	impedance associated with ξ_t $[N \cdot s \cdot m^{-3}]$
Z_3	impedance associated with ξ_c $[N \cdot s \cdot m^{-3}]$
Z_4	impedance associated with P_a $[N \cdot s \cdot m^{-3}]$
k_1	stiffness component of Z_1 $[kg \cdot m^{-2} \cdot s^{-2}]$
c_1	damping component of Z_1 $[kg \cdot m^{-2} \cdot s^{-1}]$
m_1	mass component of Z_1 $[kg \cdot m^{-2}]$
k_2	stiffness component of Z_2 $[kg \cdot m^{-2} \cdot s^{-2}]$
c_2	damping component of Z_2 $[kg \cdot m^{-2} \cdot s^{-1}]$
m_2	mass component of Z_2 $[kg \cdot m^{-2}]$
k_3	stiffness component of Z_3 $[kg \cdot m^{-2} \cdot s^{-2}]$
c_3	damping component of Z_3 $[kg \cdot m^{-2} \cdot s^{-1}]$
k_4	stiffness component of Z_4 $[kg \cdot m^{-2} \cdot s^{-2}]$
c_4	damping component of Z_4 $[kg \cdot m^{-2} \cdot s^{-1}]$
γ	OHC force-generation gain
ω	frequency $[rad \cdot s^{-1}]$
b	ratio of ξ_b to ξ_p
g	BM to IHC lever gain

C. Geisler (1993) (G)

F_a	force applied to BM $[N]$
F_m	active axial contractile force exerted by OHC $[N]$
$F(\omega)$	frequency domain representation of F_m $[N]$
F_{fb}	feedback force $[N]$
F_0	force constant $[N]$
x	displacement of BM $[m]$
z	rotational displacement of RL $[m]$
k_b	stiffness component of a segment of BM $[kg \cdot m^{-2} \cdot s^{-2}]$
r	damping component of a segment of BM $[kg \cdot m^{-2} \cdot s^{-1}]$

m	mass component of a segment of BM $[kg \cdot m^{-2}]$
k_r	passive axial stiffness of OHC and the supporting cells $[kg \cdot m^{-2} \cdot s^{-2}]$
k_c	stiffness of the ciliary/TM complex $[kg \cdot m^{-2} \cdot s^{-2}]$
γ	angular deflection of the cilia of OHC
ω	frequency $[rad \cdot s^{-1}]$
ω_0	characteristic frequency $[rad \cdot s^{-1}]$
ω_r	cut-off frequency of the all-pass circuit $[rad \cdot s^{-1}]$
ψ	angle between $\vec{F}_a$ and $\vec{F}_m$ $[degrees]$
A	measure of the BM deflection x
B	measure of the RL deflection z
C	measure of the torque of the RL and BM
D	constant (i.e. $C + cos\psi$)
T	time delay $[s]$
n	delay factor
q	force factor

Generalised variables

p_d	pressure difference across BM $[N \cdot m^{-2}]$
p_a	pressure source in OHC $[N \cdot m^{-2}]$
v_1	displacement of the first DOF $[m]$
v_2	displacement of the second DOF $[m]$
v_3	relative displacement between the first and second DOF $[m]$
Y_p	mobility of the CP $[m^3 \cdot N^{-1} \cdot s^{-1}]$
Z_p	impedance of the CP $[N \cdot s \cdot m^{-3}]$
Z_1	impedance associated with v_1 $[N \cdot s \cdot m^{-3}]$
Z_2	impedance associated with v_2 $[N \cdot s \cdot m^{-3}]$
Z_3	impedance associated with v_3 $[N \cdot s \cdot m^{-3}]$
Z_4	impedance associated with p_a $[N \cdot s \cdot m^{-3}]$
k_1	stiffness component of Z_1 $[kg \cdot m^{-2} \cdot s^{-2}]$
c_1	damping component of Z_1 $[kg \cdot m^{-2} \cdot s^{-1}]$
m_1	mass component of Z_1 $[kg \cdot m^{-2}]$
k_2	stiffness component of Z_2 $[kg \cdot m^{-2} \cdot s^{-2}]$
c_2	damping component of Z_2 $[kg \cdot m^{-2} \cdot s^{-1}]$
m_2	mass component of Z_2 $[kg \cdot m^{-2}]$
k_3	stiffness component of Z_3 $[kg \cdot m^{-2} \cdot s^{-2}]$
c_3	damping component of Z_3 $[kg \cdot m^{-2} \cdot s^{-1}]$
k_4	stiffness component of Z_4 $[kg \cdot m^{-2} \cdot s^{-2}]$
c_4	damping component of Z_4 $[kg \cdot m^{-2} \cdot s^{-1}]$
g	OHC force-generation gain

1 Project Overview

Modelling is an important method of testing the physical properties of real systems. In many cases it is the only way to provide a comprehensive data when the system is complicated, and is vulnerable to direct measurements or reveals considerable discrepancies between *in vitro* and *in vivo* investigations. Although the idea of modelling may seem advantageous at first sight, it is, unfortunately, not devoided of drawbacks.

It is crucial for the researcher who deals with modelling, to find a good compromise between simplicity and clarity, which may initially seem uncomplicated for an experienced scientist. However, once the key assumption is stated it may reveal certain constraints, which require further development of the model. In other words, it forces an expansion in the number of parameters or introduction of new constants to which the model may be very sensitive. Finally, it may occur that the latter version of the model looses its generality.

One of the most active areas of research, which has found modelling to be a powerful tool, is modelling of the function of the cochlea. The goal of modelling of the cochlea is to uncover the mysterious phenomena of its tuning and compressive properties that could help in further development of more sophisticated models of sound perception or understanding it, in general [1, 2].

Theories of modelling cochlear micromechanics are based, in principle, on the idea of discretising the cochlear partition (CP) into a number of independent resonators. However, cochlear models comprising single resonator components cannot achieve the fine tuning of the CP observed in *in vivo* measurements. One solution is to introduce a secondary resonance, which is usually explained as being due to the tectorial membrane (TM), about one octave below the resonance frequency of the basilar membrane (BM) [5]. Whereas, the need for a two-resonant model has been widely accepted, the process of defining the form of activity of a potential internal agent varies with the different approaches.

It is postulated that the OHCs are responsible for the active processes occurring in the cochlea and hence for the fine tuning of the BM. Their motile action can be considered as a force generating mechanism, which in response to the BM deflection, damps or enhances its vibration.

A conceptual model based on the anatomical data can thus be built as a lumped component model of an independent resonator, along with a set of equations of motion defining its dynamic properties. Provided that the mechanical parameters of the system are known (usually extracted from the experimental data), their implementation into the model allows us to calculate its response for the known input.

The main purpose of the present research, driven by the reasoning of de Boer in [6], is to provide a comprehensive comparison and attempt of generalisation of two active models of the cochlea: the model of S. T. Neely and D. O. Kim [21] known as the Neely and Kim model, and the model of C. Daniel Geisler

[11]. Both the first and the second, represent classic mathematical models of the cochlear mechanics with outer hair cells (OHCs) postulated to be the active elements.

In the first step, each model will be considered independently, with the original notation, to examine its inherent assumptions. A generalised model is then presented, derived only on the basis of mechanical analysis, used to represent either of the individual models.

Next, a macromechanical model will be formulated to introduce the coupling of the individual cochlear partition elements via the cochlear fluid. Furthermore, the stability of the generalised models, defined as the negative feedback systems (inferred from the model's equations of motion), will be checked by means of *Nyquist stability criterion.*

Finally, the positive feedback system with a nonlinear network component is derived to define a quasi-linear model of the basilar membrane input-output function. The introduced nonlinear component, scheduled on the amplitude of the system's output, will adapt the gain of the overall feedback path and produce a level-dependent system, to give, under tonal excitation, a compressive and saturating characteristic.

2 Anatomy and Physiology

This section provides a brief introduction to the anatomy and physiology of the peripheral hearing system of a man. The emphasis is laid on the problems concerning the structure and functions of the human cochlea (excluding the vestibular system) regarded as the main unit involved in the processing of sound, although not the only one. In addition, a short description of the outer and middle ears is also provided. The neural pathways of the auditory system are not considered.

2.1 The Outer Ear

Figure one depicts the structure of the human peripheral auditory system. A cartilaginous flange called the pinna, including a small cavity-concha, and external auditory meatus (leftmost in Fig.1.) terminated by the tympanic membrane on the right, constitute the outer ear. Together they form a complex resonant cavity. In result, the incoming sound wave pressure is increased in the outer ear, most effectively in the 2-7 kHz range, when leading from the pinna to the tympanic membrane [23].

The second function of the outer ear is to provide cues in the localisation of sound. The intensity and timing differences of the sound waves coming at the two ears enable the localisation in the horizontal plane, whereas the cues for the vertical plane are realised by the pinna and the concha.

2.2 The Middle Ear

2.2.1 The Ossicles

After the modification in the outer ear, the sound wave, through the vibrations of the tympanic membrane, is transferred to the middle ear (centre of Fig.1.). The ossicular chain of auditory bones, respectively, the malleus, incus and stapes, suspended in the middle ear cavity by a series of ligaments and tendons, assembles the main middle ear apparatus. The malleus is attached to the tympanic membrane and joined relatively rigidly with the tip of the incus. The incus joins with the third of the ossicles, the stapes, which footplate is attached to the wall of the cochlea, i.e. to the flexible window called the oval window (see Fig.1.). Thus, the ossicles transfer the vibrations of the tympanic membrane to the cochlea. However, the main function of the bony chain is to match the impedance of the two media, the air, filling the outer ear and the fluid, which fills the cochlea. The matching mechanism bases on three principles.

First, as the area of the tympanic membrane, A_1 is larger then that of the footplate of the stapes, A_2, the force F, transferred from the tympanic membrane,

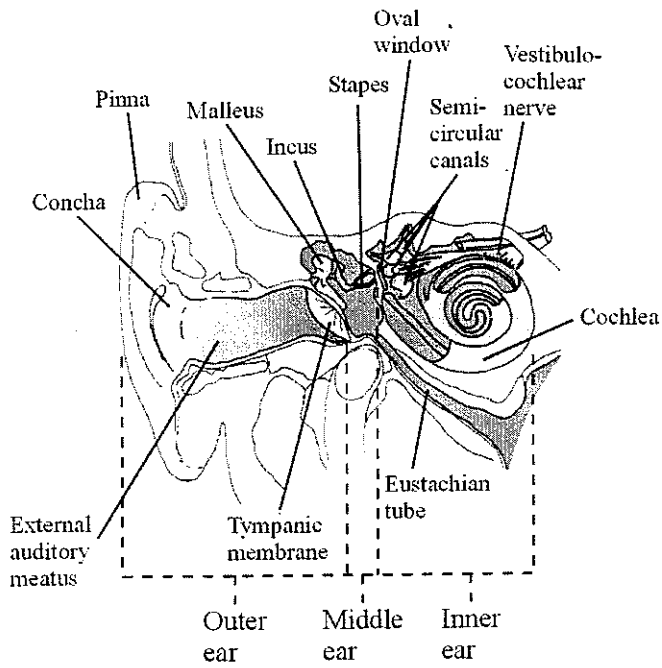

Figure 1: The peripheral auditory system of a man with the indication of the three main divisions: the outer, the middle and the inner ear.

applies a higher pressure to the oval window due to the ratio of A_1 and A_2

$$F = p_1 A_1 = p_2 A_2, \tag{1}$$

hence

$$\frac{p_2}{p_1} = \frac{A_1}{A_2}, \tag{2}$$

where p_1 denotes the pressure on the tympanic membrane and p_2, the pressure at the stapes.

The lever action between the longer, l_1, and the shorter, l_2, arms of the malleus and incus, respectively, contributes the second component to the impedance matching. The length difference, in effect, leads to an increase of the driving force at the incus and hence at the stapes, F_2, comparably to the force applied to the malleus, F_1. Furthermore, the increase of the force causes a proportional decrease of the velocity at the stapes, v_2:

$$F_1 l_1 = F_2 l_2, \tag{3}$$

thus

$$\frac{l_1}{l_2} = \frac{F_2}{F_1}, \tag{4}$$

which implicates

$$\frac{F_2}{F_1} = \frac{v_1}{v_2}, \tag{5}$$

where v_1 denotes the velocity of the malleus.

The third factor of the matching mechanism also results in the increase of the force, thus the decrease of the velocity at the stapes, however, caused by the buckling motion of the tympanic membrane.

Though the complexity of the matching mechanism, the contribution of the second and third principle described above is comparatively small, hence the impedance matching is mainly realised by the difference between the tympanic membrane and the stapes footplate areas.

2.2.2 The Middle Ear Muscles

The movement of the ossicles is controlled by two muscles, tendon tensor tympani muscle and tendon stapedius muscle, which are mainly responsible for the middle ear reflexes. The reflex contractions of both muscles stiffen the ossicular chain and reduce the transmission of sound. In general, the middle ear muscles function, to some extent, as a protective mechanism and maintain the input level at the cochlea relatively constant.

2.2.3 The Eustachian Tube

As depicted in Fig.1., the middle ear cavity proceeds to a long tube called the Eustachian tube, which allows, when opened (e.g. by swallowing, yawning or sneezing), the drainage of the fluids, ventilation and static pressure equalisation on both sides of the tympanic membrane.

2.3 The Inner Ear

The last division of the peripheral auditory system, shown in Fig.1. (right), is the inner ear, with the cochlea as its main apparatus, the semicircular canals and the vestibulo-cochlear nerve innervating the two structures.

The semicircular canals are a part of the peripheral vestibular system and, responding to angular acceleration of head, participate in the sense of balance. However, the vestibular system will not be discussed here.

The vestibulo-cochlear nerve (Fig.1.), is the most foremost part of the auditory neural pathways, which, as mentioned before, are not a subject of present research. Nevertheless, the cochlea innervation will be shortly described.

2.3.1 The Structure of the Cochlea

The cochlea is a bony structure, coiled around the bony tube called the modiolus and deep embedded in the temporal bone. Its shape reminds the shell of a

snail with 2.5 coils. The overall dimensions amount to 1 cm in width and 5 mm in height from base to apex.

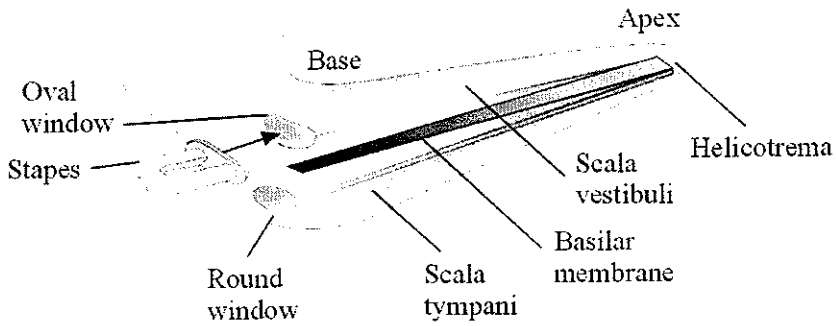

Figure 2: A schematical view of an uncoiled cochlea.

It is presented very often as an uncoiled system. Figure two presents the view of an uncoiled cochlea and Figure three, its cross-sectional view. The cochlea tapers along the whole length from the base to the apex. Two membranes, the Reissner's membrane and basilar membrane (BM) running through almost entire length of the cochlea, divide it into three compartments, the scala vestibuli, scala media, and scala tympani. The two utmost scalae are joined by the small opening at the apex of the cochlea called helicotrema. The third, scala media, creates an inner closed compartment. Furthermore, at the base of the cochlea, the upper and the lower cochlear channels are terminated by the membranous, oval, and round windows, respectively (see Fig.2.).

The scalae are filled with two kinds of fluids, which differ in the ionic composition. The scala vestibuli and scala tympani are filled with the perilymph with high sodium ions content, whereas the scala media, with the endolypmh, a fluid with high potassium ions content. The properties of the cochlear fluids are similar to those of the sea water and assumed to be inviscid and incompressible.

The length of the BM is estimated to 35 mm. Though the cochlea's width tapers from the base to the apex, the BM, widens from its narrow basal end to the apex. Furthermore, the radial stiffness of the BM, is highest at the base and decreases exponentially to the apex.

As shown on the Fig.3., an organ, called the organ of Corti (OC) rests on the BM. It is a specialised structure containing receptor cells, the hair cells, innervating the cochlea through the connection with the synaptic ends of the auditory nerve fibres (see Fig.4.).

There are two types of the hair cells in the OC. First, the flask-shaped inner hair cells (IHCs), approximately 3500 in all, innervated mainly by the afferent

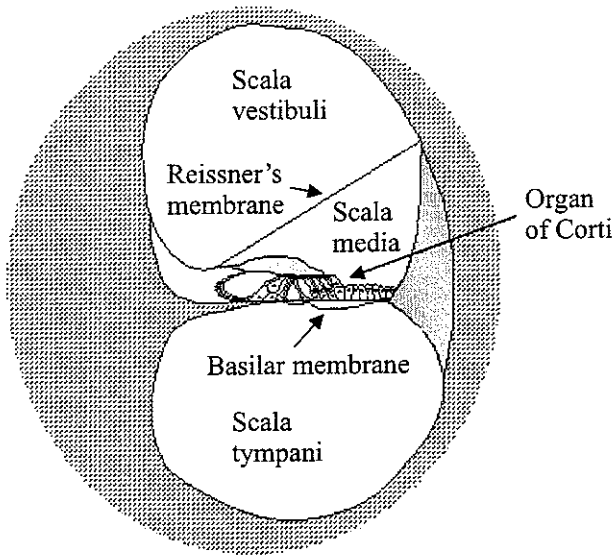

Figure 3: A cross-sectional view of the cochlea with indication of the cochlear channels.

(centripetal) nerve fibres and formed in one row running along the cochlea. The second type, are the cylindrically shaped outer hair cells (OHCs), of which there are about 12000, supported by the Deiters' cells and innervated mainly by the efferent (centrifugal) nerve fibres. The OHCs form three to five rows along the cochlea. The rows of the hair cells increase their length along the cochlea, from the base towards the apex. Both, the IHCs and the OHCs, separated by the pillar supporting cells, are embodied in the OC, surrounded by specialised cells and all bound tightly to form a close knit layer at their tops, the reticular lamina (RL) (Fig.5.).

A small ciliary bundles, the stereocilia, emerge from the top of each hair cell. The cilia are organised in rows of an increasing length outward the modiolus and are connected to their sides and tips by the cross- and tip-links, respectively. The cilia rows shape a shallow "U" on the IHC and "W" or "V" on the OHC tops [3].

The tops of the highest OHC stereocilia rows are embedded in the tectorial membrane (TM), a gelatinous structure expanding over the OC, whereas the IHC cilia are thought to be freely projecting from the cell's body. The TM mass changes along the cochlea increasing from the base to the apex.

2.3.2 The Cochlear Physiology

The BM dynamics, was studied in the XIX century by the German physicist Herman von Helmholtz after the findings of the contemporary anatomists, revealed the tonotopic organisation of the BM. Helmholtz introduced the idea of the hypothetical radially mounted set of strings (simple harmonic oscillators)

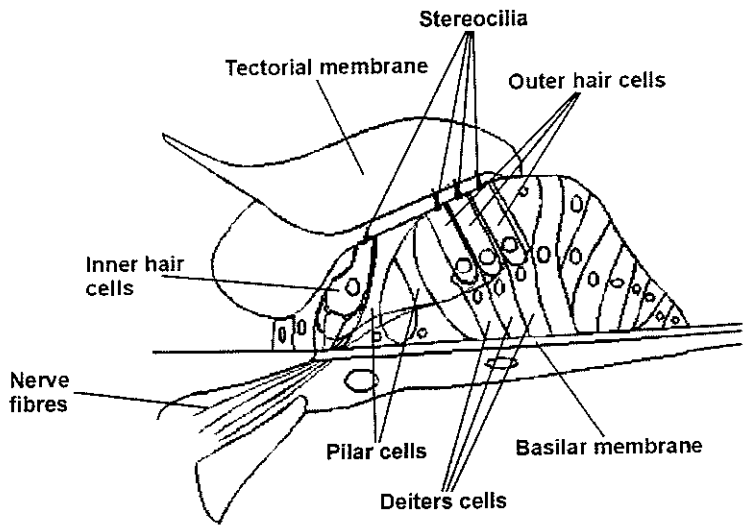

Figure 4: A schematical view of the organ of Corti.

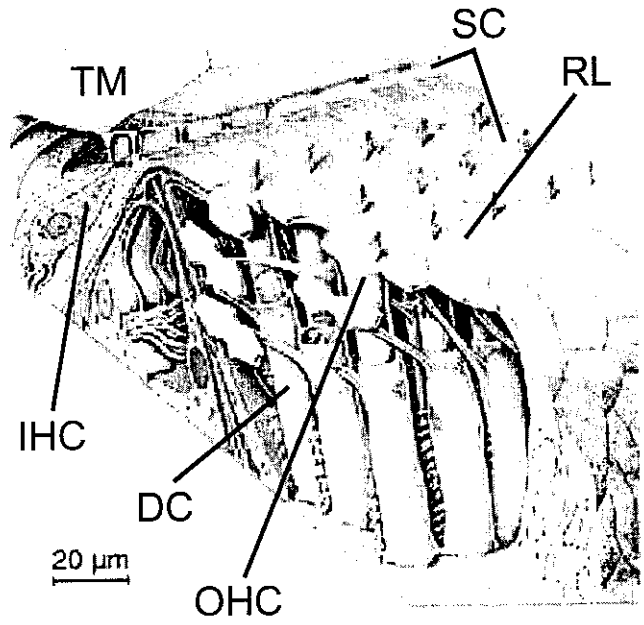

Figure 5: The view of the main structures of the organ of Corti after uncovering the tectorial membrane (DC-Deiters' cells, SC-stereocilia, see text for others).

constituting the BM, each to be excited at the characteristic place specific to the stimulus input frequency. Though innovatory and sometimes regarded as a first attempt of mechanical modelling of the cochlea, it was revised in 1928 by the Hungarian scientist Georg von Békésy and confirmed in 1943 by the results of series of his ingenious experiments on human cadaver cochleae, discovering the travelling waves in the cochlea.

Since the Reissner's membrane impedance is small, the scala vestibuli and scala media form one compartment, called often the upper cochlear channel. However, the BM, due to its impedance, constitutes a flexible border between the upper cochlear channel and the scala tympani, hence called the lower channel. The BM with the OC fixed on it and the TM, are often presented as a one, jointly moving structure called the cochlear partition (CP).

The piston-like movements of the stapes cause a disturbance in the vicinity of the stapes footplate, thus generates changes in pressure in the cochlear fluids [3]. The pressure changes along the cochlea set the CP into vibration.

While the cochlear fluids are assumed to be inviscid and incompressible, the disturbance propagates as a very fast wave but produces no forces on the CP. However, due to the pressure difference between the fluids in the upper and lower cochlear channels and a small impedance of the membranous round window, which allows a pressure gradient wave to develop along the cochlea, the CP is set into a travelling vibration, the von Békésy travelling wave. Figure six presents a travelling wave in an uncoiled cochlea.

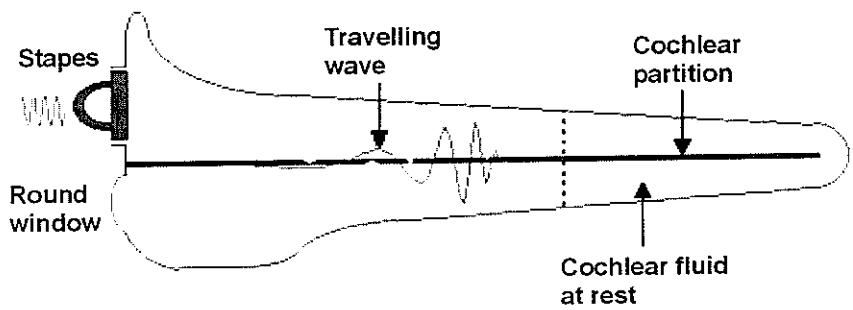

Figure 6: The travelling wave. The arrows indicate the pressure fluctuations along the cochlea exerting on the cochlear partition and inducing the travelling wave.

The processes described above, referring to the study of the interactions between the cochlear fluids and the CP, are known as the cochlear macromechanics. The cochlear micromechanics, on the other side, refers to the study of the mechanics within the CP, i.e. the interactions of the OC structures and the BM.

The vibrations of the BM cause the stereocilia of the hair cells to deflect. The deflections of the OHCs stereocilia are induced by the shearing force due to the

BM transversal vibrations and the TM radial movement, whereas the IHCs cilia, by the outward fluid flow from the closed space between the RL and the TM, which decreases when they draw towards each other.

Through the deflection of the cilia, the tip-links open a putative ionic channels, allowing the flow of the K^+ ions from the endolypmh to the hair cell. Hence, due to the difference in the endolypmh, $+80\,mV$, and the intracellular potentials, $-45\,mV$ and $-70\,mV$ in the IHCs and OHCs, respectively, the hair cells seize a depolarisation and initiate the firing of the neural impulses. The process described above occurs when the deflection of the cilia occurs in the outward-modiolus direction. The deflection of the hair bundles in the inward-modiolus direction is inhibitory, i.e. reduces the likelihood of the neurons firing (see Fig.7.).

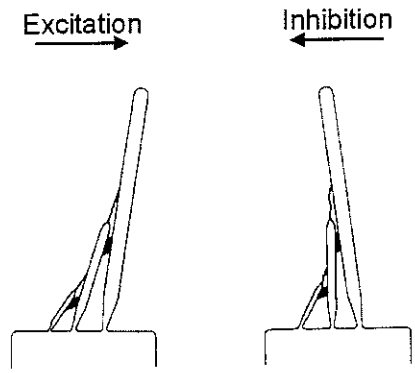

Figure 7: The deflections of the OHC stereocilia. The outward-modiolus deflections cause the excitation and the contraction, whereas the inward-modiolus, the inhibition and elongation of cells' body.

The cochlear dynamics, as described above, though consistent with the results of the experiments on the dead cochleae, did not explain the high frequency selectivity of the cochlea observed for the low sound pressure levels. The BM response patterns, observed in the live cochleae, are sharply tuned contrary to the broader response curves of the dead cochlea. Furthermore, the BM vibration is nonlinear, with a compressive characteristic for the stimuli in the range of approximately 30-90 dB SPL. This led to the hypothesis of the existence of an active mechanism within the cochlea. The active mechanism should therefore enhance and damp the BM response for the low and high sound pressure levels, respectively. With the discovery of the electromotile responses of the OHCs, the active process in the cochlea found its potential generator.

The OHCs are assumed to work as an actuator, which undergoes instantaneous contractions and elongations due to the deflections of their stereocilia. The outwards-modiolus deflections of the hair bundles depolarising the OHC, lead to its contraction, hence to the local enhancement of the BM displacement (Fig.8.).

The additional energy pumped by the OHCs to the BM is therefore mechanically described as a negative contribution to the resistive component of the BM impedance.

In result, the cochlear mechanics modelling approaches divide into the passive and active, when describing the dead or live cochleae, respectively. Figure eight depicts a schematical BM response of the passive and active cochlea.

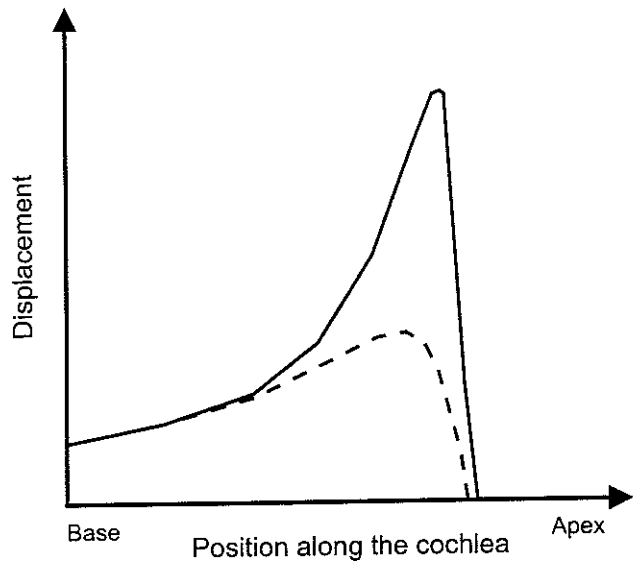

Figure 8: A schematical passive (dashed) and active (solid) basilar membrane response curve in function of position along the cochlea.

The nonlinearity of the BM, as presented in Fig.9., reveals the compressive characteristic of its response. For the stimulus input levels from 30 to 90 dB SPL, the active process tends to compress the BM displacement, whereas below and above this range the response is linear. It is assumed that the response saturates above the upper limit of 90 dB SPL and becomes linear in effect. In summary, the compression of the BM displacement in the live cochlea, reducing the gain in the active process with the increase of the sound pressure level, results in the broadening of the cochlear response curves as shown on the Fig.10. (data obtained for the BM of the guinea pig cochlea).

Further evidence of the cochlear nonlinearity is the generation of the distortion products, the $f_2 - f_1$ and $2f_1 - f_2$ combination tones, and the two-tone suppression phenomenon, which reveals in the stimulus response reduction by a second one present in the input [23].

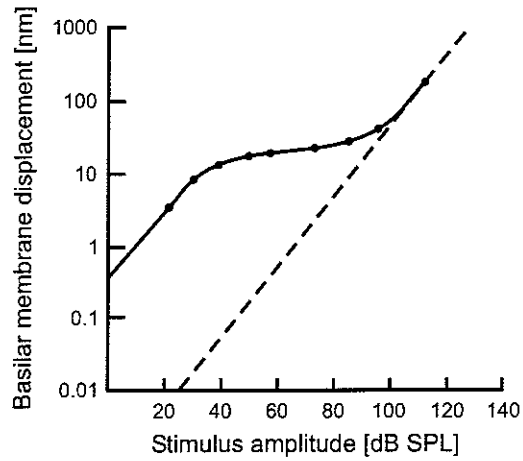

Figure 9: The input-output curve revealing the compressive nonlinearity in the live cochlea. The dashed line denotes the linear input-output function as observed in the dead cochlea.

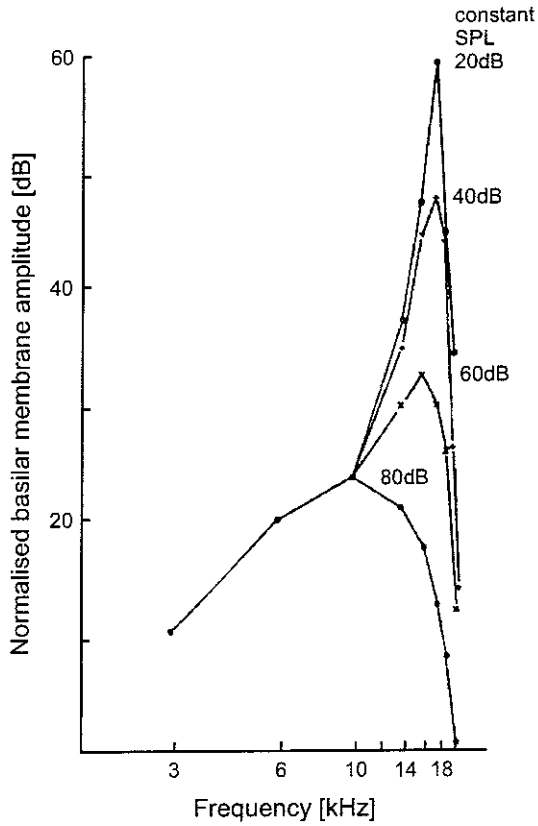

Figure 10: The normalised basilar membrane amplitude (gain) in function of the frequency (basal end of the cochlea) in the guinea pig.

3 Micromechanics

3.1 The Model of Neely and Kim

3.1.1 The Equations of Motion

The left panel of Fig.11. depicts a lumped component model of cochlear micromechanics proposed by Neely and Kim (NK). It is a two-degree-of-freedom (DOF) system with the mass of the BM lumped in the m_1 element and its stiffness and damping, represented by the spring k_1 and damper c_1, respectively. The second mass m_2, is the mass of the TM, which is attached to the spiral limbus (left boundary of the OC [3]) by the k_2 and c_2. Those two masses are coupled by the stiffness k_3 and damping c_3. Thus, the CP is now a set of components (resonators) spaced equally at each position of x.

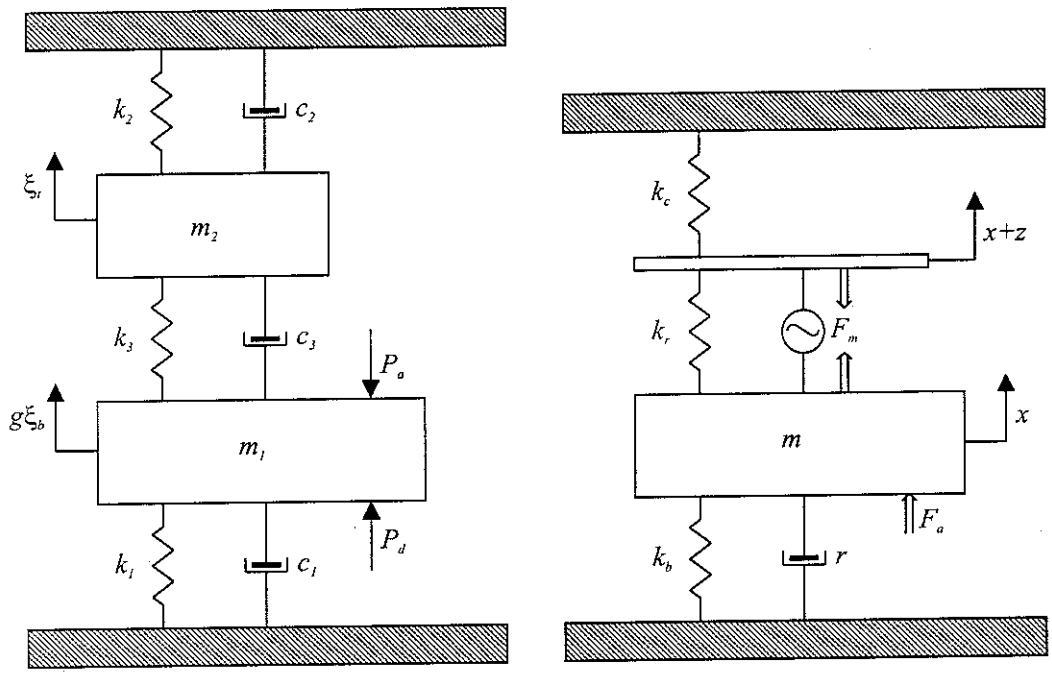

Figure 11: Lumped component systems for cochlear micromechanics: the classical model of Neely&Kim (left) and Geisler (right).

The cochlear micromechanics was described in terms of the cochlear partition impedance $Z_p(x)$ (Note that because the fluid's pressure within the cochlea is a function of position and the CF i.e. $P(x,\omega)$, therefore the CP impedance, Z_p, should be denoted as $Z_p(x,\omega)$. However, for the sake of clarity the impedances and pressures will be presented as a function of position x only.). The radial shape of the CP displacement was assumed to be independent of x. so it always

occurred in the same bending mode.

It is very important to understand that the above assumptions allow to consider the model as a linear (described by the impedance) and one-dimensional (same bending mode for any position x) system, which remarkably simplifies the mathematical formulations and imposes its deterministic behaviour at the stage of predictions. It states that there is no distortion in the waveform of the BM response, in consequence there is no need of introducing a scaling factor for the nonlinearities due to the compressive character of the function of the cochlea and the representation of the relation between the pressure and the velocity in terms of the partition impedance $Z_p(x)$, remains valid [13].

For any given position, the average displacement across the width of the CP ξ_p to the maximum displacement over the width of the BM ξ_b, was defined as the ratio b, hence

$$\xi_p(x) = b\xi_b(x), \tag{6}$$

thus $b < 1$ according to this definition.

The cochlear fluids pressure difference across the OC depicted on the Fig.11. as P_d, is driving the BM causing its vertical displacement. In addition, this vertical displacement leads to a proportional, radial shear displacement ξ_c between the RL and the TM (see Fig.2.). The relative shearing displacement is assumed to be responsible for the mechanical excitation of the sensory hair cells, both the IHCs and the OHCs.

This shearing displacement can be written as

$$\xi_c(x) = g(x)\xi_b(x) - \xi_t(x), \tag{7}$$

where $g(x)$ is the lever gain between the OC displacement ξ_t and the radial displacement of the RL and the ξ_t is the radial motion of the TM. Note that ξ_c was used to describe the hair bundle displacement of both, the IHCs and OHCs.

The equation of motion in the frequency domain for the first DOF of the system presented in Fig.11. (left) is

$$P_d(x) - P_a(x) = g(x)Z_1(x)\dot{\xi}_b(x) + Z_3(x)\dot{\xi}_c(x), \tag{8}$$

where
$Z_1 = k_1/j\omega + c_1 + j\omega m_1$,
$Z_3 = k_3/j\omega + c_3$.

The impedances Z_1 and Z_3 represent the mechanical impedance of the OC and the coupling between the OC and the TM, respectively, and P_a is an acoustical pressure source located within the OHC.

For the second DOF equation of motion is formulated by

$$0 = Z_2(x)\dot{\xi}_t(x) - Z_3(x)\dot{\xi}_c(x), \tag{9}$$

where
$Z_2 = k_2/j\omega + c_2 + j\omega m_2$,

represents the mechanical impedance of the TM.

The active source in the NK model, P_a, acts on the system due to the mechanical force generated by the OHCs and is controlled by the sensory cell displacement ξ_c. It is, though, not an independent source and takes form

$$P_a(x) = -\gamma Z_4(x)\dot{\xi}_c(x), \tag{10}$$

where
$Z_4 = k_4/j\omega + c_4$.

The γ factor, which is independent of x and ω, is an overall gain control in the active element and can be considered as a measure of the physiological condition of the cochlea. The impedance Z_4, provides a frequency-dependent phase shift between the P_a and the ξ_c.

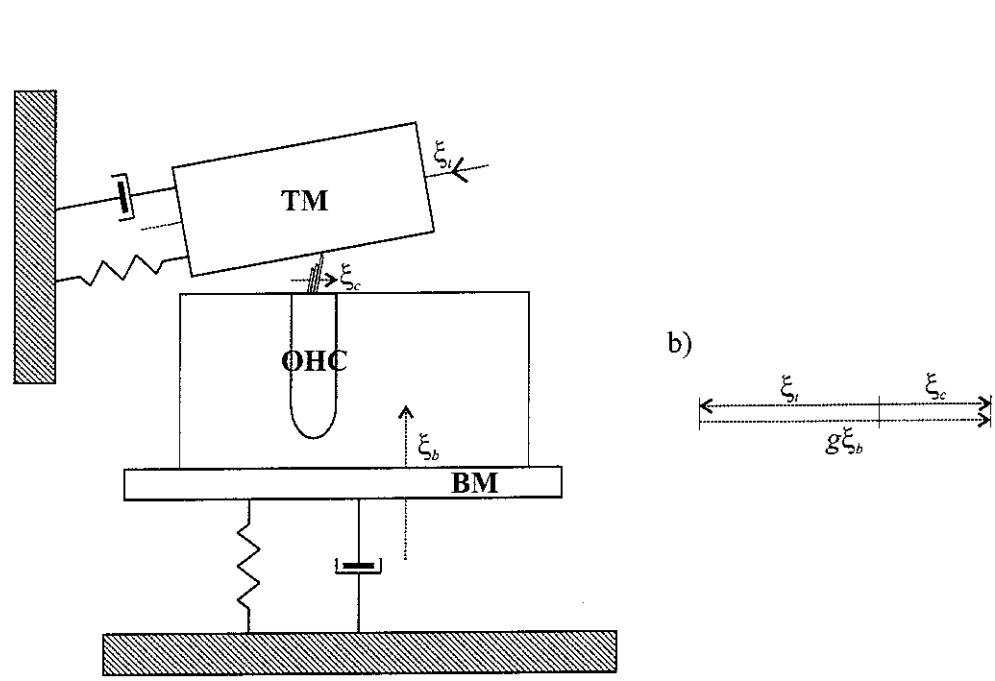

Figure 12: Schematic illustration of the Neely&Kim model components displacements. The planes of the displacements (positive direction indicated by arrows) $\xi_b(x)$, $\xi_t(x)$, $\xi_c(x)$ (a); graphic representation of Eq.7. (b).

It is surprising that, although it is known that the stereocilia of the OHCs make contact with the TM, in this model the active source is only assumed to act on the BM with no apparent reaction.

Depolarisation of the vestibular hair cell occurs when its tallest hair bundle is deflected outwards the modiolus (towards the tallest stereocilium), i.e. when ξ_c increases in the NK model. As a consequence, it leads to the OHC height shortening and could be interpreted as an internal pressure decrease in the OHC. Thus, the minus sign in Eq.10. accounts for the decrease of the pressure inside the OHC, which is isometrically transmitted to the surrounding fluid, due to the fluids incompressibility. These remarks are consistent with *in vitro* observations of the hair cells.

3.1.2 The Partition Impedance

Having formulated the equations of motion for the system in Fig.11., the driving-point impedance of the CP can be formulated as

$$Z_p = P_d/\dot{\xi}_p, \tag{11}$$

hence

$$Z_p = g/b[Z_1 + Z_2(Z_3 - \gamma Z_4)/(Z_2 + Z_3)]. \tag{12}$$

Solving the Eqs.6. and 11. for $\dot{\xi}_b$ and integrating with respect to time, the displacement of the BM ξ_b is obtained

$$\xi_b = P_d/j\omega Z_p, \tag{13}$$

and ξ_c are expressed as

$$\xi_c = g[Z_2/(Z_2 + Z_3)]\xi_b. \tag{14}$$

3.2 The Model of Geisler

3.2.1 The Equations of Motion

A lumped component model depicting a segment of the CP for the model of Geisler (G) is presented in the right panel of Fig.11. This system consists of one mass m, which is the mass of the BM, its stiffness k_b and damping r. Again the BM occurs in the traditional mass-spring-damper representation. However, there is no second mass in this case, but the RL, which is joined to the BM by the stiffness k_r that is the passive axial stiffness of the OHC and the supporting cells. The spring k_c is the stiffness of the of the ciliary/TM complex attached to the modiolus. Again, like in the NK model, the CP is represented as a set of resonators spaced equally at each longitudinal position through he cochlear channel. However, the cochlear micromechanics was described in terms of dynamic stiffness in this approach.

The total acoustic force F_a causes the BM displacement by x units (note that x now is not a longitudinal position on the BM) towards the scala vestibuli (SV), which in turn acts on the OHC deflecting its cilia by the angle of γ in the direction away from the modiolus.

According to *in vitro* observation this ciliary deflection is excitory to the OHC, thus it results in contractile forces, which elicit on the BM and RL. In this model the RL is assumed to rotate freely about the pillar heads, so the contractions of the OHC displace the RL by additional z units towards the SV. In consequence, the total deflection of the ciliary bundle γ is proportional to the total displacement $x + z$ of the RL

$$\gamma \propto Ax + Bz, \tag{15}$$

where A and B are ratios being a measure of x and z, respectively, when forced by F_a (see Fig.13.). For the detailed geometrical analysis check the appendix in the Geisler's article [11].

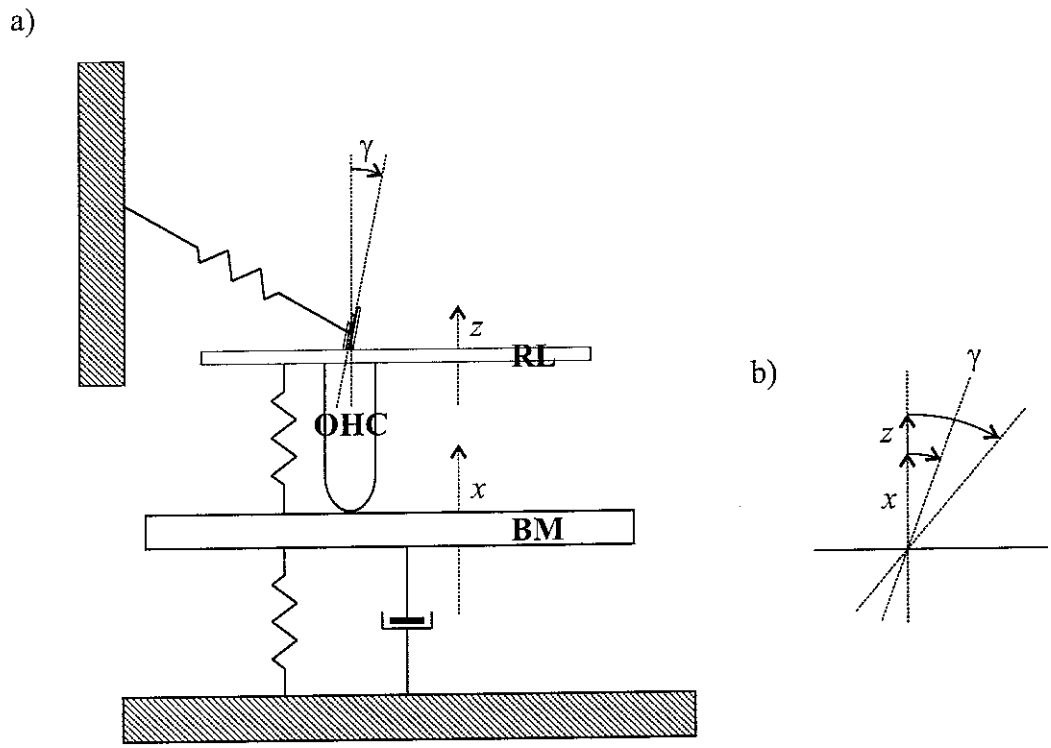

Figure 13: Schematic illustration of the Geisler model components displacements. The planes of the displacements (positive direction indicated by arrows) x, z, γ (a); graphic representation of Eq.15. (b).

The equation of motion for the first DOF of the system (right panel of Fig.11.)

takes form

$$F_a = k_b x + m\ddot{x} + r\dot{x} - F_m cos\psi - k_r cos\psi + k_c C(z + A/Bx), \qquad (16)$$

where C is the measure of the torque of the RL and BM about the ends of the pillar cells.The angle ψ is the angle between $\vec{F}_a$ and $\vec{F}_m$. Geometrical representation of the applying forces is shown in Fig.14.

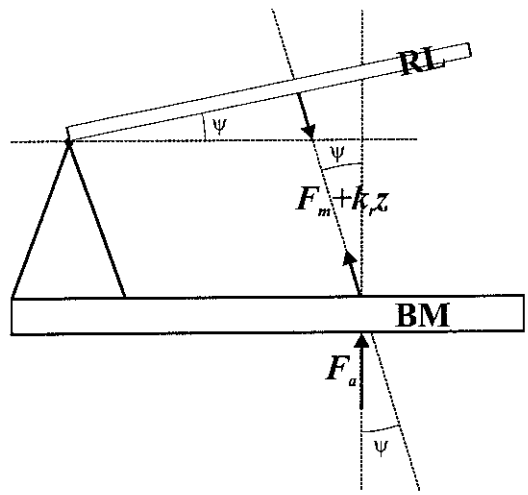

Figure 14: Geometrical sketch of the mechanical forces $\vec{F}_a$, $\vec{F}_m$ and the passive axial force $k_r z$ exerting on the BM and the RL with indication of the angle ψ between the planes of the action.

The second relationship due to the relative displacement $x + z$ (check Fig.11., right) takes form

$$0 = F_m + k_r z + k_c(z + A/Bx). \qquad (17)$$

In order to solve the model micromechanics, an explicit definition of the activity within the cochlea has to be formulated. In the G model it is assumed that

$$F_m = F(\omega) * \gamma. \qquad (18)$$

This equation implies the linear proportionality of the OHC contractile force to the angular deflection of its cilia γ. Hence, according to Eq.15., the motile force F_m is proportional to $Ax + Bz$.

3.2.2 The Partition Impedance

Solving simultaneously Eqs.16-18. for the relation of the acoustic force F_a to the BM displacement x, the dynamic stiffness of the cochlear model will be

expressed, and formulated in the frequency domain as

$$F_a/x = k_b - m\omega^2 + j\omega r + \left[\frac{k_c k_r DA/B}{k_c k_r + F_{fb}(\omega)}\right], \tag{19}$$

where
$D = C + cos\psi$,
$F_{fb} = F(\omega) * constant.$

The bracketed term in the formula above, appears in the classical negative-feedback form with the feedback force F_{fb} (check [11] for the derivation).

It is to be noted that Eq.16. takes form of the dynamic stiffness, however, dividing it by $j\omega$ will define the impedance of the cochlear partition, likewise in the NK model. First term, $k_b - m\omega^2 + j\omega r$, will account for the BM impedance and the bracketed term will state the impedance of the active load.

The mathematical representation of the G model will be completed after introducing the explicit formulation of the feedback-force F_{fb}, extracted from experimental and theoretical works. In the Fourier transform notation this feedback-force is formulated by

$$F_{fb} = F_0 \left[\frac{\omega_r - j\omega}{\omega_r + j\omega}\right] e^{-j\omega T}. \tag{20}$$

This function consists of three components. The first one, F_0, is a force constant amounting to

$$F_0 = qk_b, \tag{21}$$

where q is a force factor, which defines the cochlear activity in a way similar to γ in the NK model.

The second factor determines the transfer function of an all-pass circuit. It is specified by

$$|H(j\omega)| = 1, \tag{22}$$

and

$$\angle H(j\omega) = -tg^{-1}\left(\frac{2\omega\omega_r}{\omega_r^2 - \omega^2}\right), \tag{23}$$

thus it changes the phase of the force F_0, when passed through it. In addition, the ω_r term is a cut-off frequency that is a function of characteristic frequency (CF) ω_0

$$\omega_r = \omega_0/20. \tag{24}$$

Finally, the third component (the exponential term) of F_{fb} is a delay term. The amount of delay, set by the location of the OHC in the cochlea, is specified by T and

$$T = \frac{n\pi}{\omega_0}, \tag{25}$$

where n is a delay factor.

4 The Modes of Vibration of Neely and Kim Model

A dynamic system as one shown in Fig.11. (Neely&Kim model, left) is characterised by its natural frequencies and principal modes, number of which equals to the number of the DOFs. To find the principal modes of vibration for the NK model, an undamped free vibration of the system will be assumed. Thus all damping components will be eradicated from the equations of motion, so that the dashpots in Fig.11. (left) are omitted to give a simplified, two-degree-of-freedom system with stiffnesses and masses, as depicted in Fig.15. Furthermore, the free vibration implies no external excitation (forces/pressures) acting on the system, hence the pressures p_d and p_a are ignored.

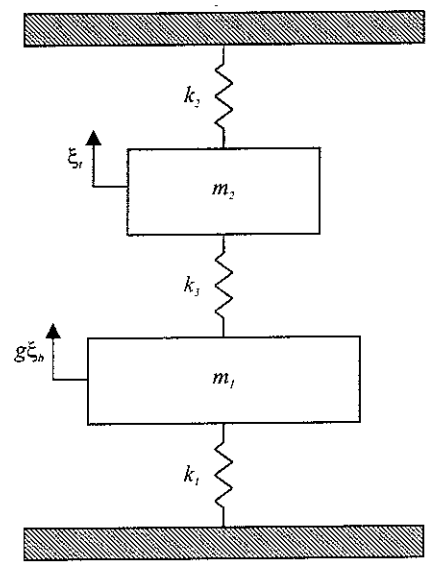

Figure 15: Lumped component Neely&Kim model as a free, undamped system.

4.1 The Equations of Motion

The equations of motion describing the system shown in Fig.15. are formulated by

$$\begin{aligned} m_1 g\ddot{\xi}_b &= -k_1 g\xi_b \quad -k_3(g\xi_b - \xi_t) \\ m_2\ddot{\xi}_t &= -k_2\xi_t \quad -k_3(\xi_t - g\xi_b). \end{aligned} \tag{26}$$

Since $g = 1$ in the NK model it can be omitted in the EOMs to give

$$\begin{aligned} m_1\ddot{\xi}_b &= -k_1\xi_b \quad -k_3(\xi_b - \xi_t) \\ m_2\ddot{\xi}_t &= -k_2\xi_t \quad -k_3(\xi_t - \xi_b), \end{aligned} \tag{27}$$

expressed equivalently, after rearrangement, as

$$\begin{aligned} m_1\ddot{\xi}_b + (k_1+k_3)\xi_b - k_3\xi_t = 0 \\ m_2\ddot{\xi}_t + (k_2+k_3)\xi_t - k_3\xi_b = 0, \end{aligned} \tag{28}$$

which in matrix notation gives

$$\begin{bmatrix} m_1 & 0 \\ 0 & m_2 \end{bmatrix} \begin{Bmatrix} \ddot{\xi}_b \\ \ddot{\xi}_t \end{Bmatrix} + \begin{bmatrix} k_1+k_3 & -k_3 \\ -k_3 & k_2+k_3 \end{bmatrix} \begin{Bmatrix} \xi_b \\ \xi_t \end{Bmatrix} = \begin{bmatrix} 0 \\ 0 \end{bmatrix}. \tag{29}$$

or, equivalently,

$$\underline{M}\,\ddot{\underset{\sim}{\xi}} + \underline{K}\,\underset{\sim}{\xi} = 0, \tag{30}$$

where

$$\underline{M} = \begin{bmatrix} m_1 & 0 \\ 0 & m_2 \end{bmatrix}, \underline{K} = \begin{bmatrix} k_1+k_3 & -k_3 \\ -k_3 & k_2+k_3 \end{bmatrix}, \ddot{\underset{\sim}{\xi}} = \begin{Bmatrix} \ddot{\xi}_b \\ \ddot{\xi}_t \end{Bmatrix} \text{ and } \underset{\sim}{\xi} = \begin{Bmatrix} \xi_b \\ \xi_t \end{Bmatrix}.$$

It can be noted that $\underline{M}$ and $\underline{K}$ are real, symmetric and positive with the off-diagonal terms representing the DOFs coupling, dynamic (mass) and static (stiffness) coupling, respectively.

Assuming the solutions of form

$$\begin{aligned} \xi_b &= A_1 e^{j\omega t} \\ \xi_t &= A_2 e^{j\omega t}, \end{aligned} \tag{31}$$

so that

$$\begin{aligned} \ddot{\xi}_b &= -\omega^2 A_1 e^{j\omega t} \\ \ddot{\xi}_t &= -\omega^2 A_2 e^{j\omega t}, \end{aligned} \tag{32}$$

and substituting to Eq.28. gives

$$\begin{aligned} -m_1\omega^2 A_1 e^{j\omega t} + (k_1+k_3)A_1 e^{j\omega t} - k_3 A_2 e^{j\omega t} = 0 \\ -m_2\omega^2 A_2 e^{j\omega t} + (k_2+k_3)A_2 e^{j\omega t} - k_3 A_1 e^{j\omega t} = 0. \end{aligned} \tag{33}$$

Crossing out the $e^{j\omega t}$ terms, Eq.33. is formulated by

$$\begin{aligned} -m_1\omega^2 A_1 + (k_1+k_3)A_1 - k_3 A_2 = 0 \\ -m_2\omega^2 A_2 + (k_2+k_3)A_2 - k_3 A_1 = 0, \end{aligned} \tag{34}$$

which after rearrangement will take form

$$\begin{aligned} (k_1+k_3-m_1\omega^2)A_1 - k_3 A_2 = 0 \\ (k_2+k_3-m_2\omega^2)A_2 - k_3 A_1 = 0. \end{aligned} \tag{35}$$

First relationship in Eq.35. gives the solution of a form

$$A_2 = \frac{k_1 + k_3 - m_1\omega^2}{k_3} A_1, \tag{36}$$

so that the second relationship becomes

$$\left[\frac{(k_1 + k_3 - m_1\omega^2)}{k_3}(k_2 + k_3 - m_2\omega^2) - k_3\right] A_1 = 0. \tag{37}$$

Assuming $A_1 = 0$, the trivial solution is obtained with $A_1 = A_2 = 0$, which implies no motion and the system stays at rest. Equating the bracketed term in Eq.37. to nought (expanding the characteristic determinant), however, gives a quadratic equation in ω^2 with two real and positive values for ω^2, [26], i.e.

$$(k_1 + k_3 - m_1\omega^2)(k_2 + k_3 - m_2\omega^2) - k_3^2 = 0, \tag{38}$$

and

$$\omega^4 - \left(\frac{k_1 + k_3}{m_1} + \frac{k_2 + k_3}{m_2}\right)\omega^2 + \frac{k_1k_2 + k_1k_3 + k_2k_3}{m_1m_2} = 0, \tag{39}$$

from which the natural frequencies, of the first and second modes, ω_1 and ω_2, respectively, can be calculated as two roots of quadratic in ω^2.

According to the relations in Eq.35. the ratio of the amplitudes is formulated by

$$\frac{A_1}{A_2} = \frac{k_3}{k_1 + k_3 - m_1\omega^2} = \frac{k_2 + k_3 - m_2\omega^2}{k_3}, \tag{40}$$

thus, for the two natural frequencies, after substituting ω_1

$$\frac{A_{11}}{A_{21}} = \frac{k_3}{k_1 + k_3 - m_1\omega_1^2} = \frac{k_2 + k_3 - m_2\omega_1^2}{k_3}, \tag{41}$$

and ω_2

$$\frac{A_{12}}{A_{22}} = \frac{k_3}{k_1 + k_3 - m_1\omega_2^2} = \frac{k_2 + k_3 - m_2\omega_2^2}{k_3}. \tag{42}$$

where the second index denotes the natural frequencies ω_1 and ω_2, respectively.

It should be noted that Eqs. 41-42. express the amplitude ratios, however, choosing one of the amplitudes equal to some arbitrary value, the amplitude ratio will be normalised to this value and the normal modes $\phi_{1,2}(\xi)$ obtained.

Choosing the A_{11} and A_{12} equal to one, the normal modes will be formulated as

$$\begin{aligned} \phi_1 &= \left\{ \begin{array}{c} 1 \\ A_{21} \end{array} \right\} \\ \phi_2 &= \left\{ \begin{array}{c} 1 \\ A_{22} \end{array} \right\}, \end{aligned} \tag{43}$$

where A_{21} and A_{22} can be derived from Eq.41. and 42.

Finally, the motion in the first mode will amount to

$$\left\{ \begin{array}{c} \xi_b \\ \xi_t \end{array} \right\} = \left\{ \begin{array}{c} 1 \\ A_{21} \end{array} \right\} e^{j\omega_1 t} \ , \tag{44}$$

and in the second mode

$$\left\{ \begin{array}{c} \xi_b \\ \xi_t \end{array} \right\} = \left\{ \begin{array}{c} 1 \\ A_{22} \end{array} \right\} e^{j\omega_2 t} \ , \tag{45}$$

or, equivalently

$$\left\{ \begin{array}{c} \xi_b \\ \xi_t \end{array} \right\} = \left\{ \begin{array}{c} 1 \\ A_{21} \end{array} \right\} (A sin\, \omega_1 t + B cos\, \omega_1 t) \ , \tag{46}$$

$$\left\{ \begin{array}{c} \xi_b \\ \xi_t \end{array} \right\} = \left\{ \begin{array}{c} 1 \\ A_{22} \end{array} \right\} (C sin\, \omega_2 t + D cos\, \omega_2 t) \ , \tag{47}$$

where A, B, C and D are real constants of integration, which are determined by the initial conditions [26].

The general free vibration is represented by the superposition of independent free vibrations in each of the two modes expressed in Eqs.44-45. (46, 47) thus

$$\left\{ \begin{array}{c} \xi_b \\ \xi_t \end{array} \right\} = \left\{ \begin{array}{c} A_{11} \\ A_{21} \end{array} \right\} (A sin\, \omega_1 t + B cos\, \omega_1 t) \ + \ \left\{ \begin{array}{c} A_{12} \\ A_{22} \end{array} \right\} (C sin\, \omega_2 t + D cos\, \omega_2 t) \ . \tag{48}$$

Assuming the initial conditions at $t = 0$: $\xi_b = 1$, $\xi_t = 0$, $\dot{\xi}_b$, $\dot{\xi}_t$ and taking $A_{11} = A_{12} = 1$ and applying to following relations

$$\left\{ \begin{array}{c} \xi_b \\ \xi_t \end{array} \right\} = \left\{ \begin{array}{c} 1 \\ A_{21} \end{array} \right\} (A sin\, \omega_1 t + B cos\, \omega_1 t) \ + \ \left\{ \begin{array}{c} 1 \\ A_{22} \end{array} \right\} (C sin\, \omega_2 t + D cos\, \omega_2 t) \ , \tag{49}$$

and

$$\left\{ \begin{array}{c} \dot{\xi}_b \\ \dot{\xi}_t \end{array} \right\} = \left\{ \begin{array}{c} 1 \\ A_{21} \end{array} \right\} (A cos\, \omega_1 t - B sin\, \omega_1 t) \ + \ \left\{ \begin{array}{c} 1 \\ A_{22} \end{array} \right\} (C cos\, \omega_2 t - D sin\, \omega_2 t) \ , \tag{50}$$

the constants A, B, C and D can be derived and will equal to

$$
\begin{aligned}
A &= 0, \\
B &= \tfrac{A_{22}}{A_{22}-A_{21}}, \\
C &= 0, \\
D &= \tfrac{A_{21}}{A_{21}-A_{22}}.
\end{aligned}
\tag{51}
$$

In summary, the actual motion will be time harmonic at two natural frequencies, ω_1 and ω_2, and defined as

$$
\left\{ \begin{array}{c} \xi_b \\ \xi_t \end{array} \right\} = \left\{ \begin{array}{c} 1 \\ A_{21} \end{array} \right\} B cos\, \omega_1 t \; + \; \left\{ \begin{array}{c} 1 \\ A_{22} \end{array} \right\} D cos\, \omega_2 t \; , \tag{52}
$$

where B and D defined in Eq.51. are the mode shapes, while the terms in curly brackets on the right-hand side of Eq.52., the amplitudes of first (at ω_1) and second (at ω_2) mode (compare Eq.43.).

4.2 The Results

The natural (radial) frequencies, ω_1 and ω_2, were numerically evaluated using a *Matlab*® script (see Appendix C) and then the frequencies , f_1 and f_2 plotted in function of position along the cochlea, x. The distribution of the characteristic frequency, f_c ($\frac{1}{2}\pi\sqrt{\frac{k_1}{m_1}}$), along the CP, was also plotted for comparison with the f_1 and f_2 resonance frequencies. Additionally, the ratio of f_2/f_1 in function of position x was presented.

Next, after taking $A_{11} = A_{12} = 1$, the relative amplitudes A_{21} and A_{22} were calculated and also presented in function of position on the CP, x.

Finally, the amplitudes B and D were obtained for one position on the CP i.e. $x = 0.0185\,m$, so that the displacements ξ_b and ξ_t, for the first and second mode, could be plotted. In both cases the time vectors were set to show two periods of vibration.

The mechanical parameters used for the computations were taken from the Neely&Kim article (converted to SI) as listed in Table 1.

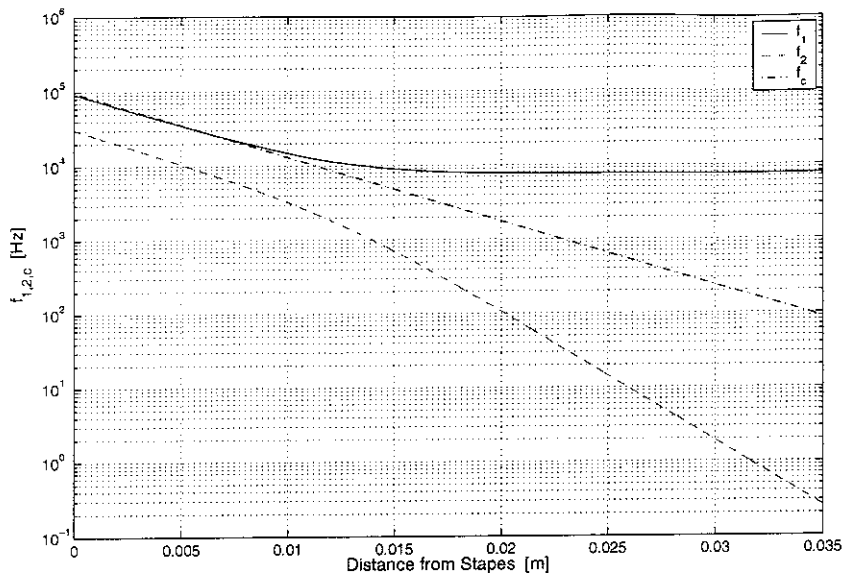

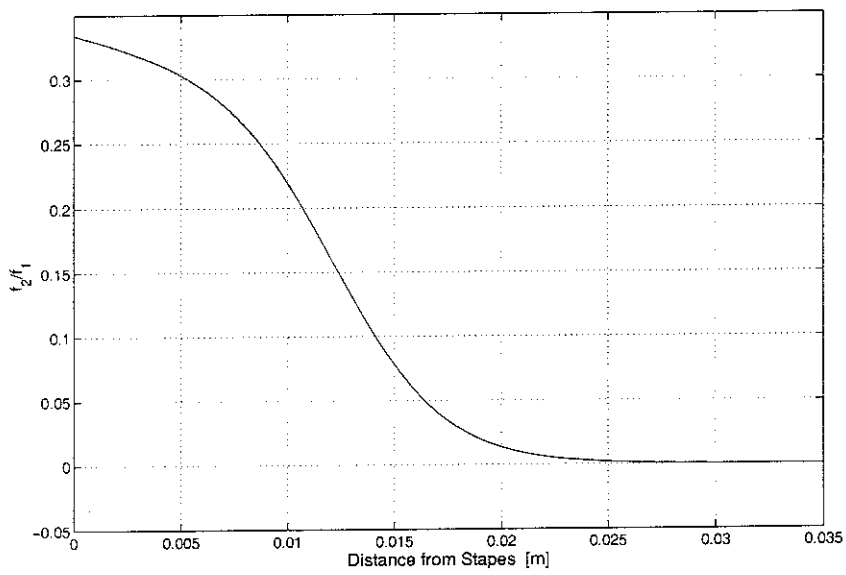

Figure 16: Resonance frequencies of the first and second mode of vibration, f_1 and f_2, respectively, with the characteristic frequency, f_c, (upper panel) of the two-degree-of-freedom system (Neely and Kim model) depicted in Fig.15. and the ratio of f_2/f_1 (lower panel), in function of the position on the cochlear partition, x.

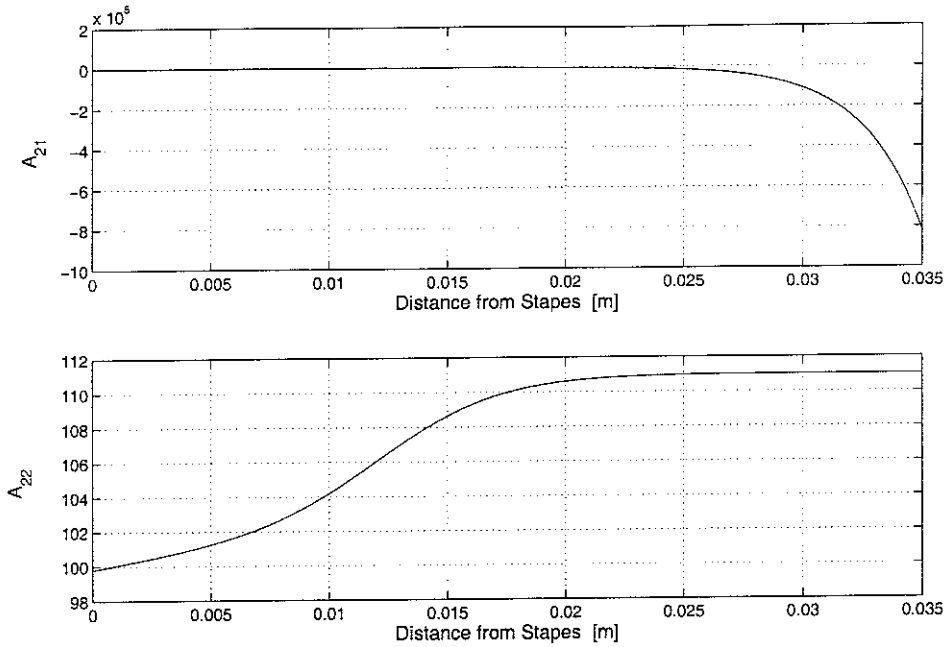

Figure 17: Amplitudes of the TM vibration with respect to the BM vibration for the first mode, A_{21}, and the second mode, A_{22}, in function of position along the cochlea.

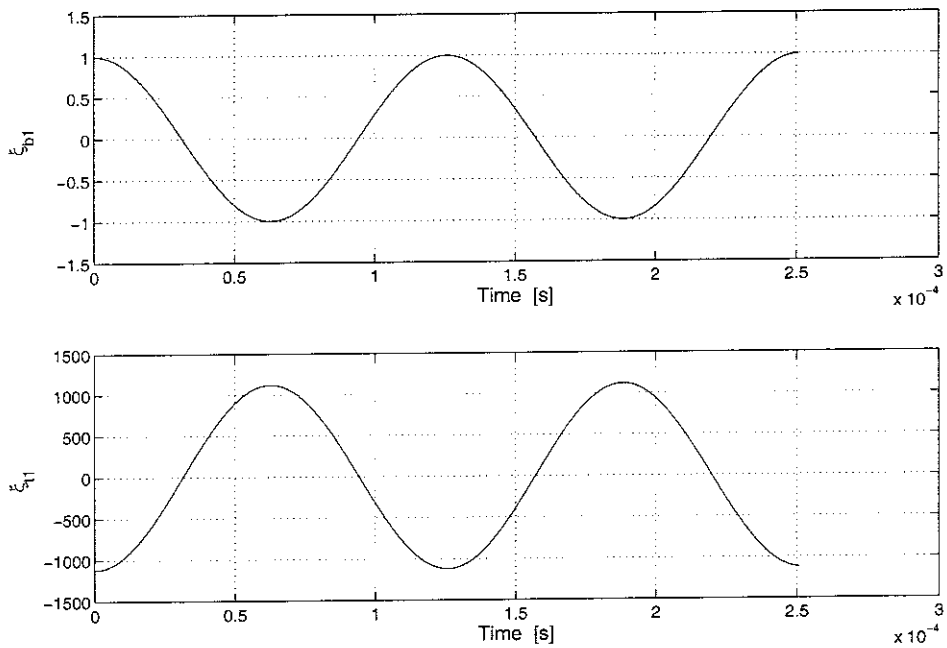

Figure 18: Displacements ξ_b and ξ_t for $x = 0.0185m$ at the first mode of vibration.

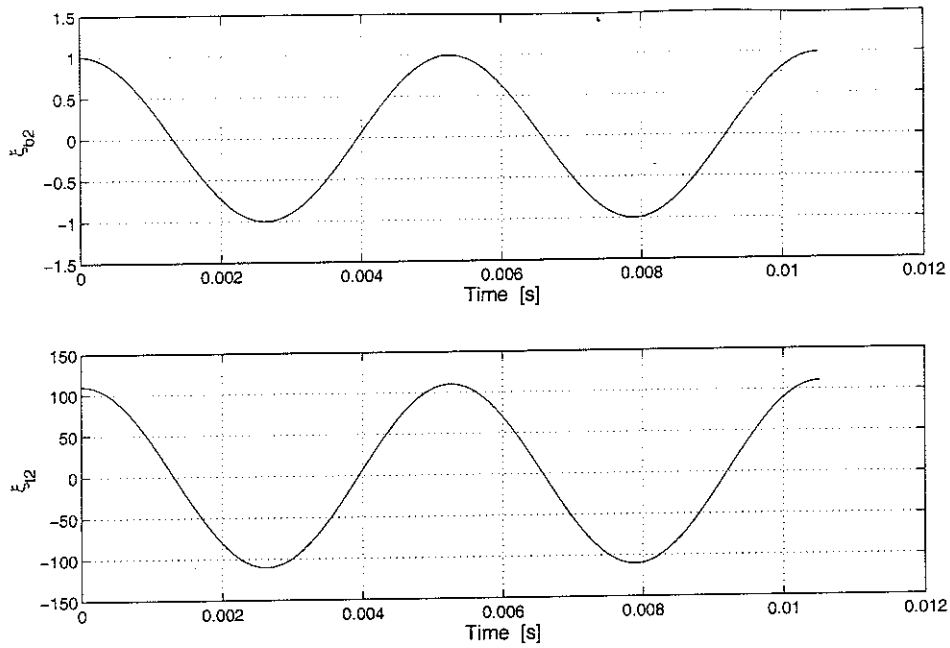

Figure 19: Displacements ξ_b and ξ_t for $x = 0.0185\,m$ at the second mode of vibration.

4.3 Discussion

The resonance of the BM occurs at higher frequencies than the one of the TM according to Fig.4.2. Distribution of the first resonance frequency, f_1 along the cochlea starts at the value of 92.106 kHz (see Fig.4.2., solid line), which corresponds approximately to the estimated value of characteristic frequency, f_c, at $x = 0$, equal to $96.373kHz$ but the difference between f_1 and f_c increases with the position, x. Furthermore, the values of f_1 and f_c for $x = 0$ do not agree with the upper limit of the characteristic frequency derived for the cat cochlea i.e. $\approx 57kHz$ [17]. The value of resonance frequency of the second mode of vibration, f_2, equals to $30.764\,kHz$ for the position $x = 0\,m$, which is about one third lower then the f_1 as mentioned above (check the ratio f_2/f_1 in Fig.16.).

The amplitudes of the TM vibration for the first and second mode, A_{21} and A_{22}, respectively, calculated with respect to the unit BM vibration amplitude reveal that the amplitude of vibrations at the second mode is higher at the first mode for all positions along the cochlea e.g. $A_{21} = 10.526$ $A_{22} = 99.791$ at $x = 0$. The difference in amplitudes is increasing rapidly above the characteristic place, $x = 0.0185\,m$, with relatively small difference of the amplitude at the first mode as depicted in Fig.17.

Figures 18. and 19. show that the BM and TM vibrate in antiphase and in phase at the first and second mode of vibration, respectively. There is also a significant difference between the BM, ξ_b, and the TM, ξ_t, displacement, of 10^3 and 10^2 order for the first and second mode of vibration, respectively.

The results are also in contrast to the measurements of Lukashkin and Russel [19] who found that in addition to the resonance at the characteristic frequency, at which the BM and TM are out of phase, a 'second resonance', at low levels, is observed about half an octave below the main resonance, at which the BM and TM are in phase.

5 Generalisation

It was shown that the EOMs can be derived using the lumped component models in Fig.11. The NK model (left in Fig.11.) has two DOFs with the mass m_1, stiffness k_1, damping c_1 and the mass m_2, stiffness k_2, damping c_2 as the parameters of the first and second DOF, respectively. The masses are coupled by the stiffness k_3 and damping c_3.

The model of Geisler (right in Fig.11.) can be considered, similarly to the NK model, as a two-degree-of-freedom system with the mass of the second DOF set to zero and attached to the rigid bone by the stiffness k_c. The first DOF, corresponding to the BM, is represented by the mass m, stiffness k_b and damping r. These two components are coupled by k_r, which is the passive axial stiffness of the OHC.

Note that the only significant difference in the dynamics of two presented models lies in the assumed action of the active source. Therefore introducing some generalisations, in order to obtain a comprehensive model, the above assumption will be justified.

Denoting k_b, k_c and k_r as k_1, k_2, k_3, respectively, r as c_1 and finally m as m_1, the EOMs and partition impedance Z_p for both models as a function of generalised variables will be derived. Now the mechanical parameters occur in the same form for both models. Furthermore, for complete representation, acting forces with resulting displacements have to be designated.

The pressure P_d in the NK model and the force F_a in the G model are acoustic sources acting upon the BM. Despite different representations, the character of these acoustic sources remains physically the same because of the interaction mechanism between cochlear fluids and the BM. Therefore, for the purpose of uniformity, p_d (Note the lower case) will define the acoustic source causing the BM motion for both models.

For both models the active source is assumed to be located in the OHCs, however, in the G model it exerts upon the first and the second DOF, whereas in the NK model only upon the first DOF (BM). These sources act in a way described in the previous sections and are assumed to be linearly proportional to ξ_c in the NK model and $z + x$ in the G model. In the general case it will be represented in terms of the pressure located in the OHC and denoted as p_a. The gain factor appearing as γ in the NK model and q in the G model will be replaced by gain g in the general approach.

In summary, after introducing new displacements v_1 (1DOF), v_2 (2DOF) and v_3 (relative displacement) the complete set of the new generalised variables will be as follows:

p_d	pressure difference across the BM
p_a	pressure source in the OHC

v_1	displacement of the first DOF
v_2	displacement of the second DOF
v_3	relative displacement between the first and second DOF
k_1	stiffness component of Z_1
c_1	damping component of Z_1
m_1	mass component of Z_1
k_2	stiffness component of Z_2
c_2	damping component of Z_2
m_2	mass component of Z_2
k_3	stiffness component of Z_3
c_3	damping component of Z_3
k_4	stiffness component of Z_4
c_4	damping component of Z_4
g	OHC force-generation gain

In consequence, the new lumped component models (NK-left and G-right) of cochlear micromechanics was proposed as presented in Fig.20.

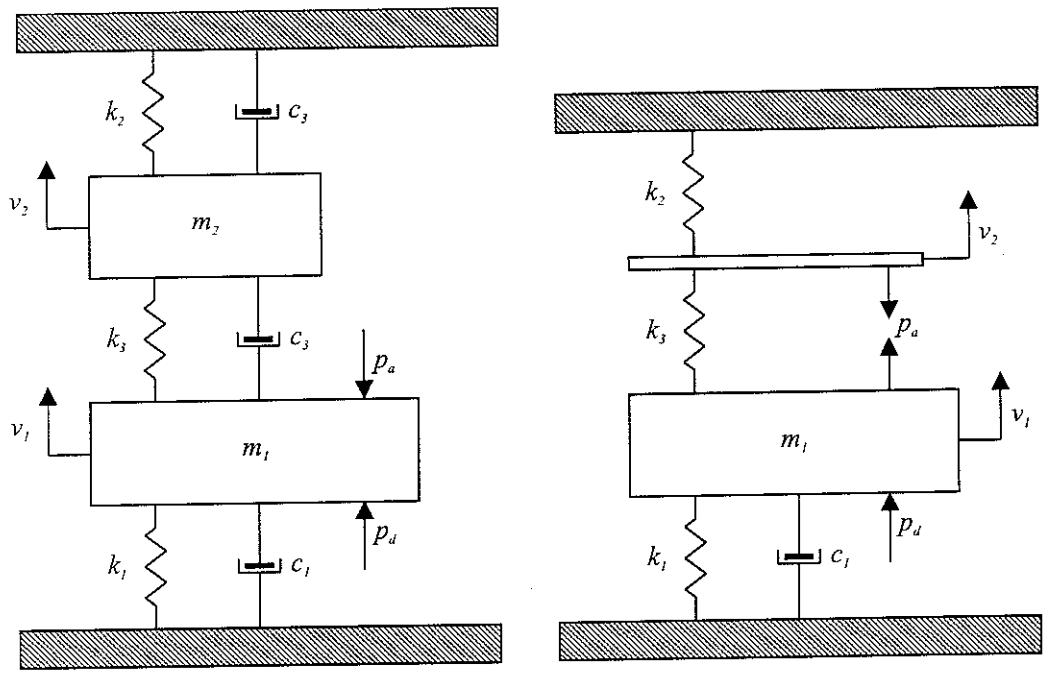

Figure 20: Generalised lumped component models of cochlear micromechanics: NK (left) and G (right).

5.1 The Model of Neely and Kim

5.1.1 The Equations of Motion

In section 4, the new generalised variables were introduced. Now, the generalised EOMs according to the systems shown in Fig.20. will be formulated. First, the relative displacement in the generalised NK (Fig.20., left) model takes form

$$v_3(x) = v_1(x) - v_2(x). \tag{53}$$

The generalised EOM for the first DOF for this lumped model is

$$p_d(x) - p_a(x) = Z_1(x)\dot{v}_1(x) + Z_3(x)\dot{v}_3(x), \tag{54}$$

where
$Z_1 = k_1/j\omega + c_1 + j\omega m_1$,
$Z_3 = k_3/j\omega + c_3$.

The generalised EOM for the second DOF is expressed by

$$0 = Z_2(x)\dot{v}_2(x) - Z_3(x)\dot{v}_3(x), \tag{55}$$

where
$Z_2 = k_2/j\omega + c_2 + j\omega m_2$,
$Z_3 = k_3/j\omega + c_3$.

Finally, the active pressure source $p_a(x)$ is represented by

$$p_a(x) = -gZ_4(x)\dot{v}_3(x), \tag{56}$$

where
$Z_4 = k_4/j\omega + c_4$.

The meaning of the impedances Z_1, Z_2, Z_3 and Z_4 remains the same as in the section 3.1.1.

5.1.2 The Partition Impedance

Once the generalised EOMs has been formulated, the CP impedance Z_p for the generalised variables can be stated. The CP impedance for the generalised NK model (left in Fig.20.) is given by

$$Z_p = Z_1 + \left[\frac{Z_2(Z_3 - gZ_4)}{Z_2 + Z_3}\right]. \tag{57}$$

5.2 The Model of Geisler

5.2.1 The Equations of Motion

The right panel of Fig.20. characterises the lumped component model of cochlear micromechanics based on the G model with a new variables. The relative displacement v_3 appears in the same form as in Eq.53. and just to recall

$$v_3(x) = v_1(x) - v_2(x). \tag{58}$$

For the first DOF of this structure the generalised EOM is formulated as

$$p_d(x) + p_a(x) = Z_1(x)\dot{v}_1(x) + Z_3(x)\dot{v}_3(x), \tag{59}$$

where
$Z_1 = k_1/j\omega + c_1 + j\omega m_1$,
$Z_3 = k_3/j\omega$.

The impedances Z_1 and Z_3 are the impedance of the OC and the impedance of the ciliary/TM complex, respectively.

The generalised EOM for the first DOF is

$$0 = -Z_2(x)\dot{v}_2(x) + Z_3(x)\dot{v}_3(x) + p_a(x), \tag{60}$$

where
$Z_2 = k_2/j\omega$,

and represents the coupling between the OC and the RL.

Finally, the formulation of the active source in the Eq.58. expresses p_a as

$$p_a(x) = gZ_4(x)\dot{v}_3(x), \tag{61}$$

where
$Z_4 = k_1/j\omega$.

The Z_4 impedance in the formula above signifies the impedance in the feedback loop acting as a resistive force in response to the BM displacement and controlled by the OHC contractions.

Note that p_a is a positive quantity in this case. However, if the negative sign accounts for the pressure decrease in the OHC (check Eq.10. with description), the positive value of p_a can, on contrary, account for the pressure increase within the OHC. Consequently, this increase should reflect in the elongation of the hair cell body, hence denote its activity.

5.2.2 The Partition Impedance

Like for the NK generalised model, the partition impedance Z_p for the new system in the right panel of Fig.20. is introduced and takes form

$$Z_p = Z_1 + \left[\frac{Z_2 Z_3}{Z_2 + Z_3 + gZ_4}\right]. \tag{62}$$

6 Calculated Results for Basilar Membrane Motion

6.1 The Parameters

6.1.1 Introduction

For examination of the generalised theoretical model described in Section 5, the mobility of the cochlear partition, Y_p ($Y_p = 1/Z_p$), will be plotted. Thus, the mechanical parameters of the Z_p have to be stated.

The impedance parameters used to verify presented models were extracted from the Liberman tonotopic function for cat cochleae [17]. This function was derived from the experiment using labelling of auditory nerve fibres of known characteristic frequency. Base of the cochleae was tuned to $57\,kHz$ and the apex to $90\,Hz$. The partition natural resonance frequency ω_0 for location x can be found from

$$\omega_0 = \omega_{st} e^{-\alpha x/2}. \tag{63}$$

The quantity ω_{st} represents the natural frequency of the partition at the stapes [rad/s], and α is a place-frequency length parameter $[m^{-1}]$ [3].

For the position of x equal to the length of the cochlea, namely $x = L$ (L-length of the cochlea), ω_0 would represent the natural frequency of the CP at the apex ω_{ap}. Hence, Eq.63. can be rearranged and solved for α

$$\alpha_{|_{x=L}} = \frac{-2\ln(\omega_{ap}/\omega_{st})}{L}. \tag{64}$$

Having evaluated α, after rearrangement of Eq.63. the stiffness k and damping c can be estimated. While

$$\omega_0 = \sqrt{\frac{k}{m}}, \tag{65}$$

hence

$$k(x) = m\omega_{st}^2 e^{-\alpha x}, \tag{66}$$

and, while $c = k/\omega_0$,

$$c(x) = m\omega_{st} e^{-\alpha x/2}. \tag{67}$$

6.1.2 The Data

The mechanical parameters were implemented into the *Matlab* script (see Appendix C) solving the partition mobility, Y_p, given in Eqs.57. and 62., for the generalised variables. Thus, the comparison was conducted only for the generalised models with reduced number of factors.

The generalised NK model was examined using the parameters listed in Table 1. of the Neely&Kim article [21]. As concerns to the generalised model of G, mechanical parameters were evaluated by the present authors on the basis of theory [3] and the information given by Geisler in his article.

It was said, in the previous section, that the impedance parameters were extracted from the tonotopic function for cat cochleae, with tuning to 57 kHz and 90 Hz at the base and the apex of the cochleae, respectively. Hence, $\omega_{st} = 2\pi \cdot 57000\, rad/s$ and $\omega_{ap} = 2\pi \cdot 90\, rad/s$. Furthermore, the length parameter α was estimated using ω_{st} and ω_{ap}, according to Eq.64., with $L = 0.035\, m$ (Note that, although the mechanical parameters were extracted for the cat's cochleae, the value of L has been extrapolated to $0.035\, m$ corresponding to the length of the human cochlea. The explicit relation between the position on the BM for the cat and the human cochleae is given in Appendix A). This amounts the value of α, for the G generalised model, to $368\, m^{-1}$. Next, knowing α, ω_0 was fixed to $2\pi \cdot 57000e^{-184x}\, rad/s$ (see Eq.32.). The mass of the BM, m_1, (the generalised variables) is equal to $0.5\, kg/m^2$ (m-the mass in the G model). In the work of G, the stiffnesses k_r, k_c and the damping coefficient r, were set to
$k_r = 1.17k_b$,
$k_c = 0.59k_b$,
$r = 0.6k_b/\omega_0$.

In consequence, for the generalised variables
$k_3 = 1.17k_1$,
$k_2 = 0.59k_1$,
$c_1 = 0.6k_1/\omega_0$.

As for the active component of the Z_p, the stiffness k_4 (in terms of the generalised variables) takes form of the stiffness k_1 according to Eq.21. and the representation of Z_4 in Eq.61. Furthermore, the active impedance Z_4 was multiplied by two factors representing the all-pass circuit and time delay according to F_{fb} in Eq.20.

The OHC force-generation gain g was fixed to values of 1 ('fully' active) and 0 (passive) for both models. Furthermore, the time delay T was set to $2\pi/\omega_0$ and $0.4\pi/\omega_0$ for comparison, thus n equals 2 and 0.4, respectively (check Eq.25.).

Recapitulating, all quantities of mechanical parameters are presented in the SI unit system and are placed in Table 1.

PARAMETER	NEELY&KIM	GEISLER
$k_1(x)\ [kg \cdot m^{-2} \cdot s^{-2}]$	$1.1 \cdot 10^{10} e^{-400x}$	$6.4 \cdot 10^{10} e^{-368x}$
$k_2(x)\ [kg \cdot m^{-2} \cdot s^{-2}]$	$7 \cdot 10^{7} e^{-440x}$	$3.8 \cdot 10^{10} e^{-368x}$
$k_3(x)\ [kg \cdot m^{-2} \cdot s^{-2}]$	$10^{8} e^{-400x}$	$7.5 \cdot 10^{10} e^{-368x}$
$k_4(x)\ [kg \cdot m^{-2} \cdot s^{-2}]$	$6.15 \cdot 10^{9} e^{-400x}$	$6.4 \cdot 10^{10} e^{-368x}$
$c_1(x)\ [kg \cdot m^{-2} \cdot s^{-1}]$	$1.1 \cdot 10^{10} e^{-200x}$	$1.8 \cdot 10^{5} e^{-184x}$
$c_2(x)\ [kg \cdot m^{-2} \cdot s^{-1}]$	$1.1 \cdot 10^{10} e^{-220x}$	0
$c_3(x)\ [kg \cdot m^{-2} \cdot s^{-1}]$	$1.1 \cdot 10^{10} e^{-80x}$	0
$c_4(x)\ [kg \cdot m^{-2} \cdot s^{-1}]$	$1.1 \cdot 10^{10} e^{-200x}$	0
$m_1(x)\ [kg \cdot m^{-2}]$	0.03	0.5
$m_2(x)\ [kg \cdot m^{-2}]$	$0.005 e^{x}$	0

Table 1: Mechanical parameters for the NK and the G generalised models.

6.1.3 The Results

In the following section the magnitude/phase ($|Y_p|/\angle Y_p$) and real/imaginary part ($Re\ Y_p/Im\ Y_p$) plots of the CP mobility, Y_p, as a function of frequency and distance from stapes, for the NK and G generalised models, are presented. Additionally, for the G generalised model, adequate plots with the time delay n set to 0.4 (according to the G model) are presented. In all cases the OHC generation gain g was set to 1 and 0 as it was mentioned in the previous section. Furthermore, in the 'place-function' plots, the frequency, f, was set to $1\,kHz$. In the 'frequency-function' plots, the position on the CP, x, was set to the value corresponding to the place of maximum of absolute value of the CP mobility function, $|Y_p(x)|_{max}$ (place-function), calculated for $1\,kHz$ stimulus frequency in every case.

The CP was divided to 1024 components for both, the NK and G generalised models. According to the G model's simulation, where optimum results were achieved for 1400 sections of the CP (integer multiples of 700 sections used [11]), the computation for the generalised G model was run for 1400 and 1024 sections revealing no discrepancies in the results. In the NK case the number of 500 sections was considered as a minimal value for the model to converge [16]. Therefore, the value of 1024 satisfies both, NK and G convergence conditions and being the power of two, it determines the best efficiency for the computation. Moreover, in the plots of mobility vs frequency, the latter was limited to $25\,kHz$ to encompass the human's audible frequencies range.

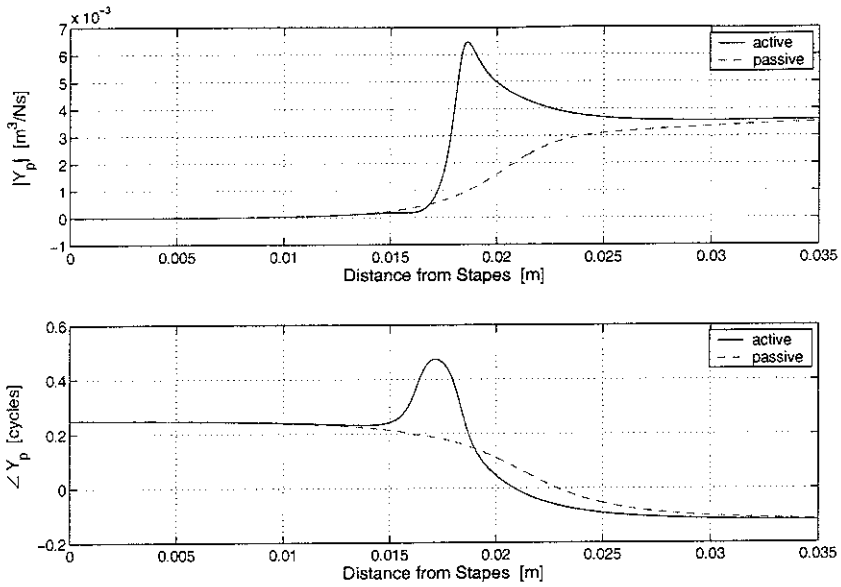

Figure 21: The magnitude and phase of the CP mobility Y_p as a function of position on the CP, for the Neely&Kim generalised model with $f = 1\,kHz$ and $g = 1$ (active, solid) and 0 (passive, dashed).

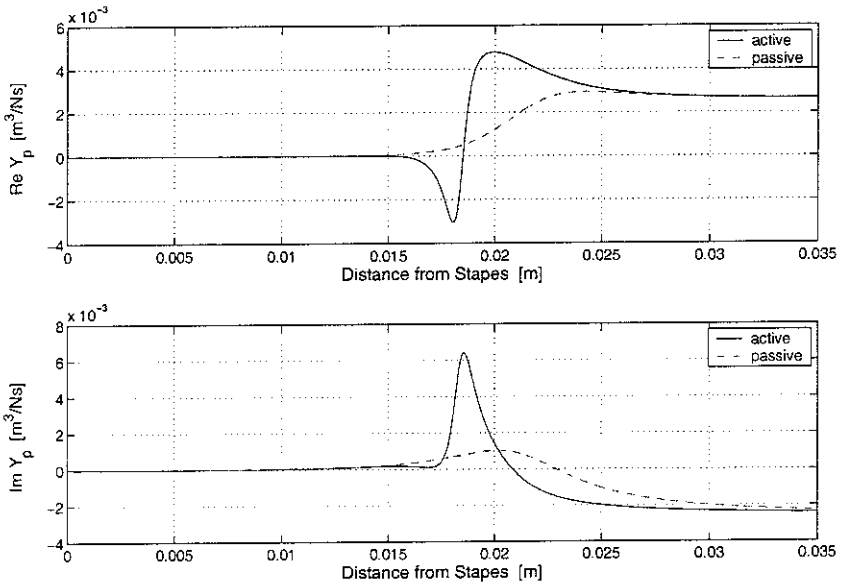

Figure 22: The real and imaginary part of the CP mobility Y_p as a function of position on the CP, for the Neely&Kim generalised model with $f = 1\,kHz$ and $g = 1$ (active, solid) and 0 (passive, dashed).

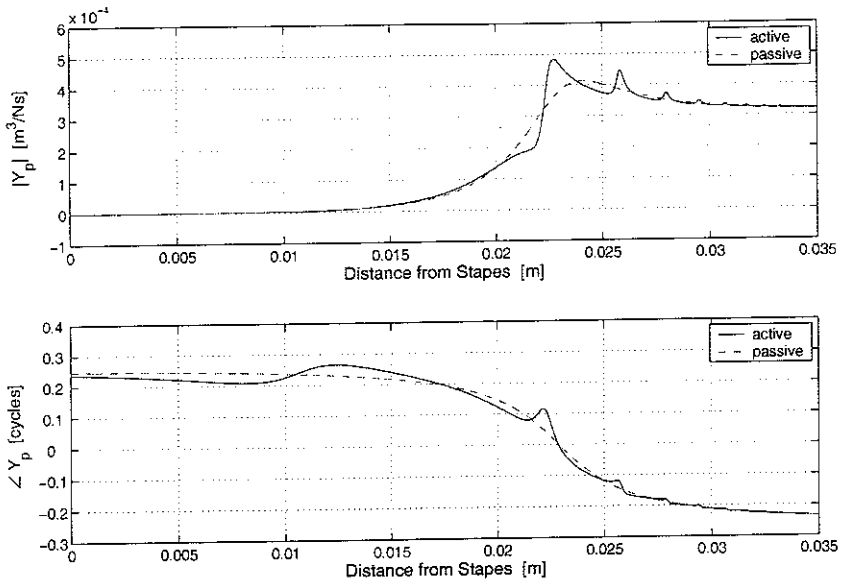

Figure 23: The magnitude and phase of the CP mobility Y_p as a function of position on the CP, for the Geisler generalised model with $f = 1\,kHz$ and $g = 1$ (active, solid) and 0 (passive, dashed).

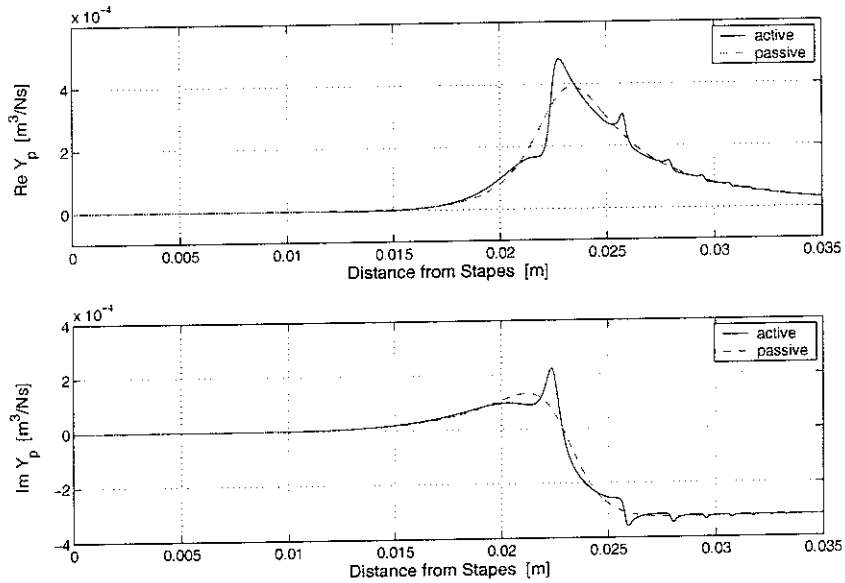

Figure 24: The real and imaginary part of the CP mobility Y_p as a function of position on the CP, for the Geisler generalised model with $f = 1\,kHz$ and $g = 1$ (active, solid) and 0 (passive, dashed).

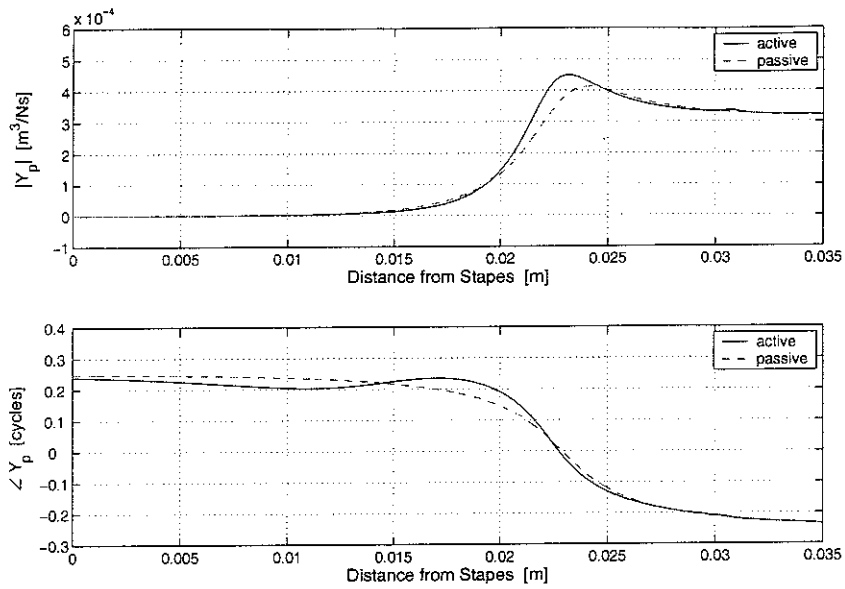

Figure 25: The magnitude and phase of the CP mobility Y_p as a function of position on the CP, for the Geisler generalised model with $f = 1\,kHz$, $g = 1$ and time delay $n = 0.4$ (active, solid) and 0 (passive, dashed).

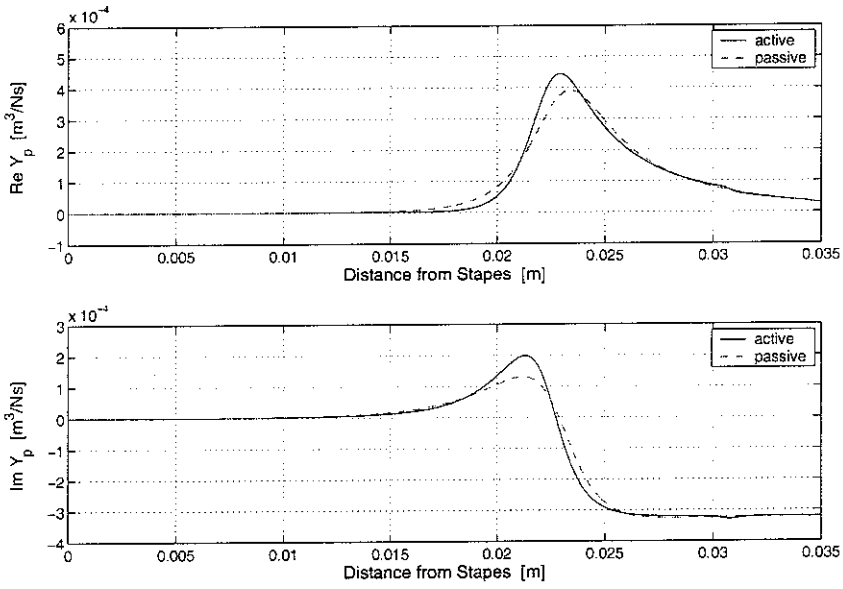

Figure 26: The real and imaginary part of the CP mobility Y_p as a function of position on the CP, for the Geisler generalised model with $f = 1\,kHz$, $g = 1$ and time delay $n = 0.4$ (active, solid) and 0 (passive, dashed).

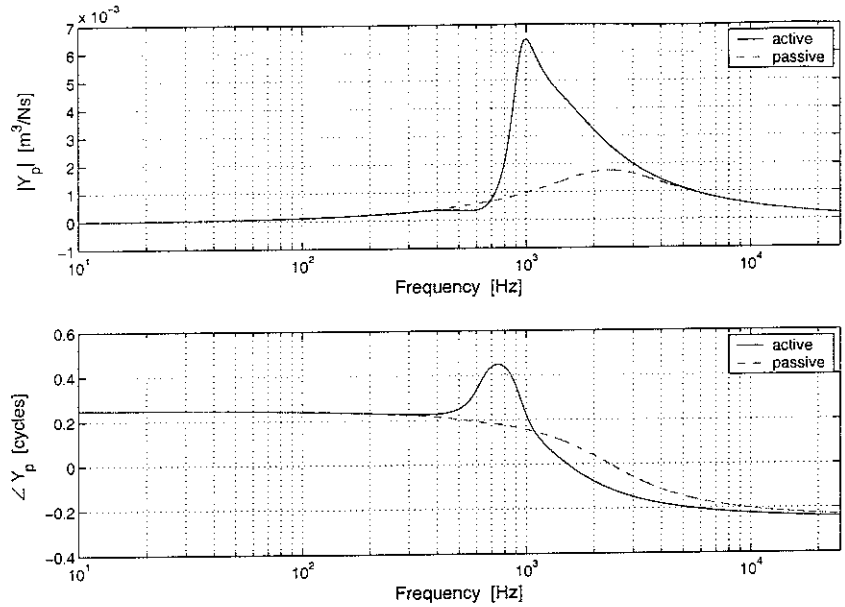

Figure 27: The magnitude and phase of the CP mobility Y_p as a function of frequency, for the Neely&Kim generalised model with $x = 0.0186\,m$ and $g = 1$ (active, solid) and 0 (passive, dashed).

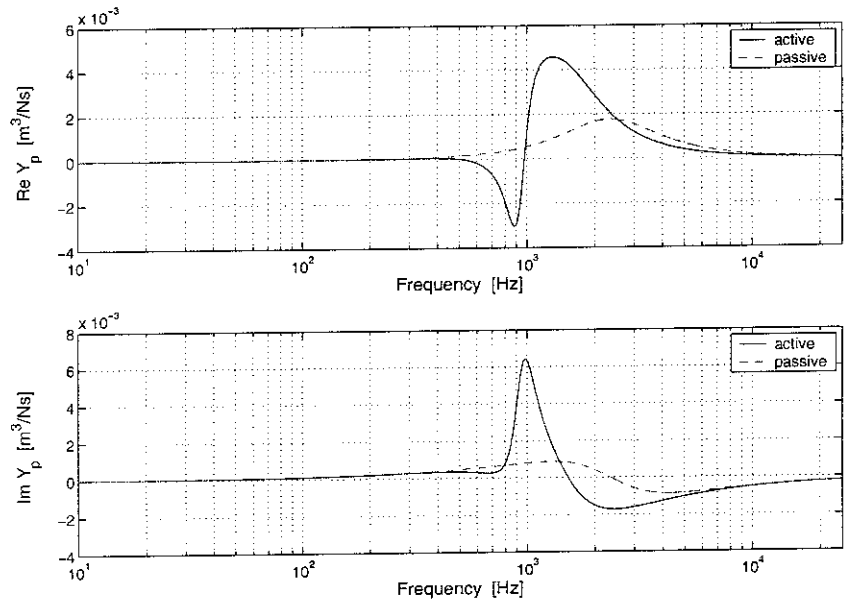

Figure 28: The real and imaginary part of the CP mobility Y_p as a function of frequency, for the Neely&Kim generalised model with $x = 0.0186\,m$ and $g = 1$ (active, solid) and 0 (passive, dashed).

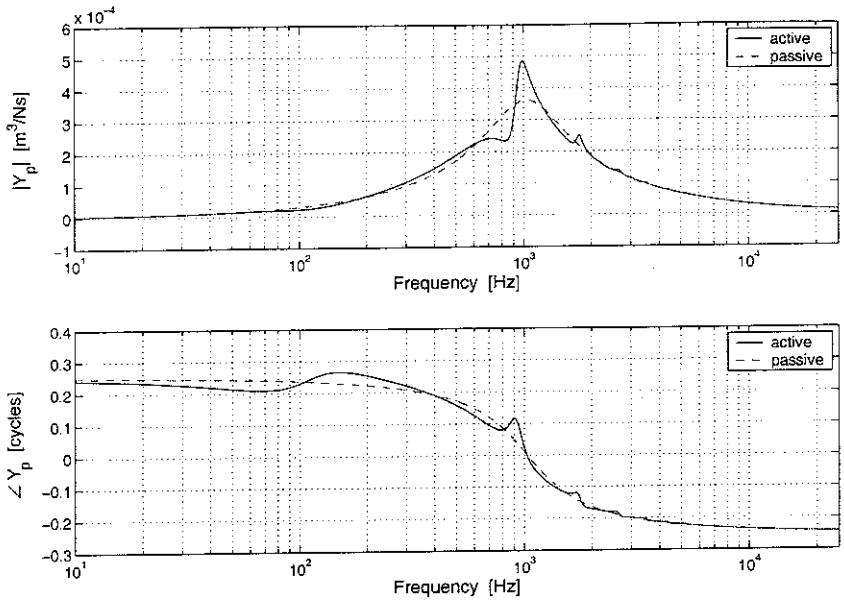

Figure 29: The magnitude and phase of the CP mobility Y_p as a function of frequency, for the Geisler generalised model with $x = 0.0227m$ and $g = 1$ (active, solid) and 0 (passive, dashed).

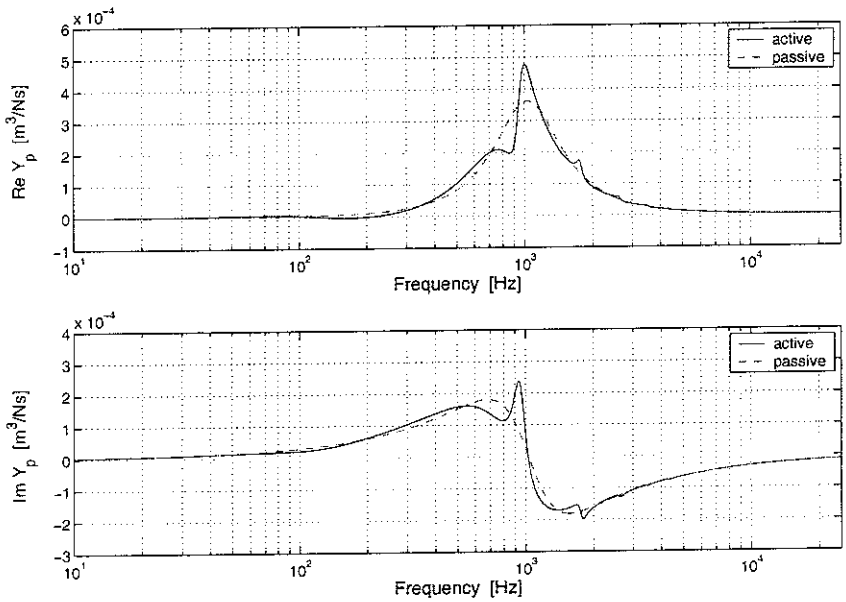

Figure 30: The real and imaginary part of the CP mobility Y_p as a function of frequency, for the Geisler generalised model with $x = 0.0227m$ and $g = 1$ (active, solid) and 0 (passive, dashed).

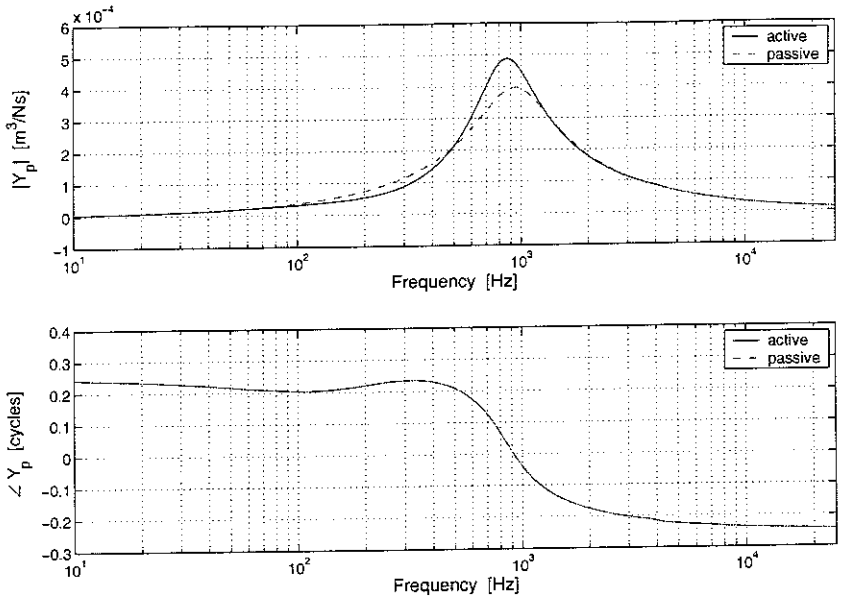

Figure 31: The magnitude and phase of the CP mobility Y_p as a function of frequency, for the Geisler generalised model with $x = 0.0232\,m$, $g = 1$ and time delay $n = 0.4$ (active, solid) and 0 (passive, dashed).

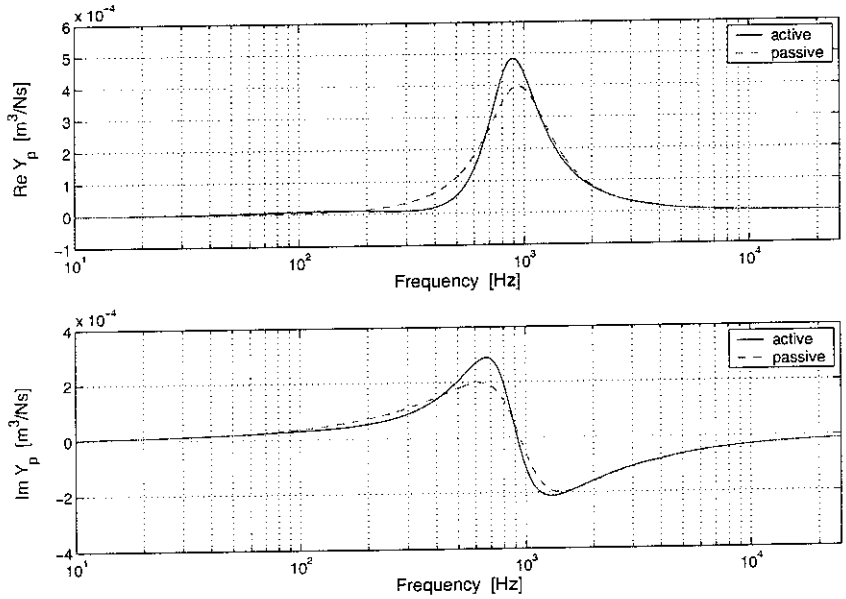

Figure 32: The real and imaginary part of the CP mobility Y_p as a function of frequency, for the Geisler generalised model with $x = 0.0232\,m$, $g = 1$ and time delay $n = 0.4$.

6.2 Discussion

The behaviour of the magnitude/phase and real/imaginary parts of the CP mobility, Y_p, reveals a significant difference between the active and passive cases only for the NK generalised model. The active process simulated in the model generates a big boost in the magnitude of the mobility forming a sharply tuned peak. The same boost can be also noticed in the plot of the real component of the partition mobility, which corresponds to a drop in the resistive component of the partition impedance, Z_p. This, in consistency with the assumption of Neely&Kim, accounts for pumping of energy, expressed as a negative resistance in the partition impedance, by the OHCs to the system. Thus, the reduction of variables (generalisation) does not change the character of the mobility of the CP.

The curves calculated for the G generalised model resemble only a passive characteristic and does not differ qualitatively from the passive case of the NK generalised model i.e. there is a difference of about one order (10^{-3} and 10^{-4} for the NK and G generalised model, respectively, see Sec.6.1.3) in value of any corresponding quantity excluding phase, which range in the same order of values but with a steeper slope in the G generalised model. This is consistent with the mathematical formulation for the CP impedance, Z_p, where setting the gain, g, to zero will eradicate the active term from Eqs.57. and 62., hence expressing the NK generalised model's impedance as equivalent with the one calculated for the G generalised model. The discrepancies in the passive plots of both models are therefore due to the divergence in the mechanical parameters implemented in the calculations (Note that Neely and Kim and Geisler refer to the same source from which the parameters have been evaluated [21, 11], namely from the physiological data of Liberman [17]). Furthermore, setting the delay factor, n, to 0.4, an optimum proposed by Geisler (compare [11]), provides even curves in comparison with the curves obtained for the delay factor of 2. In summary, the reduction of variables (generalisation) does change the mobility of the CP in case of the G generalised model through the loss of active characteristic.

7 Macromechanics

7.1 Introduction

In previous sections the micromechanical properties of the NK and G cochlear models were examined. The description of the CP by the mechanical impedance was a straightforward implication of the assumption, that there was no longitudinal, mechanical coupling between the single components [5]. However, for the computation of the CP response the aforementioned interactions between the CP and the cochlear fluids, referred to cochlear macromechanics (see section 2.3.2), have to be defined.

To facilitate the analysis, the geometry of the cochlea has been simplified. Figure 33. depicts the geometry of the cochlea with indication of the coordinate system and the cochlea dimensions. The cochlea is divided into two channels (Reissner's membrane ignored due to its negligible impedance) of equal cross-sections, which are connected by the helicotrema.

The cochlear fluids (properties compared to water), are assumed to be incompressible and inviscid, which implies the fluid velocity to be equal at any location of the cochlea as well as at the oval and round windows but with opposite phase. Furthermore, the linearity condition holds also in this case.

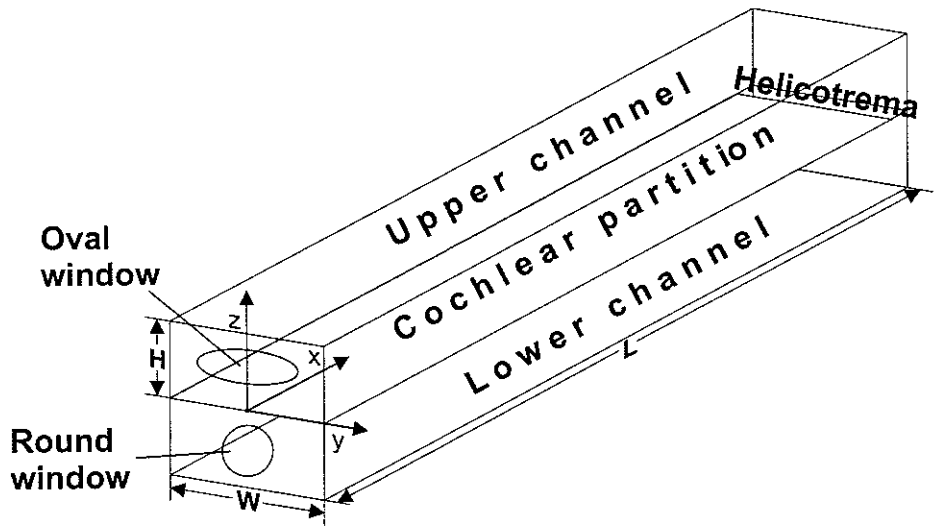

Figure 33: A schematical drawing of the simplified geometry of the cochlea with indication of its main parts, dimensions (i.e. L-length, W-width, H-height) and coordinate system.

The following assumptions and derivations base on the ones commonly used in the literature, but gathered and profoundly described in [18].

The response of the CP is defined by means of the fluid pressure and fluid velocity vectors [5, 18]. According to the coordinate system depicted in Fig.33. and neglecting the lateral changes of the pressure and velocity [5, 18] (note that the ξ_p and the ξ_b were averaged over the width of the CP and the BM, respectively), the macromechanical variables at an instant of time t, take form

$p_f(x,z,t)$ fluid pressure
$u_f(x,z,t)$ fluid x-velocity vector
$v_f(x,z,t)$ fluid z-velocity vector

and the velocities at the fluid boundaries

$u_{st}(z,t)$ stapes x-velocity vector
$u_{rw}(z,t)$ round window x-velocity vector
$v_p(x,t)$ the CP z-velocity vector

The symmetry of the model and incompressibility of the cochlear fluids imply that in case, when a identical force loading is applied to both windows (see Fig.33.), a fast wave is propagating through the channels inducing no transverse, z, displacement of the CP. When the loading forces applied are opposite, the pressure difference between the upper and lower cochlear channels generates the CP deflection travelling along the cochlea, a travelling wave described in section 2.3.2. Both cases are described often by imaging the cochlear fluids driven by two identical pistons at the stapes and round window, applying equal and in/opposite phase (the 'push-push'/'push-pull' condition) forces [18].

Mathematical representation of the above conditions postulates the combination of the semi-sum, p_s (push-push), and semi-difference, p_d (push-pull), pressures for the complete description of the wave propagation in the cochlea. However, according to the assumption of the incompressibility of the cochlear fluids only the semi-difference pressure, p_d, contributes to the generation of the travelling wave. Therefore the semi-sum pressure, p_s, or push-push case will not be considered here (for details check [18]).

The pressure difference generating the travelling wave, is defined as

$$p_d(x,z,t) = \frac{1}{2}p_f(x,z,t) - \frac{1}{2}p_f(x,-z,t), \tag{68}$$

for $0 < z < H$, and is a complex, sinusoidally varying variable taking form of $e^{j\omega t}$ [5].

Also fluid's velocity is unaffected by the 'push-push' case due to the incompressibility of the cochlear fluids. Together with the pressure it demonstrates given antisymmetry

$$u_{rw}(-z,t) = -u_{st}(z,t), \tag{69}$$

$$u_f(x,-z,t) = -u_f(x,z,t), \tag{70}$$

$$v_f(x,-z,t) = v_f(x,z,t), \tag{71}$$

$$p_f(x,z,t) = -p_f(x,-z,t). \tag{72}$$

Equations 69-71. are presented schematically in Fig.34. (after [18]). Moreover, it occurs from Eqs.68. and 72., that the pressure difference, p_d, amounts to

$$p_d(x,z,t) = p_f(x,z,t). \tag{73}$$

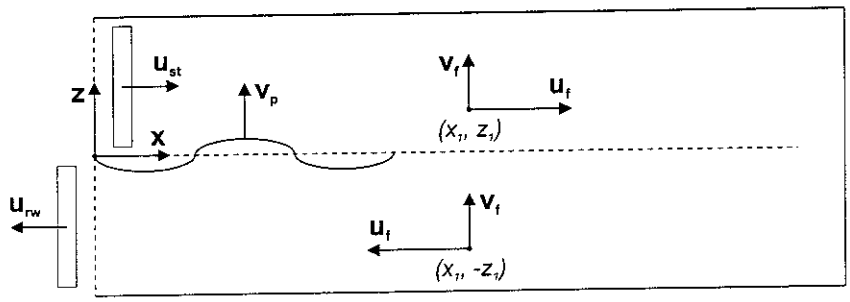

Figure 34: A graphical representation of the symmetry conditions in Eqs.69-71. The velocity arrows indicate the direction of motion (positive sign according to the coordinate system). The quantities u_1, v_1, are the velocity scalars and x_1, z_1, the positive displacements.

7.2 The Wave Equation

For the derivation of the wave equation of the cochlear travelling wave, conducted after [5, 18], a convenient long-wave approximation is used. The long-wave assumption states that the wavelength of the propagating travelling wave is substantially larger then the height (perimeter) of the cochlear channels. As a consequence the transverse coordinate, z, is eliminated from the wave equation obtaining a one-dimensional case, representing the pressure distribution in the x direction (longitudinal position on the CP).

Though the long-wave approximation simplifies the macromechanical representation, it is not devoided of drawbacks. In the region of the maximum displacement of the CP, the long-wave assumption is not as evident as for the rest

of the cochlea. Therefore, in general description, the cochlear travelling wave is often featured as a combination of the long-wave and short-wave cases (check the Appendix B) [3].

Nevertheless, the highest frequency used in the present model amounts to 25 kHz, thus taking the value of the speed of sound in water $c \approx 1500\ m/s$, the wavelength, λ, equals $\approx 60\ mm$, which is twice the length of the cochlea ($L = 35\ mm$ in the present model) and sixty times the height of the cochlea ($H = 1\ mm$ in the present model).

The incompressibility condition (fluid's density ρ is constant) formulated by the relation

$$div\ \vec{v} = 0, \tag{74}$$

in terms of the u and v fluid velocity component vectors takes form

$$\frac{\partial u_f(x,z,t)}{\partial x} + \frac{\partial v_f(x,z,t)}{\partial z} = 0 \tag{75}$$

Furthermore, the conservation of momentum (nonlinear terms neglected due to the small displacements and velocities of the cochlear fluid) applies to the, p_d, u_f and v_f as follows

$$\frac{\partial p_d(x,z,t)}{\partial x} = -\rho \frac{\partial u_f(x,z,t)}{\partial t} \tag{76}$$

in the x direction, and

$$\frac{\partial p_d(x,z,t)}{\partial z} = -\rho \frac{\partial v_f(x,z,t)}{\partial t} \tag{77}$$

in the z direction.

The boundary conditions at the stapes, where the x-velocity is assumed to be independent of z, and the helicotrema ($\forall z, t$), are formulated

$$u_f(0,z,t) = u_{st}(t), \tag{78}$$

$$u_f(L,z,t) = 0. \tag{79}$$

The boundaries at $z = 0$ (CP) and $z = H$ (ceiling of the upper cochlear channel) ($\forall x, t$), are stated as, respectively

$$v_f(x,0,t) = v_p(x,t), \tag{80}$$

$$v_f(x,H,t) = 0. \tag{81}$$

According to the Eqs.80-81. and provided $v_f(x,z,t) << u_f(x,z,t)$ (check Eq.77.), the linear variation of the fluid across the cochlea in he long-wave approximation amounts to

$$v_f(x,z,t) = \left(1 - \frac{y}{H}\right) v_p(x,t). \tag{82}$$

Differentiation of the Eq.82. with respect to z and substitution into Eq.75. gives

$$\frac{\partial u_f(x,z,t)}{\partial x} = \frac{v_p(x,t)}{H}. \tag{83}$$

It appears from the Eq.83. that, since its right side is independent of z, the left side must be also independent of z. Furthermore, evaluation of the above equation at the stapes and the assumption of the u_{st} independence of z, leads to the conclusion of $u(x,z,t)$ being independent of z too. Consequently, as, after Eq.76., the pressure becomes 'z-independent', it remains (together with the x-velocity) uniform across the channel and the z-independent variable may be eradicated from the equations [18].

Differentiation of the Eq.76. with respect to x gives

$$\frac{\partial^2 p_d(x,t)}{\partial x^2} = -\rho \frac{\partial u_f(x,z,t)}{\partial x \partial t}, \tag{84}$$

which combined with Eq.83. previously differentiated with respect to t, leads to

$$\frac{\partial^2 p_d(x,t)}{\partial x^2} = -\frac{\rho}{H} \frac{\partial v_p(x,t)}{\partial t}, \tag{85}$$

or, having said that p_d is a complex exponential of the form of $e^{j\omega t}$, equivalently in the frequency domain

$$\frac{\partial^2 p_d(x,\omega)}{\partial x^2} = -\frac{j\omega\rho}{H} v_p(x,\omega). \tag{86}$$

As it was mentioned before, in the macromechanical representation, the travelling wave is determined by the CP impedance, which is related to the CP velocity, v_p, by

$$Z_p(x,\omega) = -2\frac{p_d(x,\omega)}{v_p(x,\omega)}, \tag{87}$$

where the '-2' factor indicates that only the upper, stapes-driven, cochlear channel was taken into account and following from the assumption of the semi-difference pressure, p_d, being antisymmetric with regard to the CP [5].

Rearranging the Eq.87. for the v_p and substituting to the Eq.86. gives

$$\frac{\partial^2 p_d(x,\omega)}{\partial x^2} - \frac{2j\omega\rho}{H Z_p(x,\omega)} p_d(x,\omega) = 0. \tag{88}$$

By redefining the last equation to the form of the one-dimensional Helmholtz equation (Note that the Eq.88. is distributed and frequency dependent) it appears in the form

$$\frac{\partial^2 p_d(x,\omega)}{\partial x^2} + k_{tw}^2(x,\omega)p_d(x,\omega) = 0, \tag{89}$$

where the wave number of the cochlear travelling wave, $k_{tw}(x,\omega)$, is expressed as

$$k_{tw}(x,\omega) = \frac{\omega}{c_{tw}^2(x,\omega)}, \tag{90}$$

and the wave speed c_{tw}

$$c_{tw}^2(x,\omega) = \frac{j\omega H Z_p(x,\omega)}{2\rho}. \tag{91}$$

Finally, the boundary condition, referring to the Eq.88., at $x = 0$ and for known stapes velocity, u_{st}, is formulated as

$$\frac{dp_d(0)}{dx} = -2j\omega\rho u_{st}, \tag{92}$$

while at $x = L$, provided the input frequencies are high enough i.e. the travelling wave extinguishes basally with respect to the helicotrema [3], is given by

$$p_d(L) = 0. \tag{93}$$

7.3 The Finite Difference Approximation

In Section 3 the micromechanics of the NK and G models has been examined. The CP was discretised into a number of independent two-degree-of-freedom systems with their mechanical properties changing with the position x. Having introduced the wave equation of the cochlear travelling wave, consequently the CP properties will be examined again in such way, that the aforementioned independent components will be presented as immersed in the fluid and therefore coupled through it (the Z_p term in the Eq.88.) to form a continuous system (check Fig.35.). However, to solve the problem numerically, the wave equation will be replaced by its *Finite Difference Approximation* [16].

After the implementation of the finite difference approximation the Eq.88., for $2 < i < N - 1$, takes form

$$\frac{p_d(i) - 2p_d(i) + p_d(i-1)}{\Delta} - \frac{2j\omega\rho}{HZ_p(i)}p_d(i) = 0, \tag{94}$$

where N is the number of points and Δ is the component length expressed as

$$\Delta = \frac{L}{N-1}. \tag{95}$$

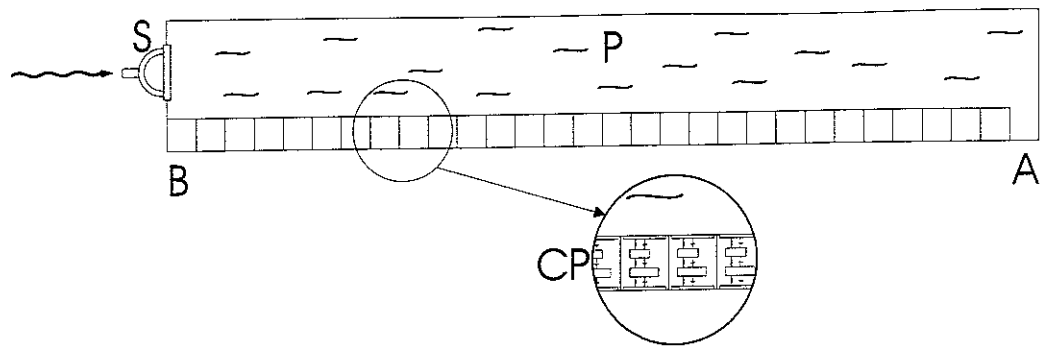

Figure 35: A schematical drawing of the cochlea upper channel (following the p_d antisymmetry assumption) where the CP is represented by a number of independent two-degree-of-freedom systems coupled via the cochlear fluid (B-base, A-apex, P-perilymph, S-stapes).

Respectively, the boundary conditions are formulated by

$$\frac{p_d(2) - p_d(1)}{\Delta} = -2j\omega\rho u_{st}, \tag{96}$$

at the stapes, while at the helicotrema

$$p_d(N) = 0. \tag{97}$$

Taking the $Y_p = 1/Z_p$, the Eq.94., 96-97. can be conveyed to a matrix representation [16] and formulated as

$$(C - M)p_d = q, \tag{98}$$

where

$$C = \frac{1}{\Delta^2}\begin{bmatrix} -\Delta & \Delta & & & \\ 1 & -2 & 1 & & 0 \\ & \ddots & \ddots & \ddots & \\ 0 & & 1 & -2 & 1 \\ & & & 0 & \Delta^2 \end{bmatrix},$$

$$M = \frac{2j\omega\rho}{H}\begin{bmatrix} 0 & & & \\ & Y_p(1) & & 0 \\ & & \ddots & \\ & 0 & & Y_p(N-1) \\ & & & & 0 \end{bmatrix},$$

$$p_d = \left\{ \begin{array}{c} p_d(1) \\ \vdots \\ p_d(i) \\ \vdots \\ p_d(N) \end{array} \right\}, \quad q = \left\{ \begin{array}{c} -2j\omega\rho u_{st} \\ 0 \\ \vdots \\ \vdots \\ 0 \end{array} \right\}.$$

The subsequent terms in the Eq.98. denote the fluid coupling matrix, C_1, the mobility matrix, M, the pressure and the source vectors, p_d and q, respectively.

Introducing a tridiagonal, $N \times N$, matrix T such, that

$$T = C - M, \tag{99}$$

the Eq.98. can be rewritten to

$$Tp_d = q, \tag{100}$$

thus according to the above, the vector of pressures, p_d, can be obtained from

$$p_d = T^{-1}q. \tag{101}$$

According to Eq.87., the p_d is formulated as

$$p_d(x,\omega) = -\frac{v_p(x,\omega)Z_p(x,\omega)}{2}, \tag{102}$$

after reintroducing the $\dot{v}_1$ (check Sec.5), Eq.102. can be rearranged to

$$p_d(x,\omega) = -\frac{\dot{v}_1(x,\omega)Z_p(x,\omega)}{2}, \tag{103}$$

thus

$$\dot{v}_1(x,\omega) = -2p_d(x,\omega)Y_p(x,\omega). \tag{104}$$

Since the pressure difference, p_d, calculated from Eq.100., and the CP mobility, Y_p, are known, the CP velocity $\dot{v}_1$ can be computed according to Eq.104. In addition, knowing that

$$v_1 = \frac{\dot{v}_1}{j\omega}, \tag{105}$$

the CP displacement can be inferred dividing Eq.104. by the $j\omega$ factor, giving

$$v_1(x,\omega) = \frac{-2p_d(x,\omega)Y_p(x,\omega)}{j\omega}. \tag{106}$$

7.4 The Results

7.4.1 The Data

The *Matlab* scripts (Appendix C) were rearranged including the components defined in Eq.98. The CP was discretised into a number of points, N, equal to 1024 (likewise Sec.6.1.3), thus the length of a single partition element $\Delta \approx 3.4 \cdot 10^{-5}$. The mechanical parameters of the CP were the same as in the previous section (check Table 1.). Furthermore, the length of the CP was set to $L = 0.035\,m$, while the height of the upper cochlear channel $H = 0.001\,m$ (see Eq.94.). The cochlear fluid was assumed to have properties of water, hence the fluid's density $\rho = 1000\,kg/m^3$. The fluid was driven by the tonal signal, which, according to Eq.96., was expressed in terms of stapes velocity u_{st}, set to unity in both models. The OHC generation gain, g, was set to 1 and 0.

7.4.2 The Results

In this section the magnitude/phase plots, in function of frequency and distance from stapes, of the pressure difference p_d, the CP velocity, $\dot{v}_1$ and the CP displacement v_1, for the NK and G generalised models, are presented. The magnitude was expressed in dB with reference of $\dot{v}_{ref} = 2 \cdot 10^{-4}\,m/s$ and $v_{ref} = 1\,nm$ for the CP velocity and displacement, respectively, and in dB SPL with $p_{ref} = 2 \cdot 10^{-5}\,Pa$ reference for the pressure difference p_d (references of $\dot{v}_{ref}$ and v_{ref} were chosen according to the values of velocity and displacement at CF neural threshold, derived from comparisons with tuning curves of single auditory nerve fibres, in cat for $CF = 33\,kHz$ as listed in Table 1. in [25]). The G generalised model was computed with the delay factor $n = 2$ and 0.4 (compare Sec.6.1.3).

For the NK generalised model, the frequency, f, was set to $1\,kHz$, in the 'place-function' plots, and in the frequency-function plots the position on the BM, x, was set to the value corresponding to the place of maximum of absolute value of, appropriately, $|p_d|_{max}$, $|\dot{v}_1|_{max}$ and $|v_1|_{max}$, calculated for $1\,kHz$ stimulus frequency (Sec.6.1.3).

However, for the G generalised model, the frequency, f, was set to $1\,kHz$, in the place-function plots, but in the frequency-function plots, the position on the BM, x, was set to the value corresponding to the place for which the characteristic frequency, CF, calculated from Eq.63. (see also Sec.6.1.2) amounts to $1\,kHz$ i.e. $x \approx 0.022\,m$.

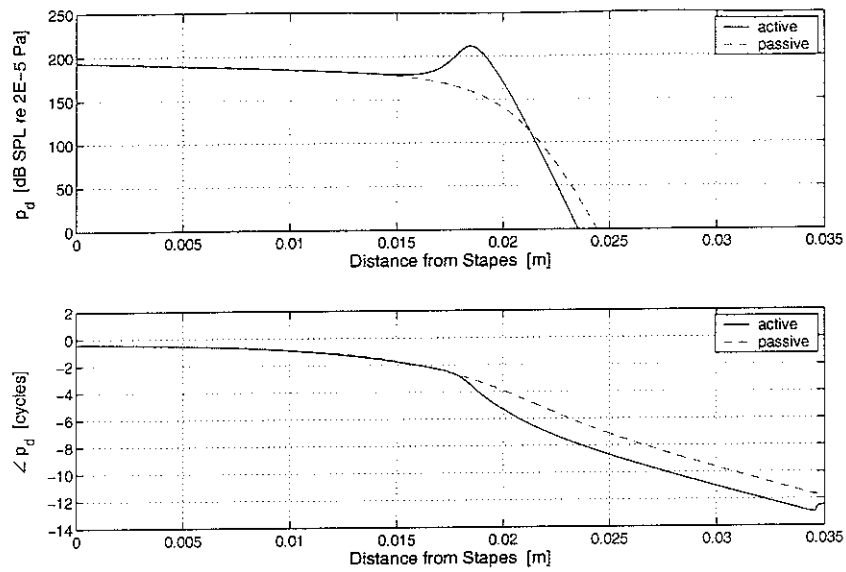

Figure 36: The magnitude and phase of the cochlear fluid's pressure difference p_d (dB SPL re $2 \cdot 10^{-5}\, Pa$) as a function of position on the BM, for the Neely&Kim generalised model with $f = 1\ kHz$ and $g = 1$ (active, solid) and 0 (passive, dashed).

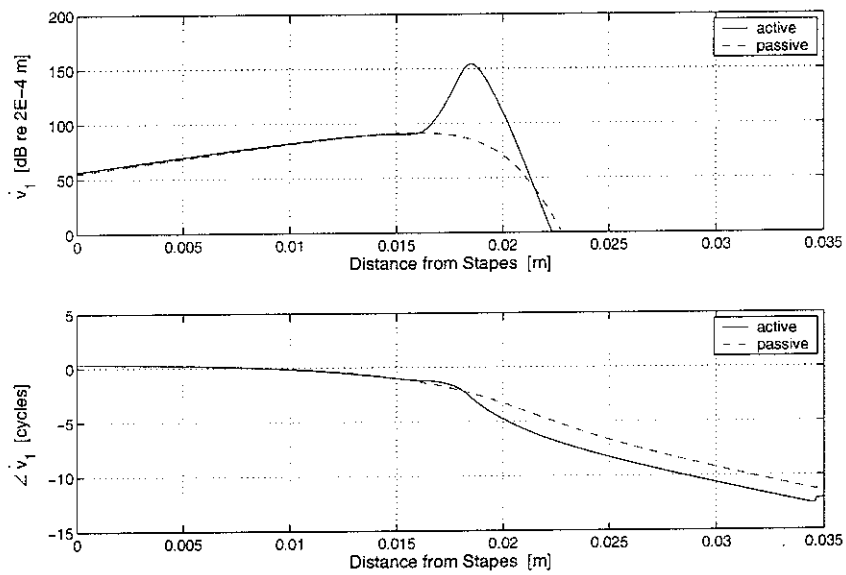

Figure 37: The magnitude and phase of the CP velocity $\dot{v}_1$ (dB re $2 \cdot 10^{-4}\, m/s$) as a function of position on the BM, for the Neely&Kim generalised model with $f = 1\ kHz$ and $g = 1$ (active, solid) and 0 (passive, dashed).

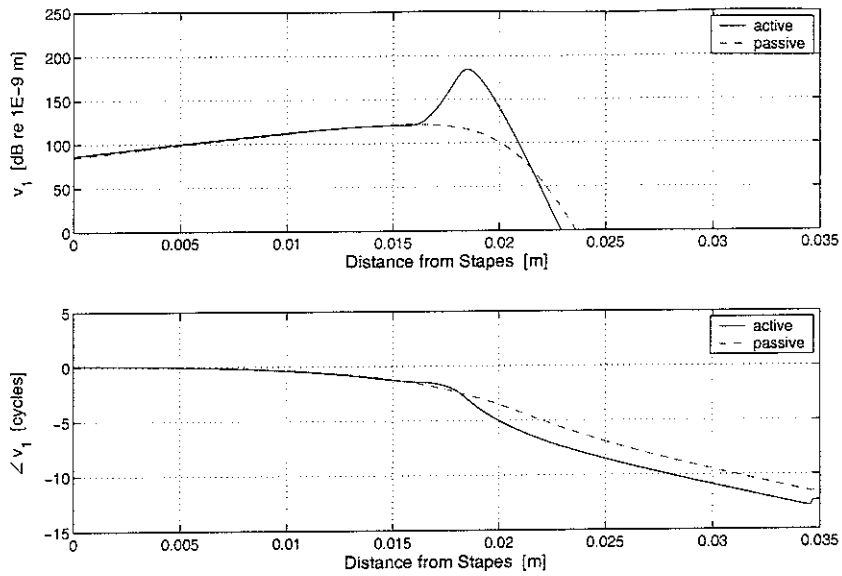

Figure 38: The magnitude and phase of the CP displacement v_1 (dB re 1 nm) as a function of position on the BM, for the Neely&Kim generalised model with $f = 1\ kHz$ and $g = 1$ (active, solid) and 0 (passive, dashed).

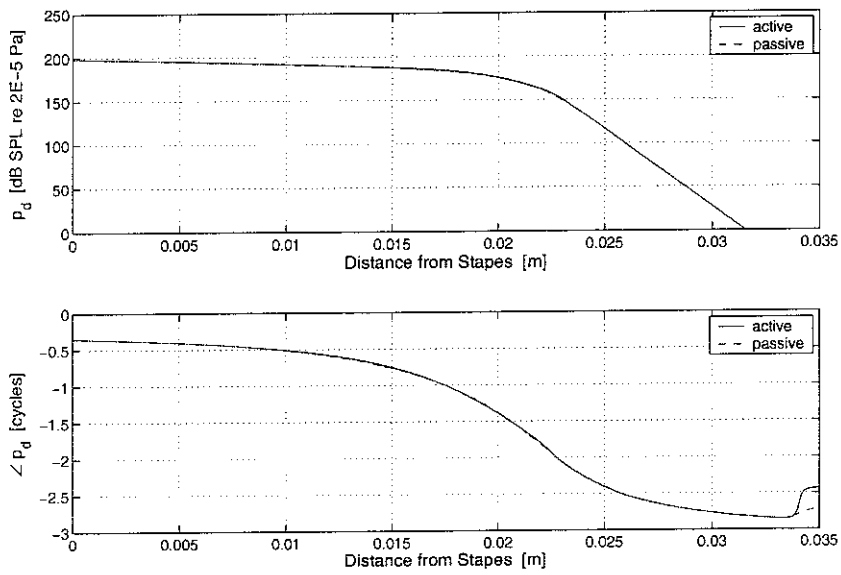

Figure 39: The magnitude and phase of the cochlear fluid's pressure difference p_d (dB SPL re $2 \cdot 10^{-5}\ Pa$) as a function of position on the BM, for the Geisler generalised model with $f = 1\ kHz$ and $g = 1$ (active, solid) and 0 (passive, dashed).

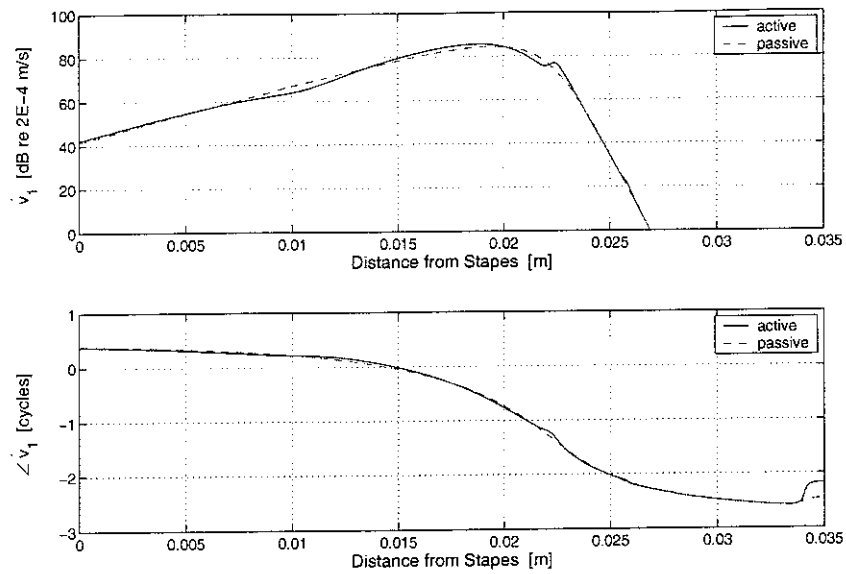

Figure 40: The magnitude and phase of the CP velocity $\dot{v}_1$ (dB re $2{\cdot}10^{-4}m/s$) as a function of position on the BM, for the Geisler generalised model with $f = 1\,kHz$ and $g = 1$ (active, solid) and 0 (passive, dashed).

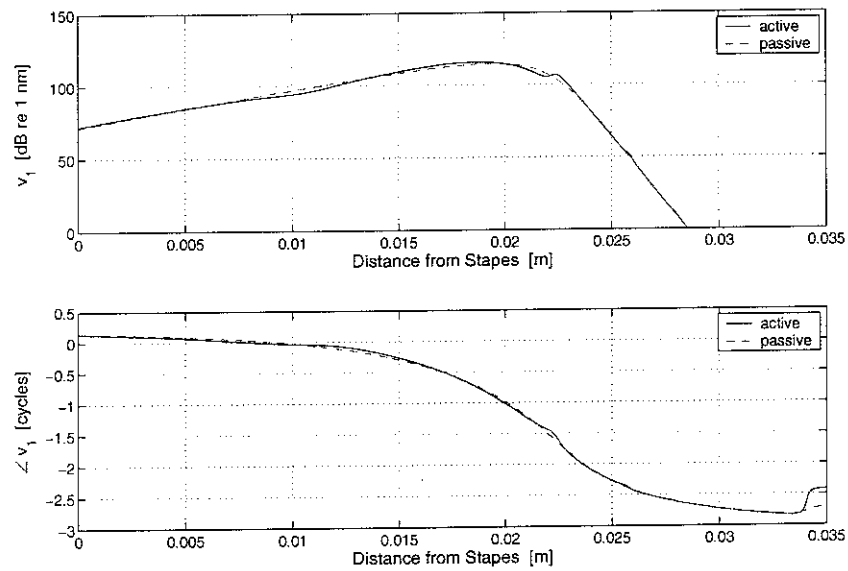

Figure 41: The magnitude and phase of the CP displacement v_1 (dB re $1nm$) as a function of position on the BM, for the Geisler generalised model with $f = 1\,kHz$ and $g = 1$ (active, solid) and 0 (passive, dashed).

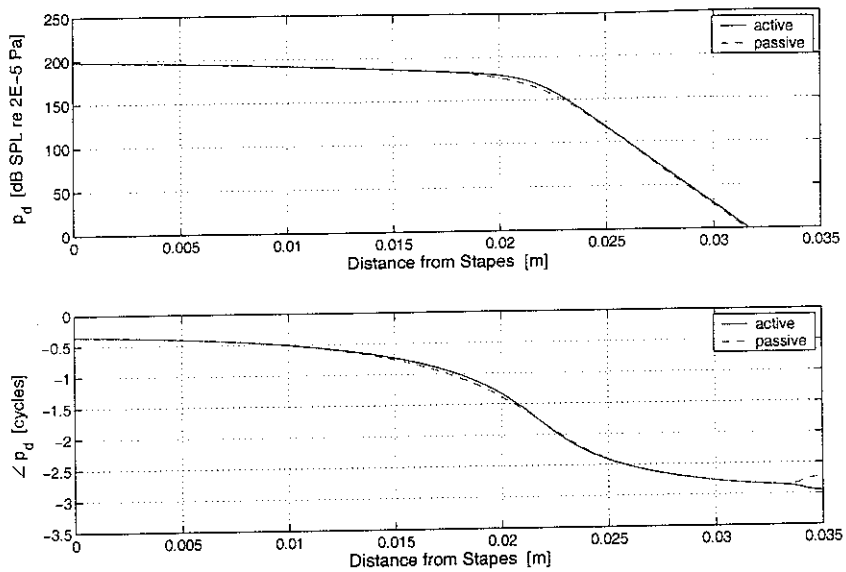

Figure 42: The magnitude and phase of the cochlear fluid's pressure difference p_d (dB SPL re $2 \cdot 10^{-5}\ Pa$) as a function of position on the BM, for the Geisler generalised model with $f = 1\ kHz$, delay factor, $n = 0.4$, and $g = 1$ (active, solid) and 0 (passive, dashed).

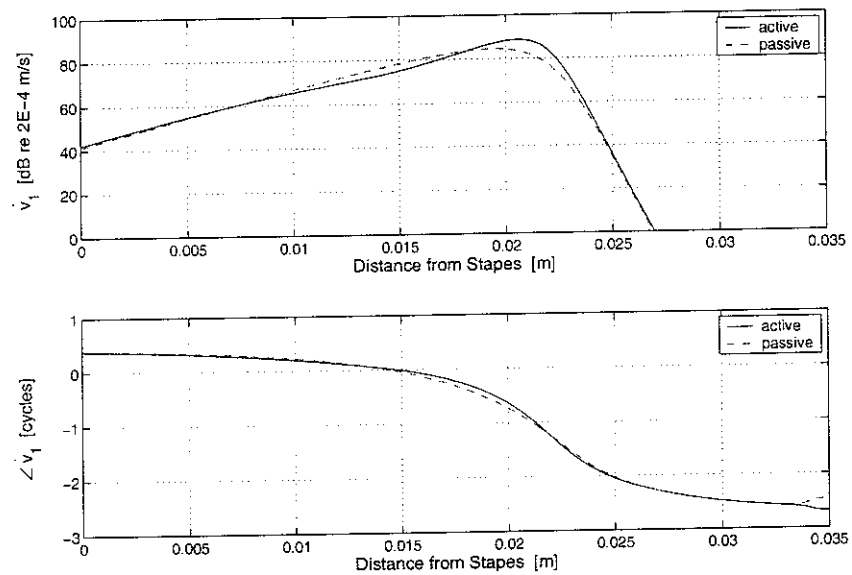

Figure 43: The magnitude and phase of the CP velocity $\dot{v}_1$ (dB re $2 \cdot 10^{-4} m/s$) as a function of position on the BM, for the Geisler generalised model with $f = 1 kHz$, delay factor, $n = 0.4$, and $g = 1$ (active, solid) and 0 (passive, dashed).

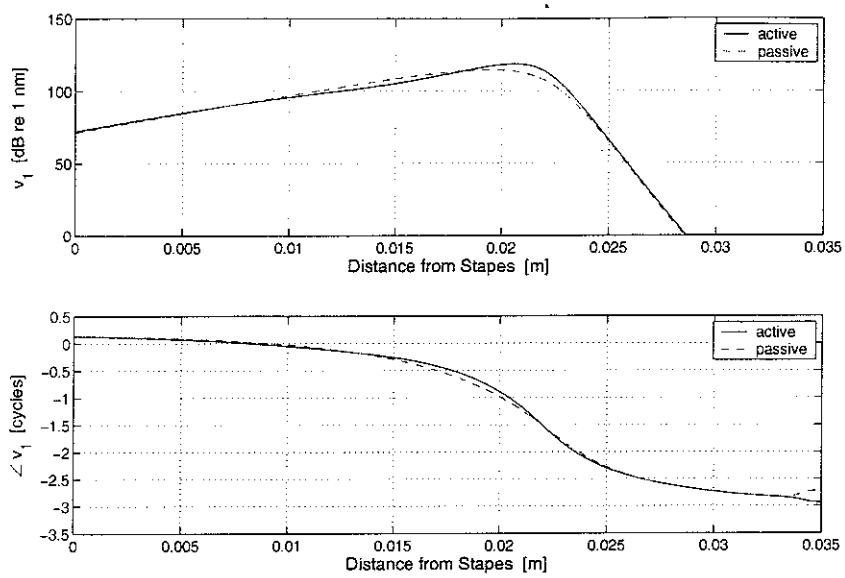

Figure 44: The magnitude and phase of the CP displacement v_1 (dB re $1nm$) as a function of position on the BM, for the Geisler generalised model with $f = 1kHz$, delay factor, $n = 0.4$, and $g = 1$ (active, solid) and 0 (passive, dashed).

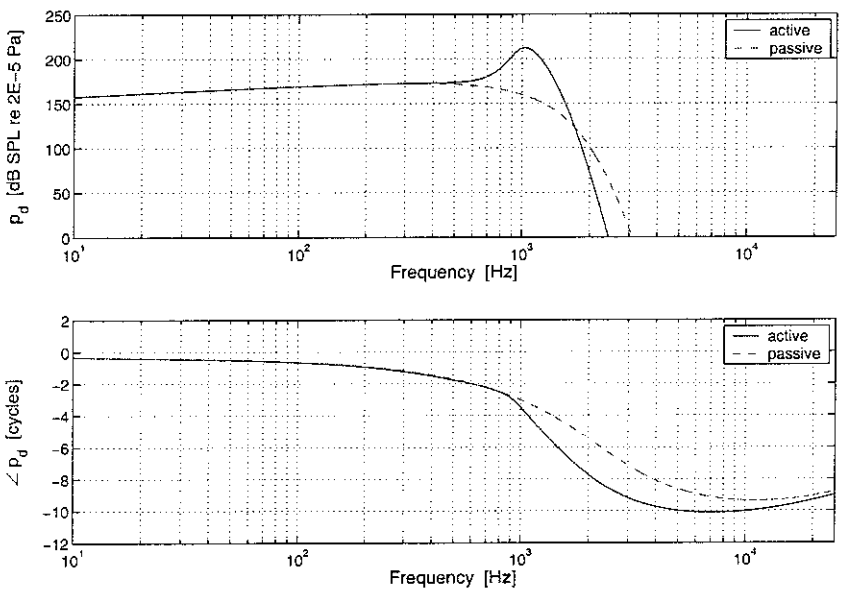

Figure 45: The magnitude and phase of the cochlear fluid's pressure difference p_d (dB SPL re $2 \cdot 10^{-5} Pa$) as a function of stimulus frequency, f, for the Neely&Kim generalised model for the position on the BM $x = 0.0185\,m$ and $g = 1$ (active, solid) and 0 (passive, dashed).

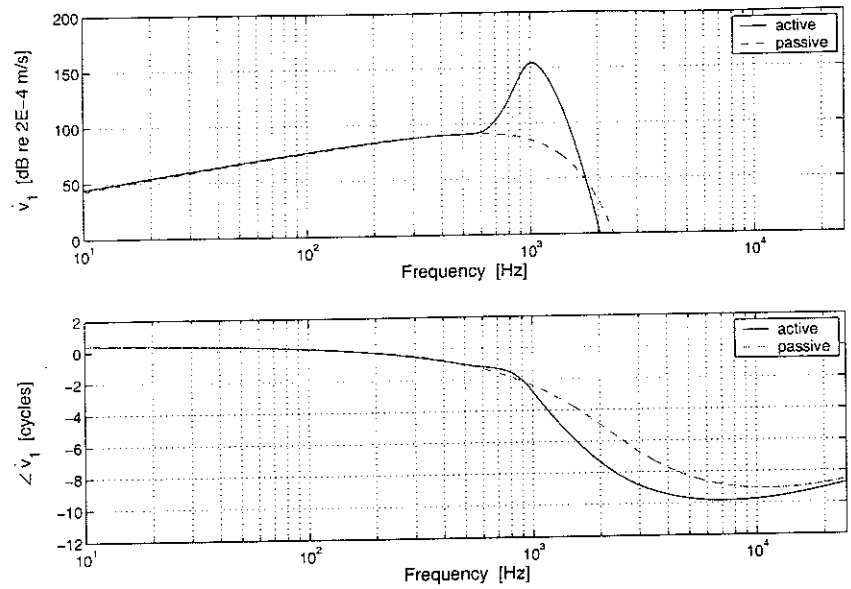

Figure 46: The magnitude and phase of the CP velocity $\dot{v}_1$ (dB re $2 \cdot 10^{-4}\, m/s$) as a function of stimulus frequency, f, for the Neely&Kim generalised model for the position on the BM $x = 0.0185\, m$ and $g = 1$ (active, solid) and 0 (passive, dashed).

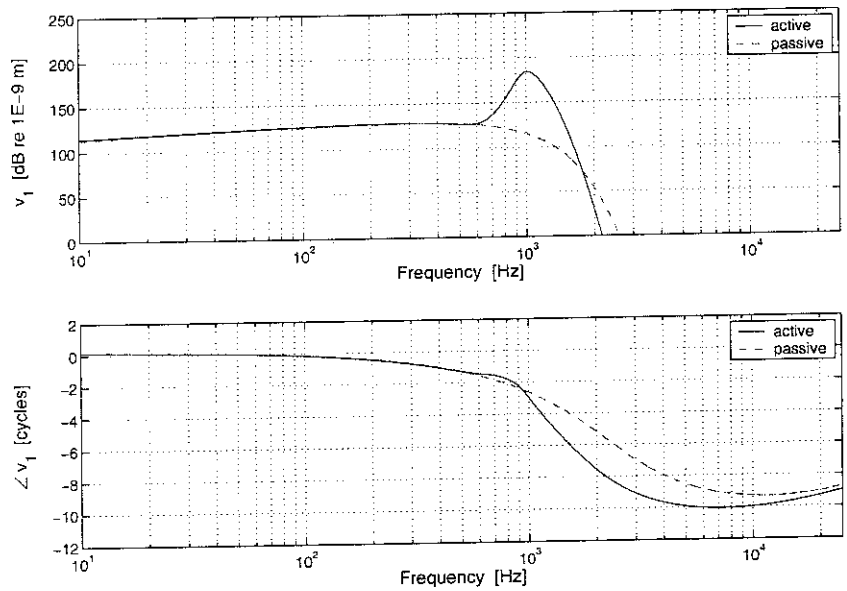

Figure 47: The magnitude and phase of the CP displacement v_1 (dB re $1\, nm$) as a function of stimulus frequency, f, for the Neely&Kim generalised model for the position on the BM $x = 0.0185\, m$ and $g = 1$ (active, solid) and 0 (passive, dashed).

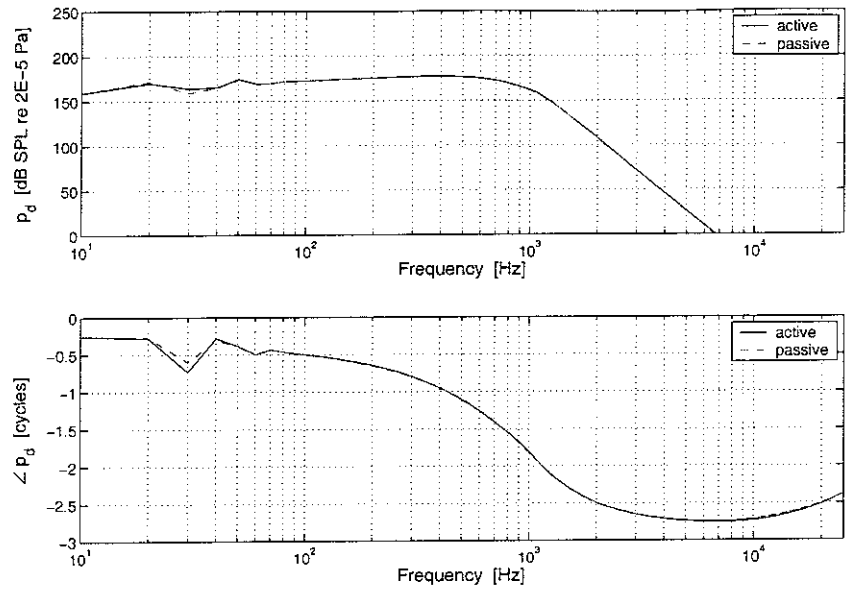

Figure 48: The magnitude and phase of the cochlear fluid's pressure difference p_d (dB SPL re $2 \cdot 10^{-5}\, Pa$) as a function of stimulus frequency, f, for the Geisler generalised model for the position on the BM $x = 0.022\, m$ and $g = 1$ (active, solid) and 0 (passive, dashed).

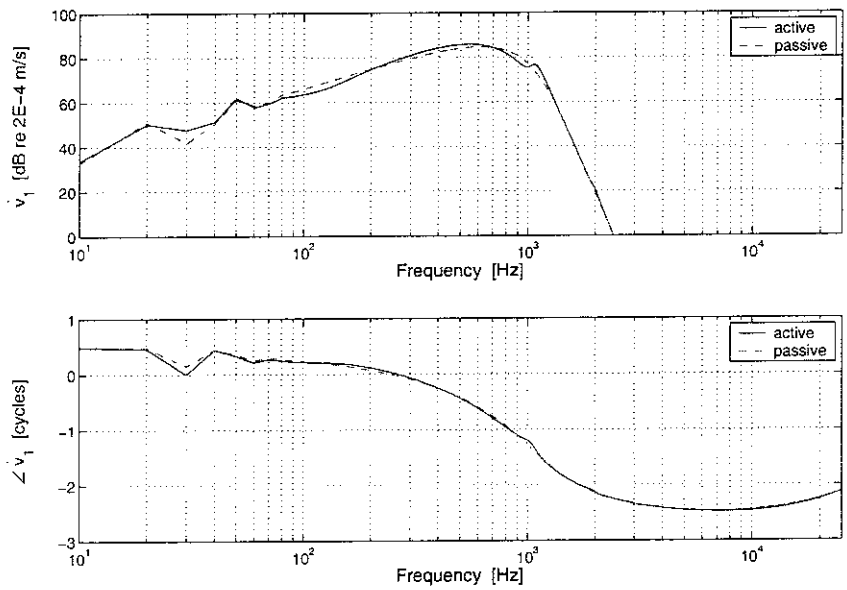

Figure 49: The magnitude and phase of the CP velocity $\dot{v}_1$ (dB re $2 \cdot 10^{-4}\, m/s$) as a function of stimulus frequency, f, for the Geisler generalised model for the position on the BM $x = 0.022m$ and $g = 1$ (active, solid) and 0 (passive, dashed).

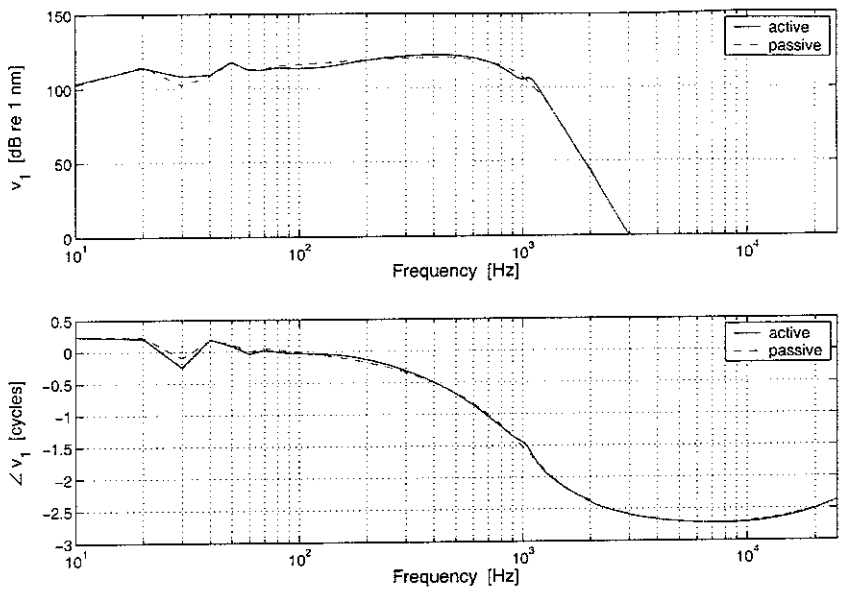

Figure 50: The magnitude and phase of the CP displacement v_1 (dB re $1\,nm$) as a function of stimulus frequency, f, for the Geisler generalised model for the position on the BM $x = 0.022m$ and $g = 1$ (active, solid) and 0 (passive, dashed).

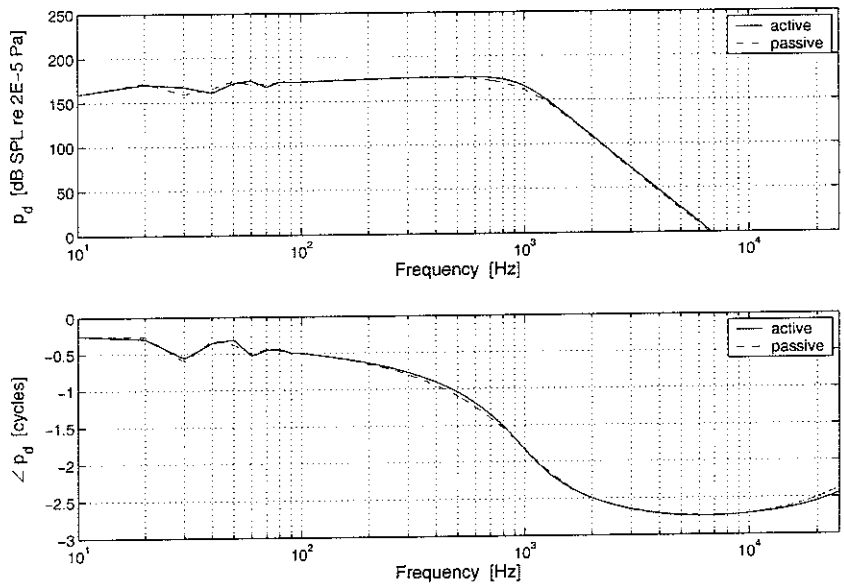

Figure 51: The magnitude and phase of the cochlear fluid's pressure difference p_d (dB SPL re $2 \cdot 10^{-5}\,Pa$) as a function of stimulus frequency, f, for the Neely&Kim generalised model for the position on the BM $x = 0.022\,m$, delay factor, $n = 0.4$, and $g = 1$ (active, solid) and 0 (passive, dashed).

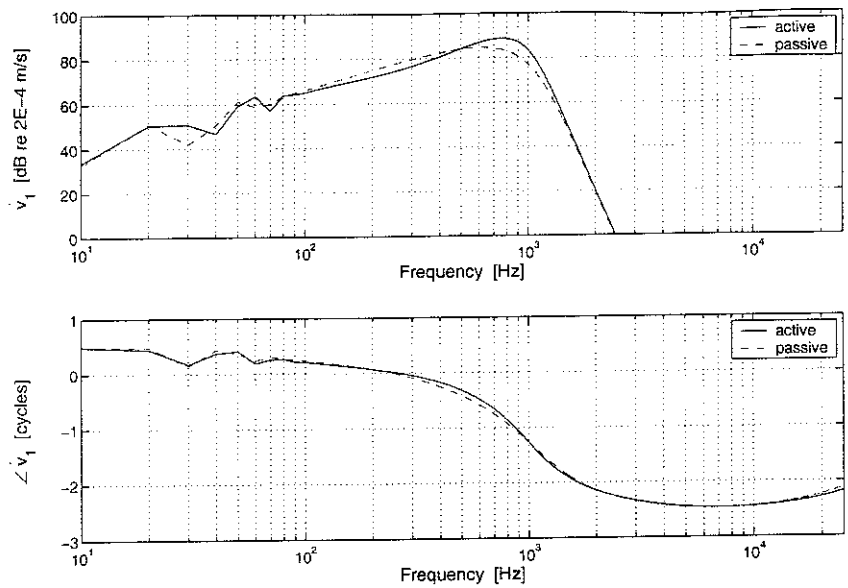

Figure 52: The magnitude and phase of the CP velocity $\dot{v}_1$ (dB re $2 \cdot 10^{-4}\, m/s$) as a function of stimulus frequency, f, for the Geisler generalised model for the position on the BM $x = 0.022\, m$, delay factor, $n = 0.4$, and $g = 1$ (active, solid) and 0 (passive, dashed).

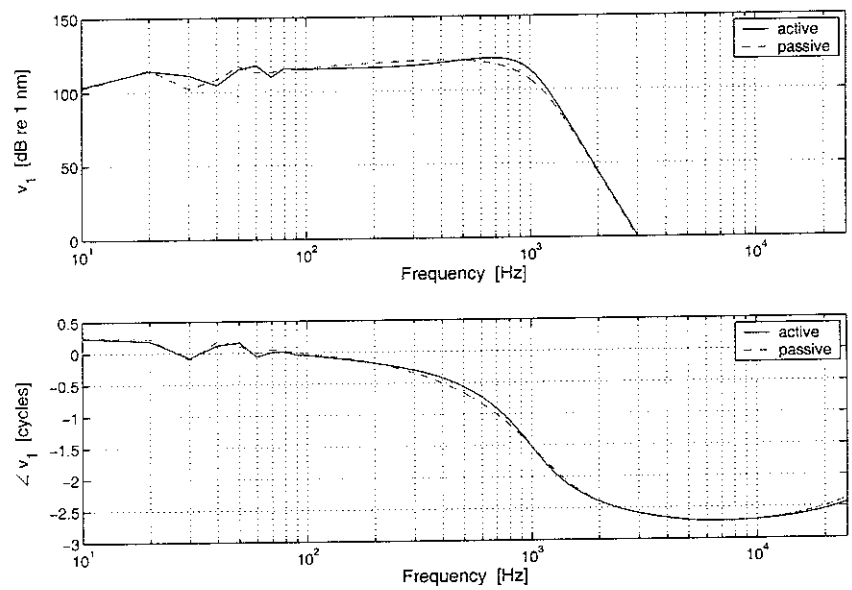

Figure 53: The magnitude and phase of the CP displacement v_1 (dB re $1\, nm$) as a function of stimulus frequency, f, for the Geisler generalised model for the position on the BM $x = 0.022\, m$, delay factor, $n = 0.4$, and $g = 1$ (active, solid) and 0 (passive, dashed).

7.5 Discussion

Presented plots, likewise in the mobility plots case (see Sec.6.1.3), reveal differences between the active and the passive modelled response only for the NK generalised model. For all quantities active response is characterised by a sharply tuned peak, stating the characteristic place of approximately 0.0185 m for the 1 kHz stimulus frequency, about 40 dB SPL above the maximum of the passive response for the pressure difference, p_d, and about 60 dB above for the partition velocity, $\dot{v}_1$, and displacement, v_1.The tuning does provide a rather steep roll-off on the apical side of the curves i.e. approximately 149 dB/octave (62 dB/octave for passive response) 154 dB/octave (57 dB/octave for passive response) and 155 dB/octave (61 dB/octave for passive response) in the pressure difference, partition velocity and partition displacement curves, respectively. Along with the increase of the response's peak a steeping of the phase slope, in comparison with the passive phase curve, can be observed. The fast increasing phase lag, characteristic in the peak region (highest activity), comparing to the slow cumulation of phase below and above the CF (characteristic place) corresponds to the real cochlea behaviour.

The active response plots of the G generalised model do not provide an enhancement characteristic for the active response of the real cochlea. Thus, in the active and passive case the same broad curves represent the response of the model. In the G generalised model, the roll-off on the apical side of the active and passive response curves amounts to about 62 dB/octave, 69 dB/octave and 76 dB/octave in the pressure difference, partition velocity and partition displacement curves, respectively (for both delay factors, $n = 2$ and 0.4, used). The slope of 62 dB/octave in the pressure difference plot corresponds to the slope of the passive generalised model of NK. However, the slopes of the partition velocity and partition displacement curves are steeper then those calculated for the NK model. The reason for such behaviour is the one order bigger value of the BM mass evaluated for the G model's parameters, though there is no second mass like the one represented by the TM in the NK generalised model (check Table 1.). Nevertheless, despite the above, reduction of the variables significantly changed the response of the model as it mentioned in Section 6.2.

Finally, there is no change in the phase behaviour of any examined quantity, between the active and passive curve. Although the slope of the phase may seem steeper then the one in the NK case, the cumulation of phase amounts only to about three cycles, whereas it ranges to approximately fourteen cycles in the NK model. This small phase cumulation also does not agree with the physiological data.

8 Backward Travelling Wave

This section, inspired by the research of Tianying Ren in [24], examines the phase behaviour of the cochlear fluid's pressure. It was assumed by Ren that the slope of the phase curves, plotted in function of the position along the cochlea, x, determines the direction of the BM vibration [24].

Considering a simple analogy of the wave propagation in an infinite duct as presented in Fig.54., phase lags of the pressure will be detected in both positive, $+x$, and negative, $-x$, directions from the source.

The phase of the pressure difference, p_d, calculated for the generalised NK and G models reveals increasing lags with the position, x, which corresponds to the positive direction of the wave propagating from the source (stapes vibration in the models) as depicted in Fig.54.

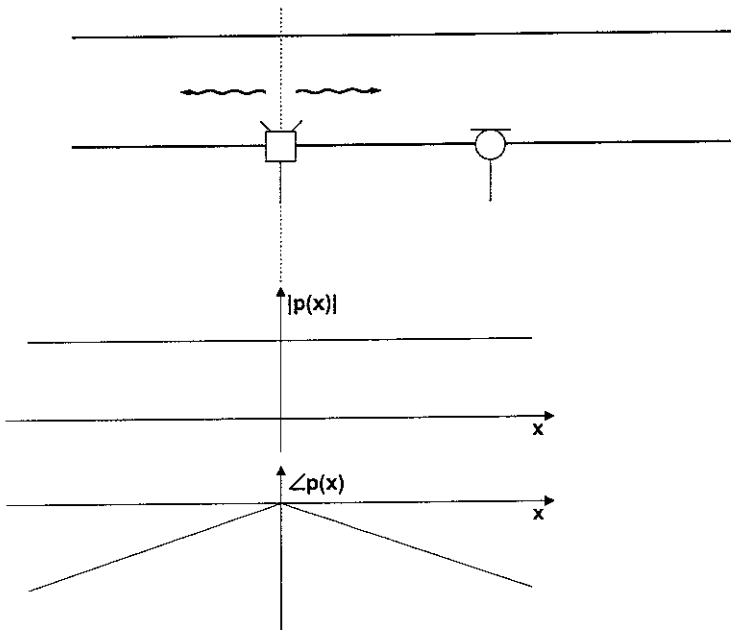

Figure 54: An infinite duct with a sound source and sound receiver (top). Phase lags of the propagating pressure wave will be observed in both, positive ($+x$) and negative ($-x$) directions from the source (bottom).

Representation of the source vector q in Eq.98. enables a change in the position of the stimulus (expressed in terms of stapes velocity, u_{st}) to any point on the CP, thus, checking the phase behaviour of the pressure waves propagating in both directions from the source.

In order to verify this assumption, the magnitude and phase of the pressure difference, p_d, evaluated from the macromechanical, generalised NK model, were examined.

8.1 The Results

The magnitude and phase of the pressure difference, p_d, were calculated likewise Sec.7.4.2 with the source set to the position of the stapes footplate, $x = 0\,m$ (q_1 in the source vector, check Eq.98.) and $x = 0.0185\,m$ corresponding to the place of the maximum value of absolute of the pressure difference, p_d, for the active ($g = 1$) NK model, computed for $f = 1\,kHz$ stimulus frequency (q_{541} in the source vector, check Eq.98.). The stimulus frequency, f, was set to $f = 1\,kHz$ and the gain, g, to 0 and 1 in both cases. The response has been evaluated for the unit stapes velocity, u_{st}.

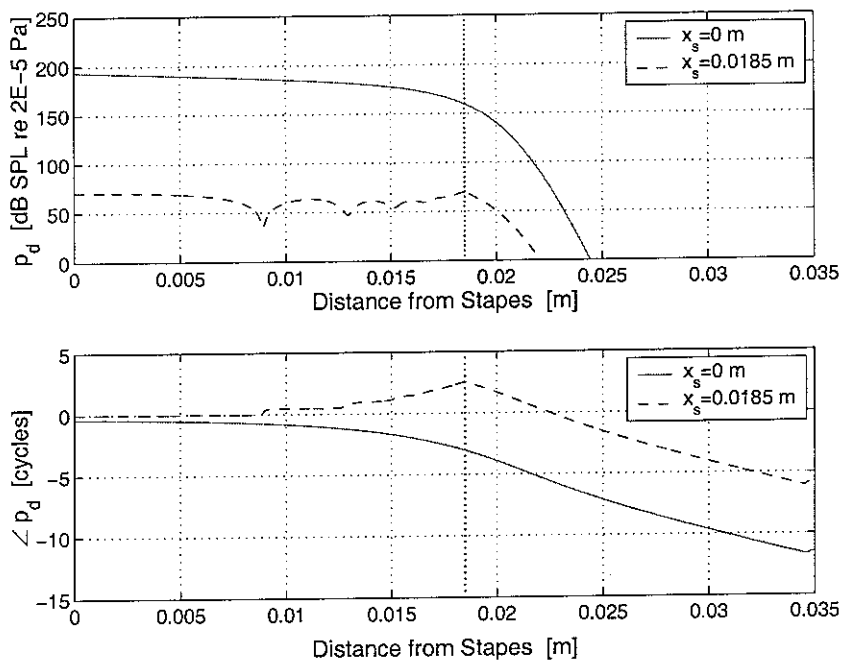

Figure 55: The magnitude and phase of the cochlear fluid's pressure difference p_d (dB SPL re $2 \cdot 10^{-5}\,Pa$) as a function of position on the BM, for the passive ($g = 0$) Neely&Kim generalised model with stimulus frequency, f, equal to $1\,kHz$. The position, marked with the dotted line, of the stimulus, $x_s = 0$ (stapes, solid line) and $0.0185\,m$ (position of $|p_d|_{max}$ for $1\,kHz$ frequency input, dashed line).

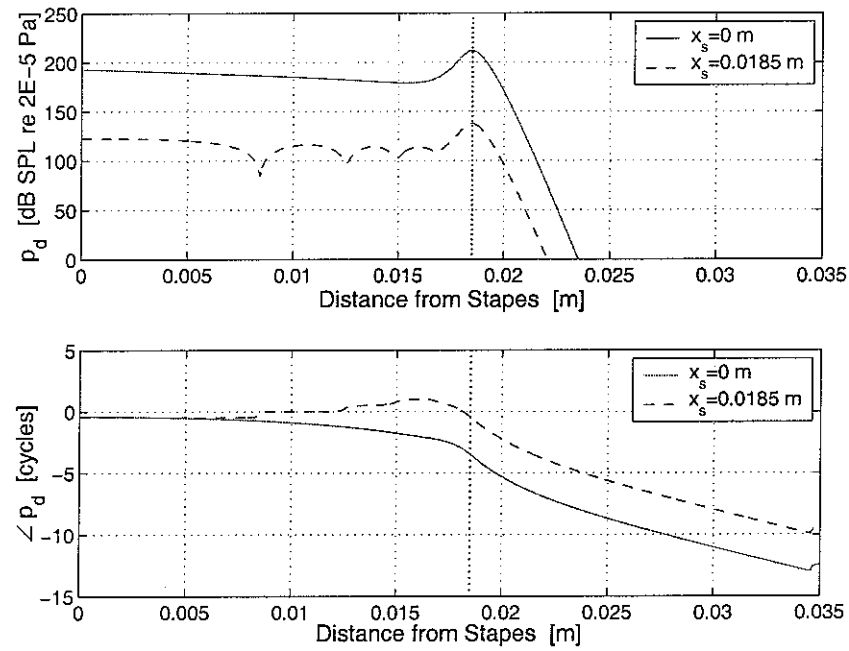

Figure 56: The magnitude and phase of the cochlear fluid's pressure difference p_d (dB SPL re $2 \cdot 10^{-5}\, Pa$) as a function of position on the BM, for the active ($g = 1$) Neely&Kim generalised model with stimulus frequency, f, equal to $1 kHz$. The position of the stimulus, $x_s = 0$ (stapes, solid line) and $0.0185\, m$ (position, marked with the dotted line, of $|p_d|_{max}$ for $1\, kHz$ frequency input, dashed line).

8.2 Discussion

The phase plots obtained for the passive generalised model of NK verify the assumed behaviour of the propagating wave from the source (the source-receiver analogy). The phase, depicted in Fig.55., lags in both directions (accordingly to $+x$ and $-x$ in Fig.54.) from the position of the stimulus i.e. $x = 0.0185\,m$ (the source in Fig.54.) towards the ends of the cochlea.

However, in the active model, the phase lags from the same position of the stimulus towards the apex (positive, $+x$, direction in Fig.54.) but a lead of about one cycle followed by the phase lag towards the base of the cochlea proceeds in the opposite direction from the position of the stimulus. Therefore discerning the direction of the BM vibration propagation by means of the phase slope seems not as unequivocal as assumed by Ren.

The phase behaviour calculated for the passive case remains consistent with the theoretical prediction, however, it reveals some peculiarities in case of the active modelled response of the cochlea. In summary, the analysis of phase data calculated from active models of the cochlea, should be approached with greater care and insight.

9 Stability

9.1 The Introduction

It is proposed that the cochlea works as a physiological control system which identification may determine its main characteristics. The models of the cochlear dynamics define its characteristics in terms of a closed-loop system identification. The open-loop characteristics (passive) of the cochlear function/response is rather well examined, however, unravelling the mechanism of the cochlear activity stimulates the investigations on the feedback component of the loop, thus the characteristic of the overall closed-loop system [14].

The active processes responsible for the sharp tuning and high sensitivity of the cochlea are represented in the NK and G models as an additional source stimulated by the deflections of the OHCs cilia and pumping the energy into the system. This mechanism (active sources) is postulated to act as a controlling device in the overall feedback loop within the cochlea.

In the NK model the feedback component in the closed loop is formulated by the active pressure p_a (Eq.10.), in which an additional element $-\gamma Z_4$ is introduced to account for the gain control and frequency-dependent phase shift between p_a and ξ_c (see Fig.57.).

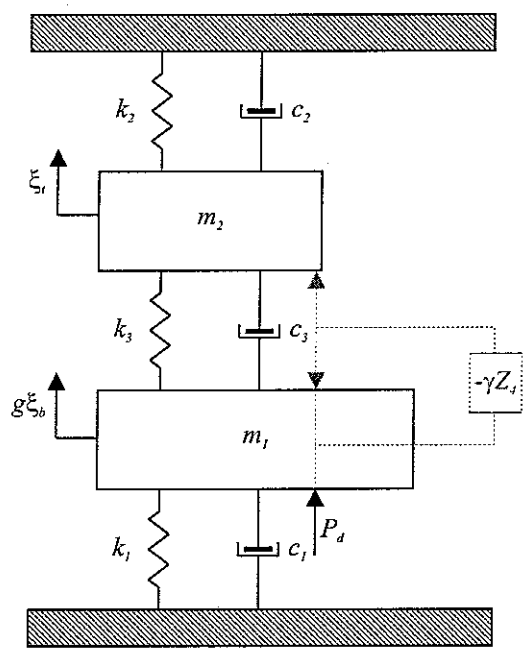

Figure 57: The lumped component system of the Neely&Kim model with indication of the feedback loop. The element $-\gamma Z_4$ accounts for the control of the input pressure P_a to acquire a particular velocity $\dot{\xi}_c$ in the output of the loop.

The fluid pressure p_d, represents the input and shearing velocity, $\dot{\xi}_c$, the output of the feedback loop for this case.

In the G model, the feedback loop is expressed by the bracketed term in Eq.19. with introduction of the feedback force $F_{fb}(\omega)$. By this formulation the negative-feedback term describes an effective loading that exerts upon the BM. Figure 58. depicts a block diagram of the feedback loop for the model of Geisler (compare Fig.2. in [10]). Here, the displacement of the BM x and the acoustic force F_a account for the input and output terms, respectively, as seen from the BM [10].

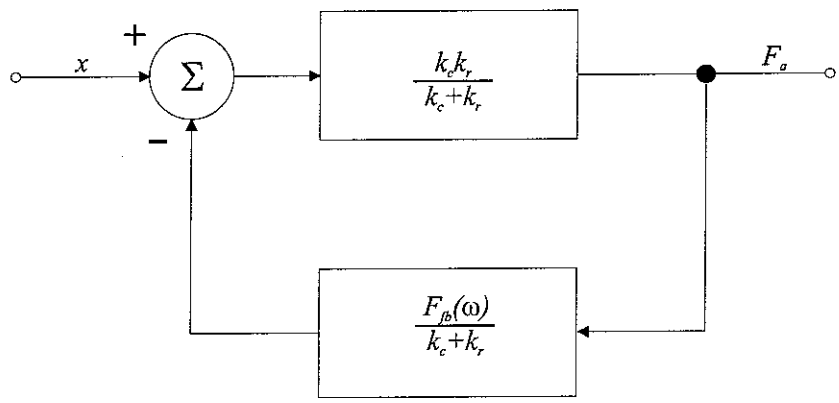

Figure 58: A block diagram of the feedback loop for the Geisler model. The 'input' x is controlled by $F_{fb}(\omega)/k_c+k_r$ (controller) to arrange particular acoustic force F_a at the output of the loop.

In this section the feedback loop systems for the generalised NK and G models will be introduced. Next, the stability of the systems will be analysed using the *Nyquist stability criterion.* The theoretical formulation of the feedback loop will be conducted on the basis of the EOMs derived in Section 5.

For both generalised models the control term will be represented by the active pressure p_a whereas the input and output of the feedback loop by the pressure difference p_d and velocity $\dot{v}_3$, respectively [16]. A block diagram of the proposed control system is shown in Fig.59., where G denotes the plant and H the controller of the feedback. Explicit formulation of the G and H will be derived from the generalised EOMs, as it was mentioned before.

9.2 The Model of Neely and Kim

Differentiating Eq.53. with respect to time gives the formulation of the relative velocity $\dot{v}_3(x)$

$$\dot{v}_3(x) = \dot{v}_1(x) - \dot{v}_2(x), \tag{107}$$

so

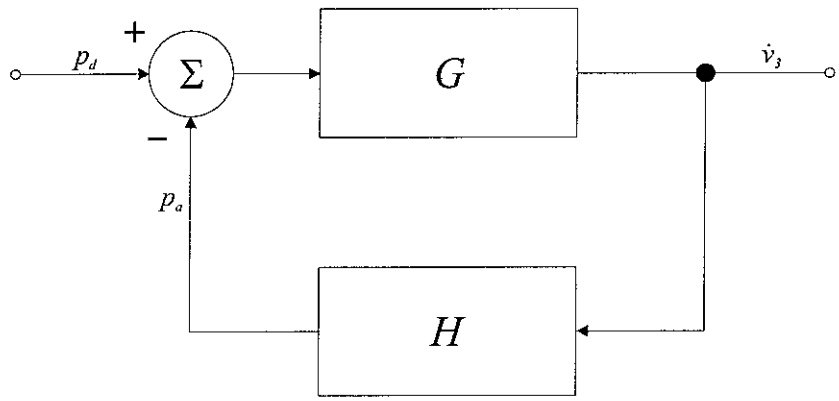

Figure 59: A block diagram of the feedback loop for the Neely&Kim and Geisler generalised models. The acoustic pressure p_d is the input and the $\dot{v}_3$ velocity the output of the feedback loop. The G and H terms denote the plant and the controller, respectively.

$$\dot{v}_1(x) = \dot{v}_3(x) + \dot{v}_2(x). \tag{108}$$

After rearranging Eq.55. the expression for $\dot{v}_2(x)$ takes form

$$\dot{v}_2(x) = \frac{Z_3}{Z_2}\dot{v}_3(x), \tag{109}$$

and substituting to Eq.108. the velocity $\dot{v}_1(x)$ equals

$$\dot{v}_1(x) = \left(1 + \frac{Z_3}{Z_2}\right)\dot{v}_3(x), \tag{110}$$

Substituting above equation and the expression for p_a from Eq.56. to Eq.54., the first DOF of the NK generalised model, the EOM takes form

$$p_d(x) - (-gZ_4)\dot{v}_3(x) = \left[Z_1\left(1 + \frac{Z_3}{Z_2}\right)\right]\dot{v}_3(x) + Z_3\dot{v}_3(x), \tag{111}$$

or equivalently

$$p_d(x) - (-gZ_4)\dot{v}_3(x) = \left[Z_1\left(1 + \frac{Z_3}{Z_2}\right) + Z_3\right]\dot{v}_3(x). \tag{112}$$

Dividing Eq.112. by the bracketed term of the right-hand side

$$\underbrace{\frac{1}{\left[Z_1\left(1 + \frac{Z_3}{Z_2}\right) + Z_3\right]}}_{G} p_d(x) - \underbrace{\frac{1}{\left[Z_1\left(1 + \frac{Z_3}{Z_2}\right) + Z_3\right]}}_{G}\underbrace{(-gZ_4)}_{H}\dot{v}_3(x) = \dot{v}_3(x). \tag{113}$$

where G denotes the plant and H the controller of the closed feedback loop.

Equation 113. expressed by means of G and H amounts to

$$Gp_d(x) - GH\dot{v}_3(x) = \dot{v}_3(x), \tag{114}$$

therefore

$$\dot{v}_3(x) = \frac{G}{1+GH}p_d(x), \tag{115}$$

which appears in the form of a classical negative-feedback system and the formulation of G and H components is given in Eq.113.

9.3 The Model of Geisler

Following the same procedure likewise in Sec.9.2, first, rearranging Eq.60. (formulation for the second DOF of the G generalised model) for $\dot{v}_2(x)$ gives

$$\dot{v}_2(x) = \frac{Z_3}{Z_2}\dot{v}_3(x) + \frac{gZ_4}{Z_2}\dot{v}_3(x). \tag{116}$$

Applying this expression to Eq.108. along with the expression of the active pressure p_a in Eq.61., the velocity $\dot{v}_1(x)$ takes form

$$\dot{v}_1(x) = \left(1 + \frac{Z_3}{Z_2} + \frac{gZ_4}{Z_2}\right)\dot{v}_3(x). \tag{117}$$

By substitution of Eq.117. and Eq.61. to Eq.59. (EOM for the first DOF in the G generalised model) the EOM will amount to

$$p_d(x) + gZ_4\dot{v}_3(x) = \left[Z_1\left(1 + \frac{Z_3}{Z_2} + \frac{gZ_4}{Z_2}\right)\right]\dot{v}_3(x) + Z_3\dot{v}_3(x), \tag{118}$$

and after rearrangement

$$p_d(x) + gZ_4\dot{v}_3(x) - \frac{gZ_1Z_4}{Z_2}\dot{v}_3(x) = \left[Z_1\left(1 + \frac{Z_3}{Z_2}\right) + Z_3\right]\dot{v}_3(x), \tag{119}$$

euivalently

$$p_d(x) - \frac{gZ_4(Z_1 - Z_2)}{Z_2}\dot{v}_3(x) = \left[Z_1\left(1 + \frac{Z_3}{Z_2}\right) + Z_3\right]\dot{v}_3(x). \tag{120}$$

Dividing Eq.120. by the bracketed term on the right-hand side gives the final form

$$\underbrace{\frac{1}{\left[Z_1\left(1+\frac{Z_3}{Z_2}\right)+Z_3\right]}}_{G} p_d(x) - \underbrace{\frac{1}{\left[Z_1\left(1+\frac{Z_3}{Z_2}\right)+Z_3\right]}}_{G} \underbrace{\frac{gZ_4(Z_1-Z_2)}{Z_2}}_{H} \dot{v}_3(x) = \dot{v}_3(x). \tag{121}$$

where G denotes the plant and H the controller of the closed feedback loop.

Formulation of Eq.121. by means of G and H is

$$Gp_d(x) - GH\dot{v}_3(x) = \dot{v}_3(x), \tag{122}$$

and

$$\dot{v}_3(x) = \frac{G}{1+GH} p_d(x), \tag{123}$$

which describes a classical negative-feedback system for the G generalised model. The formulation of G and H components is given explicitly in Eq.121.

9.4 The Results

Stability of the NK and G generalised models, expressed as the negative feedback systems, was examined by means of the Nyquist stability criterion. According to the definition, system becomes unstable when the Nyquist plot encloses the point (-1,0) in the complex plane (the pole in the inferred transfer functions of the negative feedback systems, check Eqs.113. and 121. for NK and G generalised models, respectively) when the transfer function of the loop is being evaluated for frequencies from zero to infinity [14, 9].

The contours of the $GH(j\omega)$ open loop were calculated in *Matlab* for a band of frequencies ranging from 0 to 10^6 Hz, and presented in the Nyquist plots ($Im\,GH(j\omega)$ vs $Re\,GH(j\omega)$). The stability of the considered systems was examined for different positions on the CP i.e. $x = 0.0085$, 0.0135, 0.0185, $0.0235\,m$ with the gain, $g = 1$, and for different values of gain, i.e. $g = 0.7$, 1 and 1.1, with the position, x set to 0.0085 (apical), 0.0185 (point on the CP corresponding to the maximum displacement, v_1, for 1 kHz stimulus frequency) and $0.0235\,m$ (apical region) for every model.

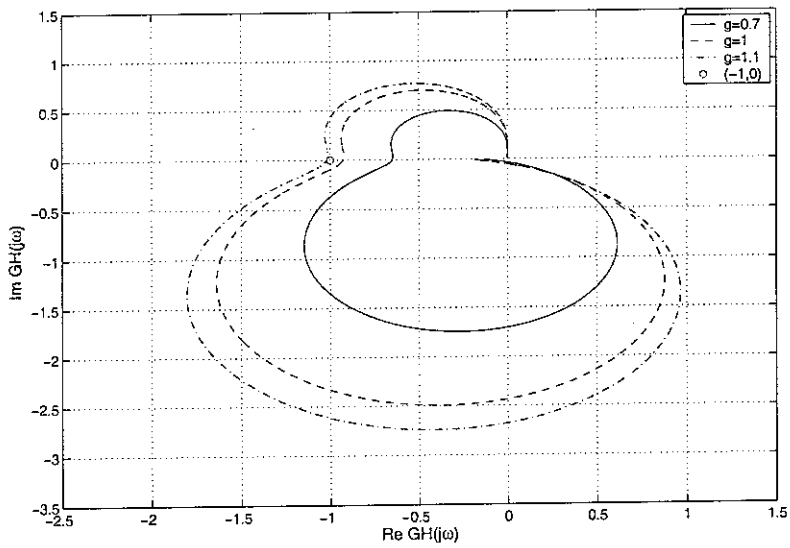

Figure 60: Nyquist plots of the negative feedback loop for $x = 0.0085\,m$ (basal site), derived for the Neely&Kim generalised model with the values of gain, g, equal to 0.7 (solid), 1 (dashed) and 1.1 (dash-dotted). The circle indicates the point (-1,0).

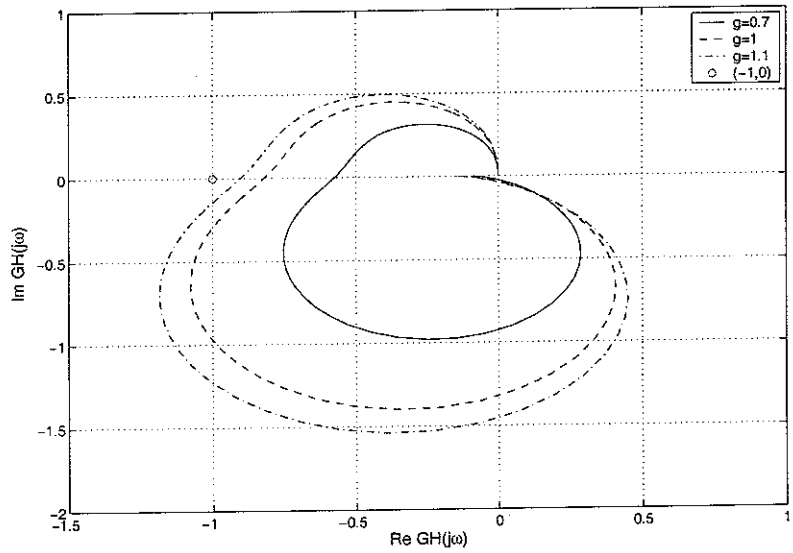

Figure 61: Nyquist plots of the negative feedback loop for $x = 0.0185\,m$ (the CP maximum displacement site for $f = 1\,kHz$), derived for the Neely&Kim generalised model with the values of gain, g, equal to 0.7 (solid), 1 (dashed) and 1.1 (dash-dotted). The circle indicates the point (-1,0).

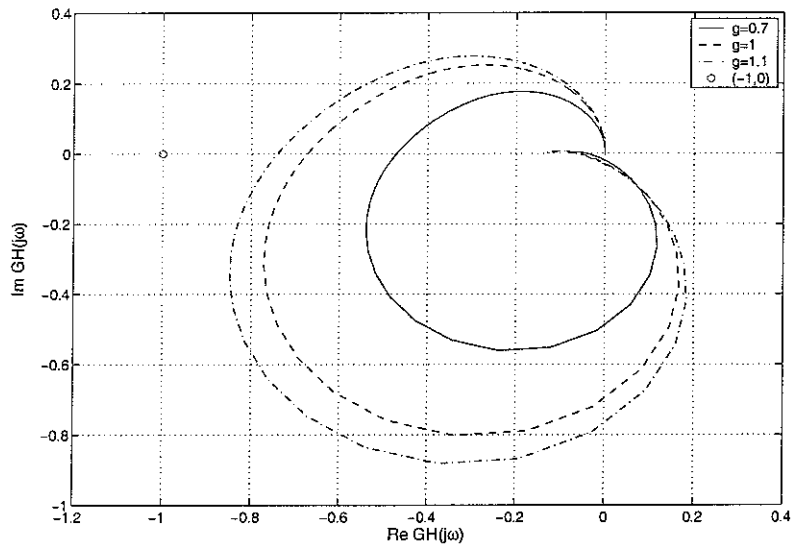

Figure 62: Nyquist plots of the negative feedback loop for $x = 0.0235\,m$ (apical site), derived for the Neely&Kim generalised model with the values of gain, g, equal to 0.7 (solid), 1 (dashed) and 1.1 (dash-dotted). The circle indicates the point (-1,0).

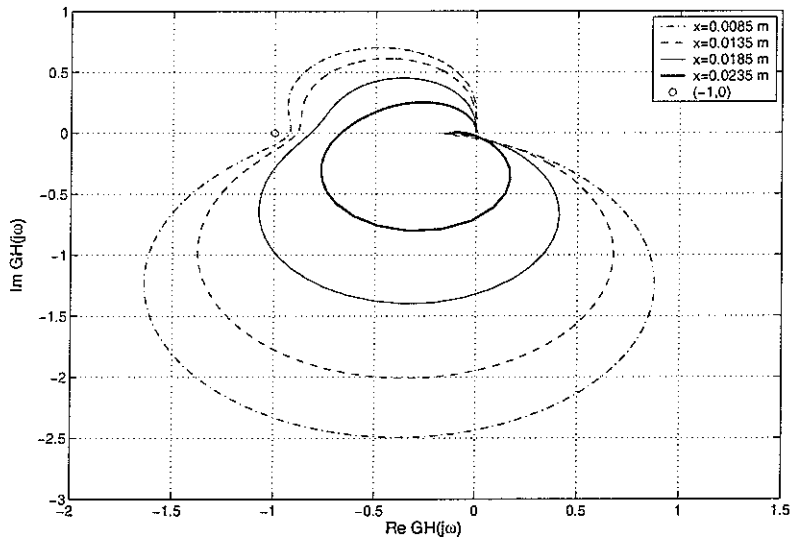

Figure 63: Nyquist plots of the negative feedback loop for $g = 1$ (active model), derived for the Neely&Kim generalised model with the values of position on the CP, x, equal to 0.0085 (dash-dotted), 0.0135 (dashed), 0.0185 (solid) and $0.0235m$ (bold). The circle indicates the point (-1,0).

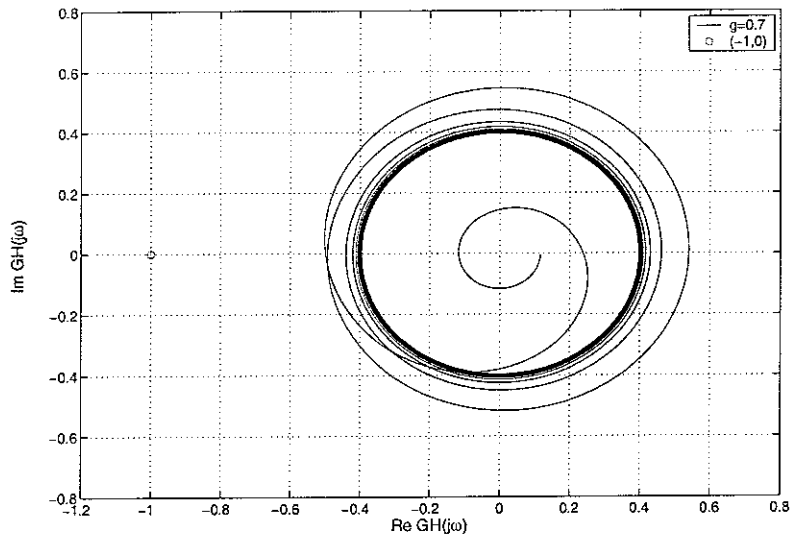

Figure 64: Nyquist plot of the negative feedback loop for $x = 0.0085\,m$ (basal site), derived for the Geisler generalised model with the value of gain, g, equal to 0.7. The circle indicates the point (-1,0).

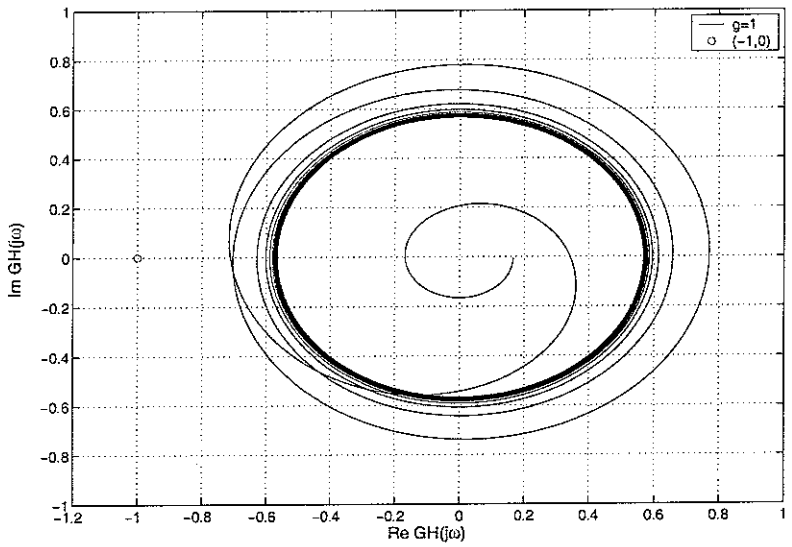

Figure 65: Nyquist plot of the negative feedback loop for $x = 0.0085\,m$ (basal site), derived for the Geisler generalised model with the value of gain, g, equal to 1. The circle indicates the point (-1,0).

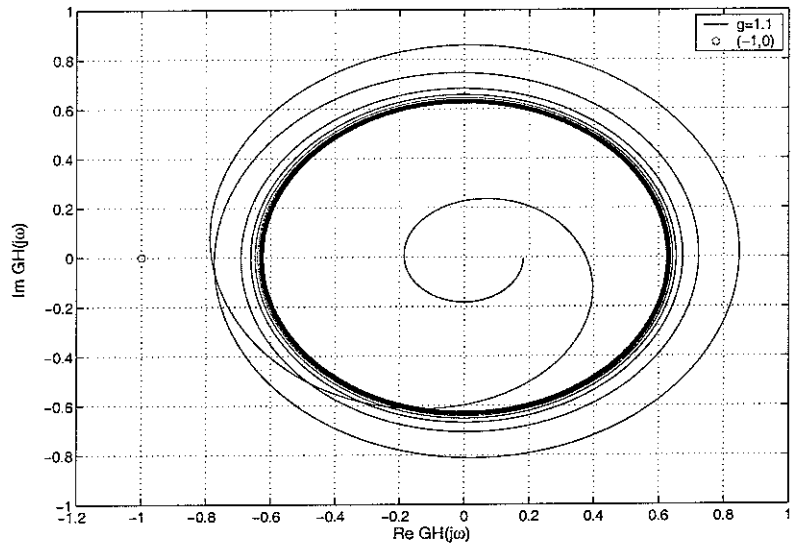

Figure 66: Nyquist plot of the negative feedback loop for $x = 0.0085\,m$ (basal site), derived for the Geisler generalised model with the value of gain, g, equal to 1.1. The circle indicates the point (-1,0).

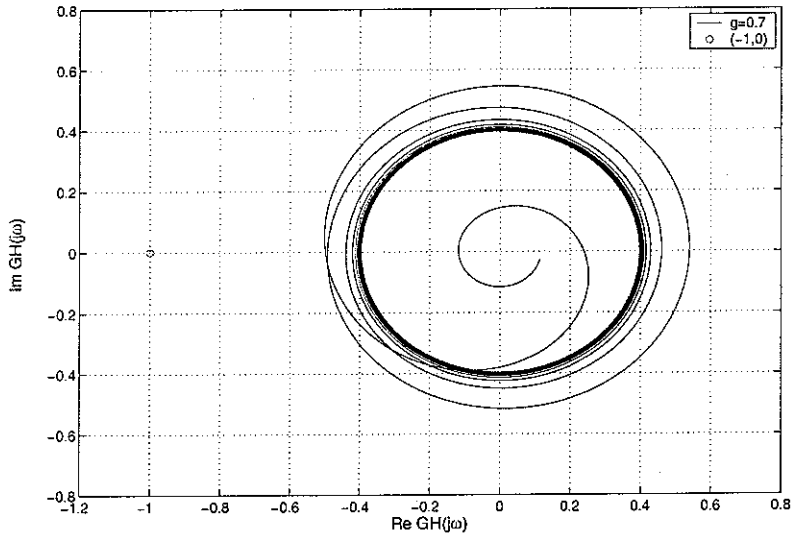

Figure 67: Nyquist plot of the negative feedback loop for $x = 0.0185\,m$ (site of the maximum displacement of the CP for $f = 1\,kHz$), derived for the Geisler generalised model with the value of gain, g, equal to 0.7. The circle indicates the point (-1,0).

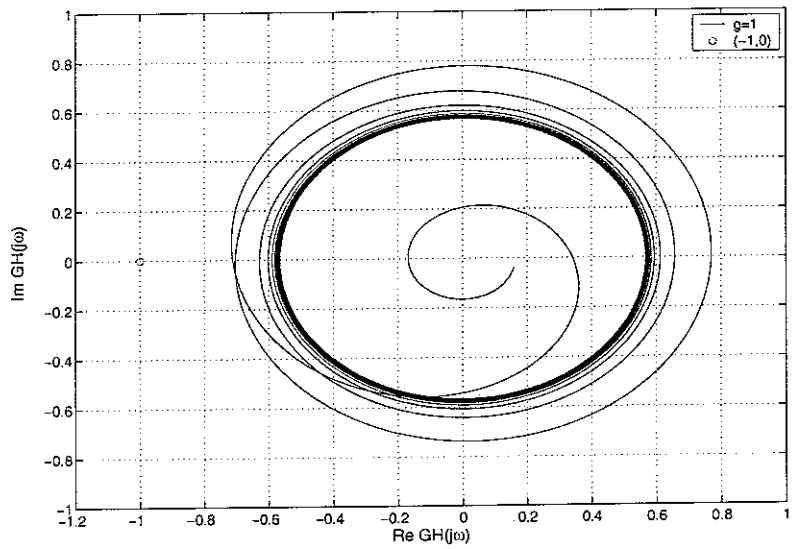

Figure 68: Nyquist plot of the negative feedback loop for $x = 0.0185\,m$ (site of the maximum displacement of the CP for $f = 1\,kHz$), derived for the Geisler generalised model with the value of gain, g, equal to 1. The circle indicates the point (-1,0).

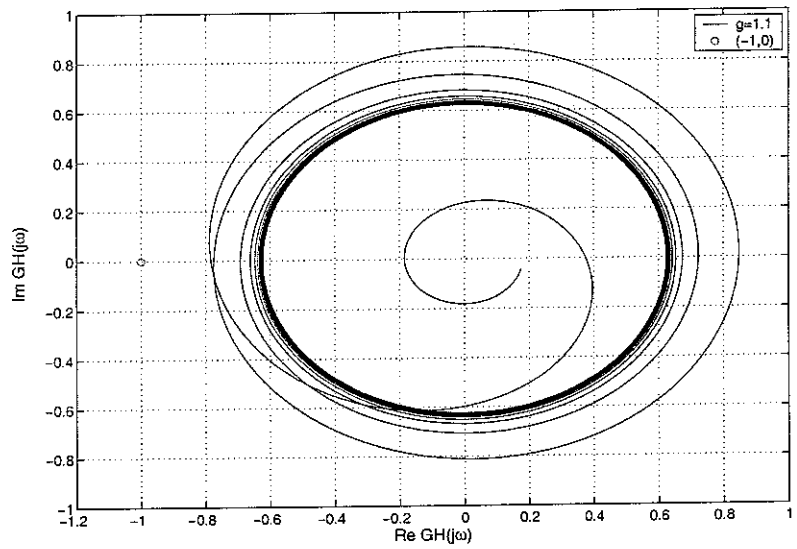

Figure 69: Nyquist plot of the negative feedback loop for $x = 0.0185\,m$ (site of the maximum displacement of the CP for $f = 1\,kHz$), derived for the Geisler generalised model with the value of gain, g, equal to 1.1. The circle indicates the point (-1,0).

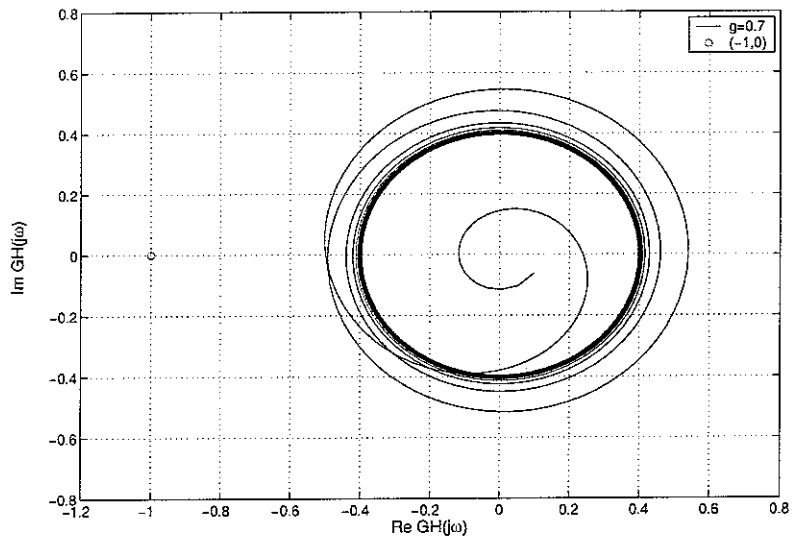

Figure 70: Nyquist plot of the negative feedback loop for $x = 0.0235\,m$ (apical site), derived for the Geisler generalised model with the value of gain, g, equal to 0.7. The circle indicates the point (-1,0).

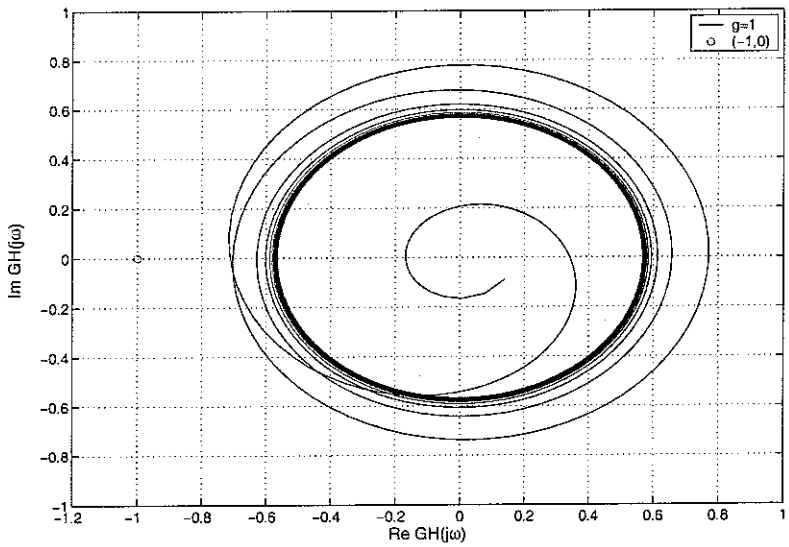

Figure 71: Nyquist plot of the negative feedback loop for $x = 0.0235\,m$ (apical site), derived for the Geisler generalised model with the value of gain, g, equal to 1. The circle indicates the point (-1,0).

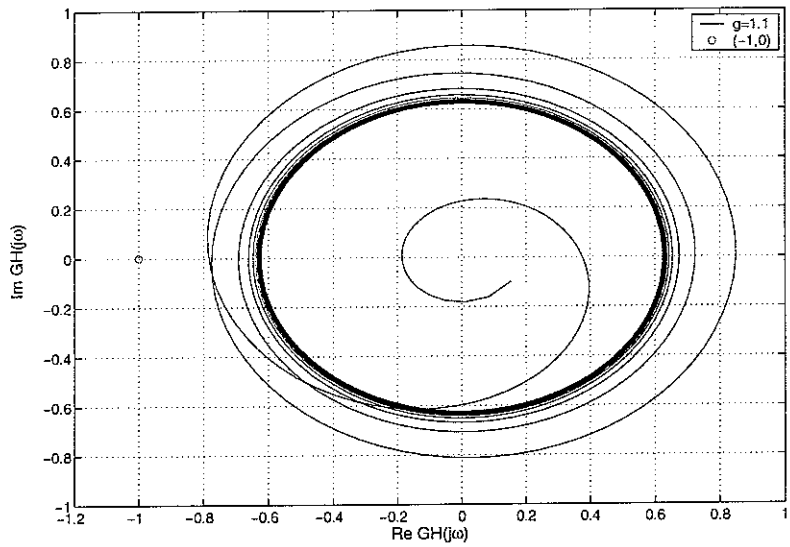

Figure 72: Nyquist plot of the negative feedback loop for $x = 0.0235\,m$ (apical site), derived for the Geisler generalised model with the value of gain, g, equal to 1.1. The circle indicates the point (-1,0).

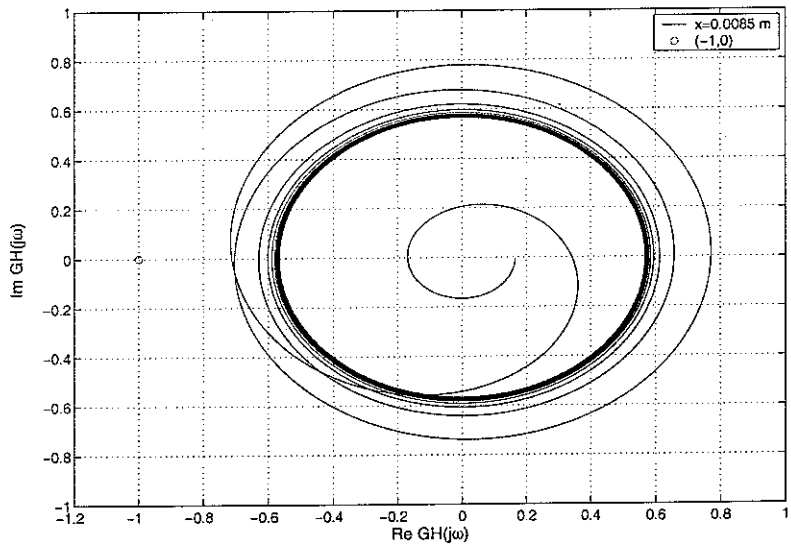

Figure 73: Nyquist plot of the negative feedback loop for $x = 0.0085\,m$ (basal site), derived for the Geisler generalised model with the value of gain, g, equal to 1. The circle indicates the point (-1,0).

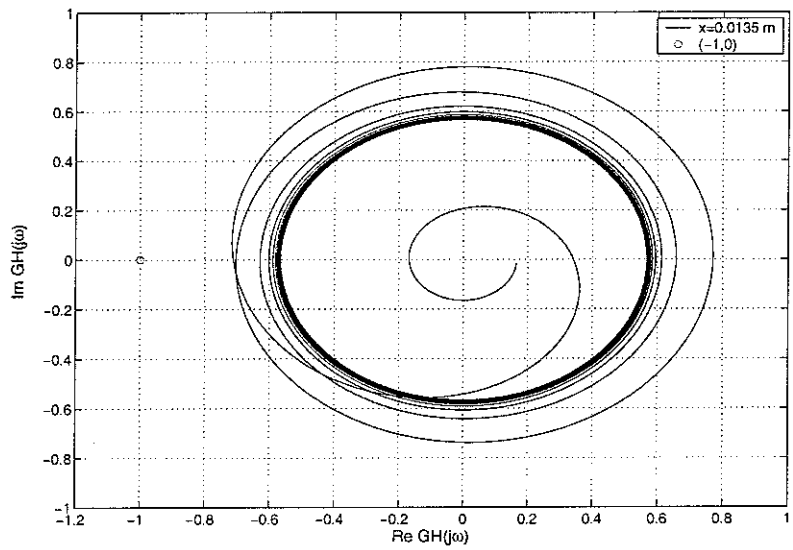

Figure 74: Nyquist plot of the negative feedback loop for $x = 0.0135\,m$, derived for the Geisler generalised model with the value of gain, g, equal to 1. The circle indicates the point (-1,0).

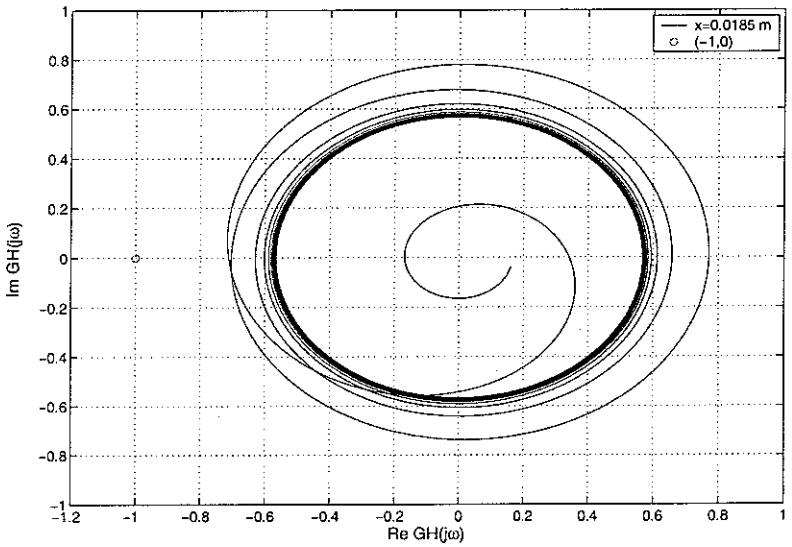

Figure 75: Nyquist plot of the negative feedback loop for $x = 0.0185\,m$, derived for the Geisler generalised model with the value of gain, g, equal to 1. The circle indicates the point (-1,0).

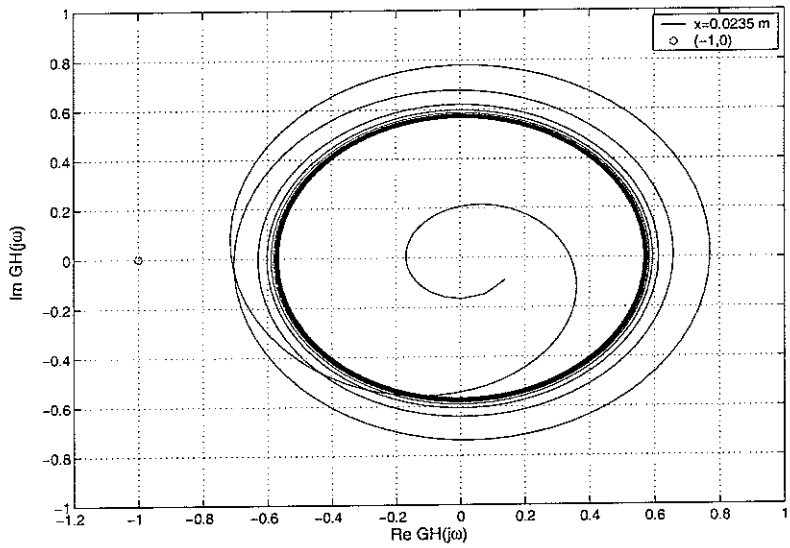

Figure 76: Nyquist plot of the negative feedback loop for $x = 0.0235\,m$ (apical site), derived for the Geisler generalised model with the value of gain, g, equal to 1. The circle indicates the point (-1,0).

9.5 Discussion

The Nyquist plots evaluated for the NK negative feedback systems show that increase in gain, g, to 1.1 leads to the instability, i.e. enclosure of the -1,0 point (circle in all figures), of the single system at $x = 0.0085\,m$ (Fig.60.), while the systems become more stable as the position shifts from the base to the apex of the cochlea (Figs.61-62.). This is qualitatively consistent with the results obtained for the NK model without generalisation examined in [16], where it was stated that the systems were set very close to instability in order to achieve the best tuning in the cochlea in regions of highest activity (basal sites). The estimation of boundary value of gain at two positions on the CP, for which the system is still stable will be presented in the next section.

Figure 63. depicts the stability check of a fully-active model for different positions along the cochlea calculated for constant gain ($g = 1$). In this case system is set close to instability at the position of $x = 0.0085\,m$ and, as the curves move further away from the -1,0 point, it becomes more stable with the increase of x.

The Nyquist plots evaluated for the G negative feedback systems, on the other hand, do not seem to prove the instability as the -1,0 point (circle in all figures) is not enclosed by any of the calculated curves. Nevertheless, there is a tendency for deterioration of stability of the single system while the gain is increased to 1.1, however, there is no significant difference between the curves calculated for corresponding gains at various positions x (compare e.g. Fig.66.,69. and 72.). Furthermore, plots in Figs.73-76. do not reveal significant differences between each other and remain stable for any examined position.

9.6 Investigation of Kolston's model

It has been argued by Kolston that an increase in the generation of the OHCs force exerting on the BM leads paradoxically to a decrease of the cochlear amplifier's gain and therefore to a decrease of the BM displacement [15].

In order to verify this result, the stability of the feedback system (with the CP velocity $\dot{v}_1$ as the system output), the magnitude and phase of the CP velocity $\dot{v}_1$ and the real and imaginary parts of the CP impedance, Z_p of the generalised model of NK has been investigated. Two cases, for stimulus frequencies $f_1 = 1kHz$ (reference) and $f_2 = 30kHz$ (Kolston's case), were computed. Additionally, for every case, three values of cochlear amplifier's gain, g, have been used: 0 (passive case corresponding to no OHC motility case in the Kolston's model), 0.5, 1 ('fully' active case corresponding to normal OHC motility-330 pN/nm case in the Kolston's model) and 1.7 ('enhanced' activity case corresponding to enhanced OHC motility-560 pN/nm case presented in [15]). The response was computed for the unit stapes velocity, $u_{st} = 1$, and referenced to the value of $2 \cdot 10^{-4}\, m/s$ (compare Sec.7.4.2).

First, the stability of the negative feedback loop as formulated in Sec.9.2 was also examined. The Nyquist plots were calculated for $x = 0.0185$ (reference) and $0.0023m$ (Kolston) (corresponding to $1kHz$ and $30kHz$ site on the CP in the NK generalised model, respectively) and three values of gain as mentioned before.

Secondly, the response (magnitude and phase) of the CP in terms of the partition velocity, $\dot{v}_1$, are presented in function of position on the BM, x, with the values of stimulus frequency and cochlear amplifier's gain as described above.

Finally, the corresponding (for $1\ kHz$, $30\ kHz$ stimulus frequency and three aforementioned values of the OHC force-generation gain, g) real and imaginary parts of the CP impedance, Z_p, have been plotted for comparison with Fig.4. (b, c, e, f) in [15].

As it was reported that the magnitude of the response tends to increase initially and then decrease with an increase of the amplifier's gain, the critical value of gain, $g_{critical}$ (i.e. the value of g as the transition from an increasing to decreasing magnitude of the response), was also estimated by calculating the peak response $|\dot{v}_1|_{max}$ for changing gain, g, from 0 to 2. The $g_{critical}$ was also estimated for two stimulus frequencies i.e. 1 and $30\ kHz$.

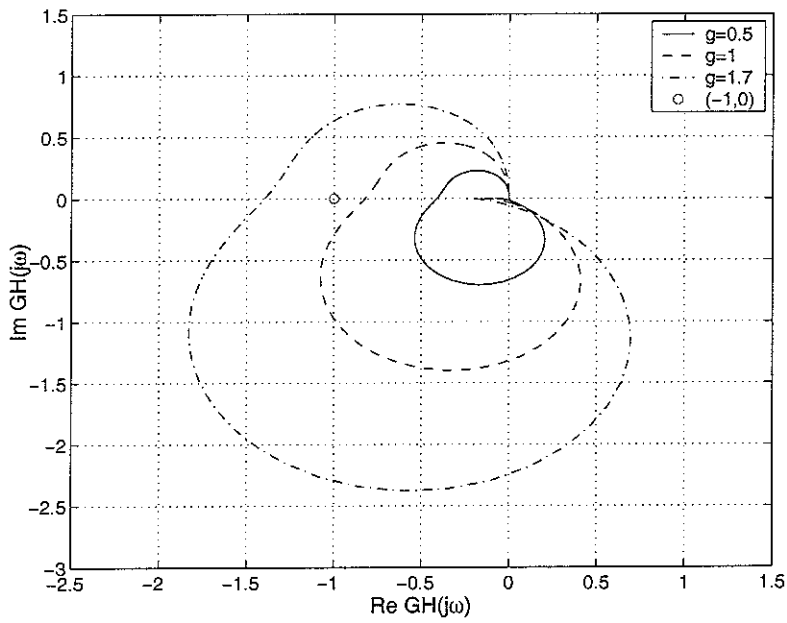

Figure 77: Stability of the negative feedback loop for $x = 0.0185\,m$ site corresponding to the maximum velocity, $\dot{v}_1$, for $f = 1\,kHz$ and $g = 1$. The solid, dashed and dash-dotted lines refer to the plots for g equal to 0.5, 1 and 1.7, respectively.

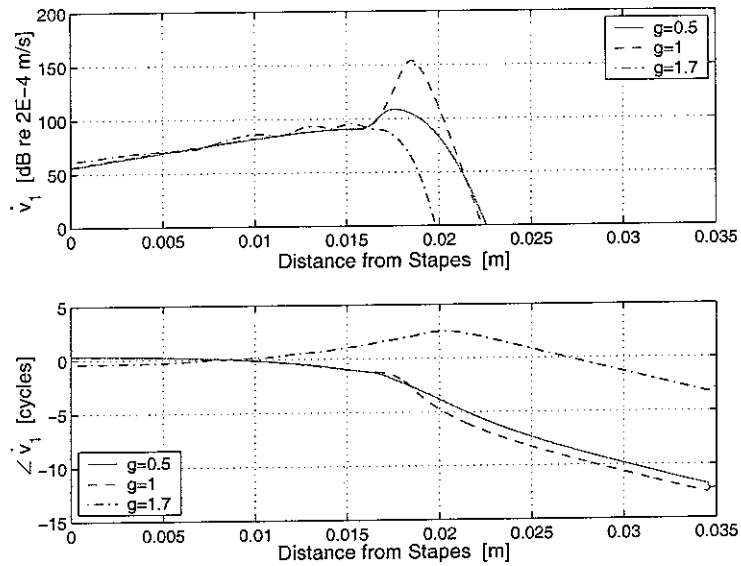

Figure 78: Magnitude (re $\dot{v}_{ref} = 2 \cdot 10^{-4}\, m/s$) and phase of the cochlear partition velocity, $\dot{v}_1$, of the generalised Neely&Kim model in function of position, x. Stimulus frequency $f = 1\, kHz$ and the OHC force-generation gain, g, set to 0.5 (solid), 1 (dashed) and 1.7 (dash-dotted).

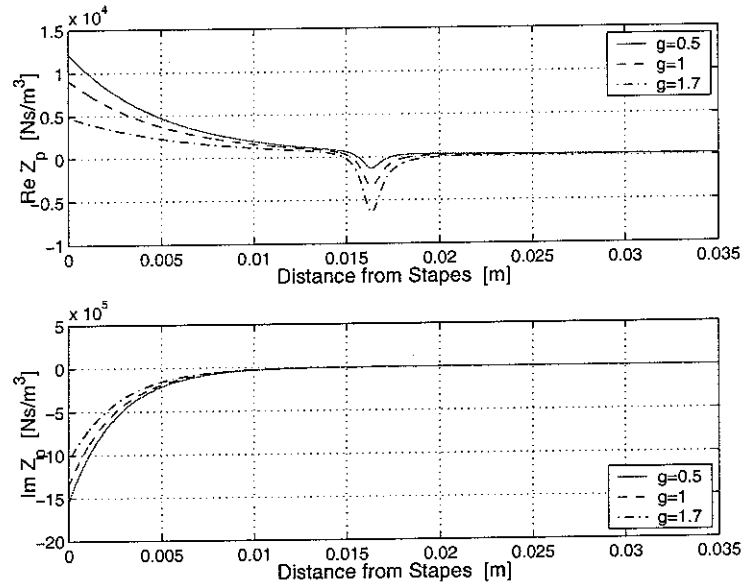

Figure 79: Real and imaginary parts of the cochlear partition impedance, Z_p, of the generalised Neely&Kim model in function of position, x. Stimulus frequency $f = 1\, kHz$ and the OHC force-generation gain, g, set to 0.5 (solid), 1 (dashed) and 1.7 (dash-dotted).

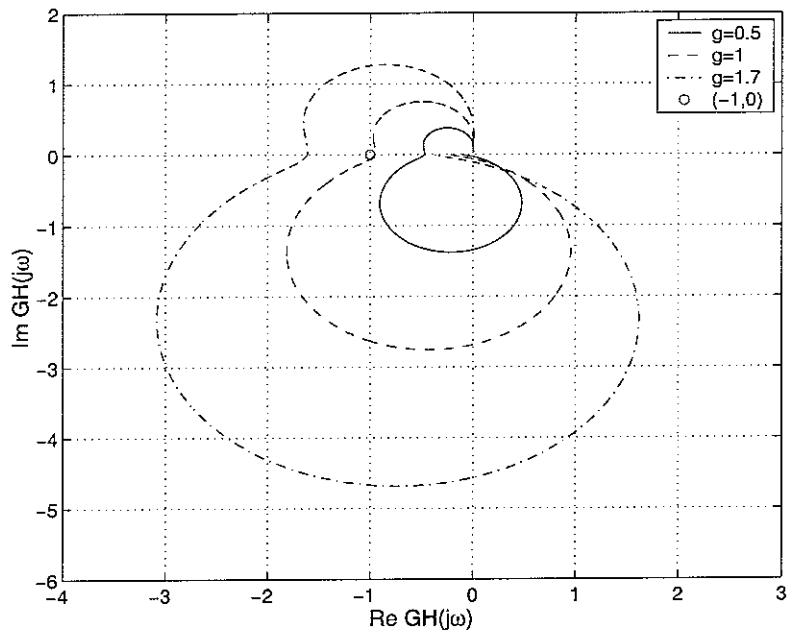

Figure 80: Stability of the negative feedback loop for $x = 0.0023\,m$ site corresponding to the maximum velocity, $\dot{v}_1$, for $f = 30\,kHz$ and $g = 1$. The solid, dashed and dash-dotted lines refer to the plots for g equal to 0.5, 1 and 1.7, respectively.

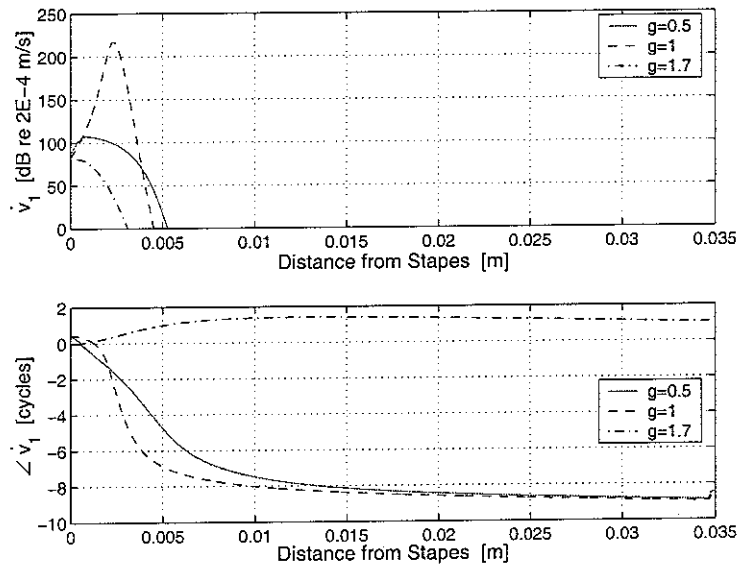

Figure 81: Magnitude (re $\dot{v}_{ref} = 2 \cdot 10^{-4}\, m/s$) and phase of the cochlear partition velocity, $\dot{v}_1$, of the generalised Neely&Kim model in function of position, x. Stimulus frequency $f = 30\, kHz$ and the OHC force-generation gain, g, set to 0.5 (solid), 1 (dashed) and 1.7 (dash-dotted).

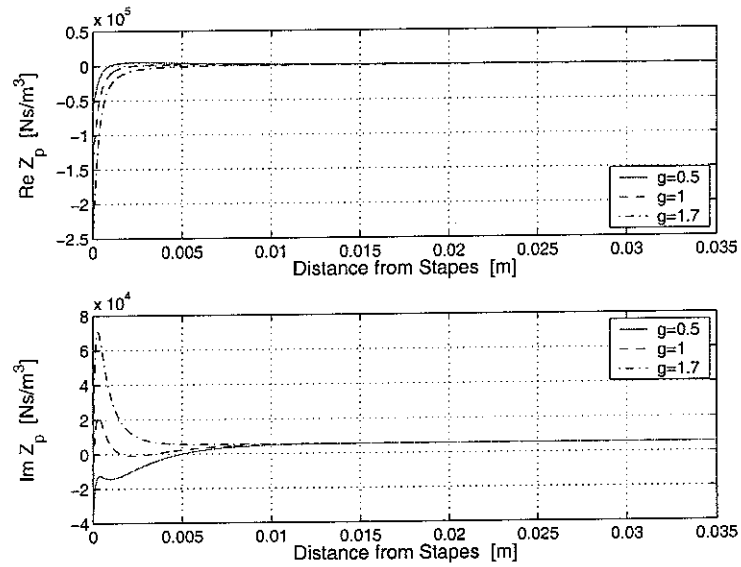

Figure 82: Real and imaginary parts of the cochlear partition impedance, Z_p, of the generalised Neely&Kim model in function of position, x. Stimulus frequency $f = 30\, kHz$ and the OHC force-generation gain, g, set to 0.5 (solid), 1 (dashed) and 1.7 (dash-dotted).

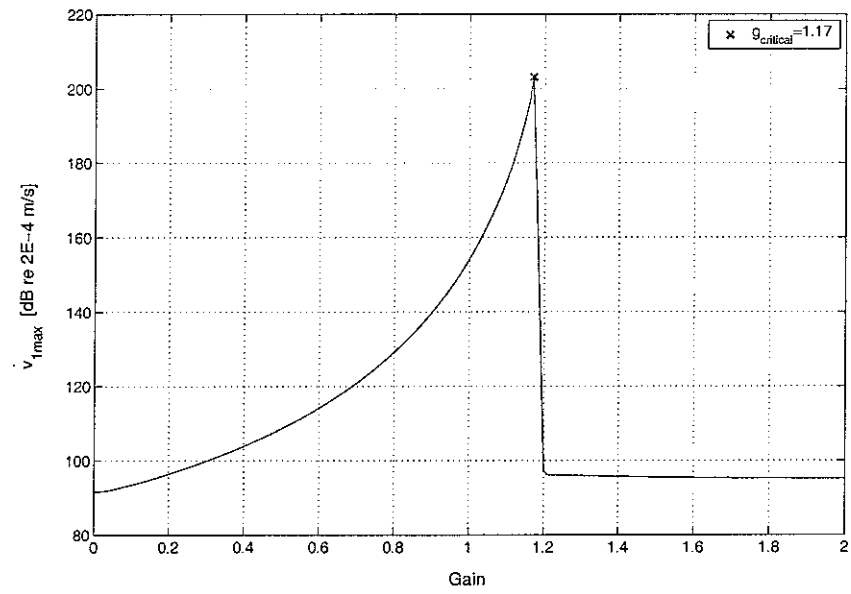

Figure 83: Apparent maximum magnitude (re $\dot{v}_{ref} = 2 \cdot 10^{-4} m/s$) of the cochlear partition velocity, $|\dot{v}_1|_{max}$, of the generalised Neely&Kim model in function of the OHC force-generation gain, g. Stimulus frequency $f = 1\, kHz$.

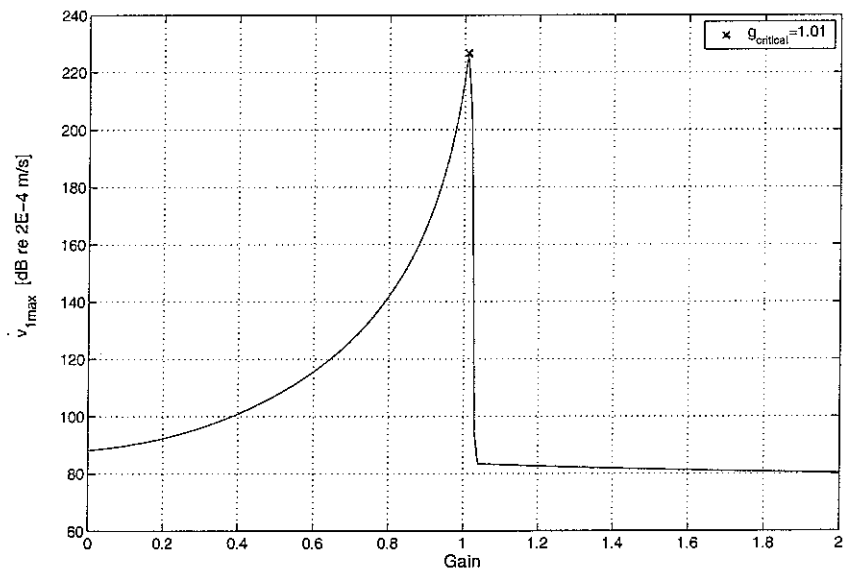

Figure 84: Apparent maximum magnitude (re $\dot{v}_{ref} = 2 \cdot 10^{-4} m/s$) of the cochlear partition velocity, $|\dot{v}_1|_{max}$, of the generalised Neely&Kim model in function of the OHC force-generation gain, g. Stimulus frequency $f = 30\, kHz$.

9.6.1 Discussion

According to Figs.78. and 81., with an increase of the gain, g, the CP velocity $\dot{v}_1$ increases subsequently to about 217 dB (active case, $g = 1$) and 154 dB (active case, $g = 1$) for $f = 1$ and $30\,kHz$, respectively, however, it decreases in the next step to about 80 and 95 dB, appropriately, though g was increased to 1.7. Appropriately, the phase plots show that the phase lags for $g = 0.5$ and 1 shift to phase lead with the increase of the amplifiers' gain to 1.7.

The system's response falls with the increasing gain but since for $g = 1.7$ the system is unstable, according to Nyquist plot in Figs.77. and 80., the frequency domain model is not valid and conclusions of Kolston not justified. Additionally, the critical value of gain, $g_{critical}$, estimated for both stimulus frequencies, $f = 1$ and $30\,kHz$, indicate that the response of the models will start to fall with values of gain higher than 1.17 and 1.01, appropriately. The maximum of the response decreases with the increase of gain as depicted in Figs.83-84. and so that the $g_{critical}$ values determine the point of singularity, which causes the instability of the system.

Furthermore, the existence of a pole/s in the right half of the $j\omega$ plane defines a *nonminimum-phase* system, which, according to de Boer [7], may represent a characteristic of a non-classical but not a classical or three-dimensional model like the one of Kolston.

Finally, the real part of the CP impedance, Z_p, resemble the characteristic of the ones presented by Kolston in Fig.4. (b, c) in [15]. However, the imaginary part plots of the partition impedance depicted in Fig.82. of present work are not consistent with the ones of Kolston for the normal ($g = 1$) and enhanced activity ($g = 1.7$) of OHCs (see Fig.4., e and f in [15]). There is some similarity for the imaginary curves in the region between 0 to $40\,\mu m$ from the spiral lamina (Fig.4. e, f in [15]) but due to the assumption that the displacement of the NK model is averaged across the width of the CP (assumption holds also for the generalised model), it may not represent the behaviour of the BM impedance imaginary part.

10 Nonlinearity

Along with the improvement in techniques for measuring the BM response, new phenomena have been discovered. The most prominent and crucial in light of the modelling efforts, was the finding of the BM nonlinearity (see Section 2.3.2). The BM displacement in function of the stimulus level, as observed first by Rhode (Rhode, 1971), revealed a highly nonlinear dependence. Precisely, the nonlinearity of the BM response appeared to be most pronounced in the region of its highest sensitivity (peak of the response), frequency dependent and, primarily, of a compressive character [1].

Initiated by the Rhode's findings, the studies on the cochlear nonlinearity confirm the former discovery and show a number of phenomena commencing with the level-dependent nonlinearity of the BM response, two-tone suppression or the generation of the distortion products (see section 2.3.2).

The level-dependent nonlinearity appears to be a mainly compressive function, even though, a case of an expansive characteristic has been also reported (see Fig.11. in [25]). Different results, however, are observed in different species, as well as some dependence on the site of the BM investigated (base or apex), which lead to different sensitivity functions and cochlear gains. The gain at the $9 - 10\ kHz$ site (more apical region) of the guinea pig cochlea showed ranges of cochlear gain from $35 - 58\ dB$, for example, while the value of $35\ dB$ at the $17-18kHz$ site (more basal region) of the chinchilla cochlea (Table 1. in [25]. The gain is measured in terms of displacement and defined by the difference between the peaks in the sensitivity functions estimated for low- and high-intensity tones or *in vivo* and *post-mortem* responses [25]). In conclusion, since the activity in the cochlea (cochlear amplifiers gain) appears to be inseparably related with the nonlinear effects (most pronounced in the peak region of the BM response), the building of a nonlinear, active model of the cochlea seems to be important for the full understanding of the cochlear dynamics as well as for elimination of the discrepancies in the physiological results by verification of the experimental artefacts resulting from the measurement method used or condition of the cochlea preparation.

In the following section a nonlinear cochlear model will be presented. A compressive nonlinearity was introduced into the NK and G generalised, active models solved in Section 5. The model works by iteratively calculating the level and hence the nonlinear gain and so is similar to the quasilinear approach of [13, 16].

10.1 The Nonlinear Positive Feedback System

It was suggested by Yates that a nonlinear cochlear model can be considered as a simple positive feedback system with source of energy as input, some sort of output and a nonlinear element in feedback path [27, 28]. Figure 85. shows

a block diagram of such conceptual model in which the feedback path consists of a plant G (feedforward gain), nonlinear network Φ and a frequency-selective network, β (a bandpass filter to select the fundamental component of $v(t)$, the loop output). The latter network provides the gain to the input signal (also β), which amplifies the fundamental frequency and attenuates the harmonics when the input is tonal [8].

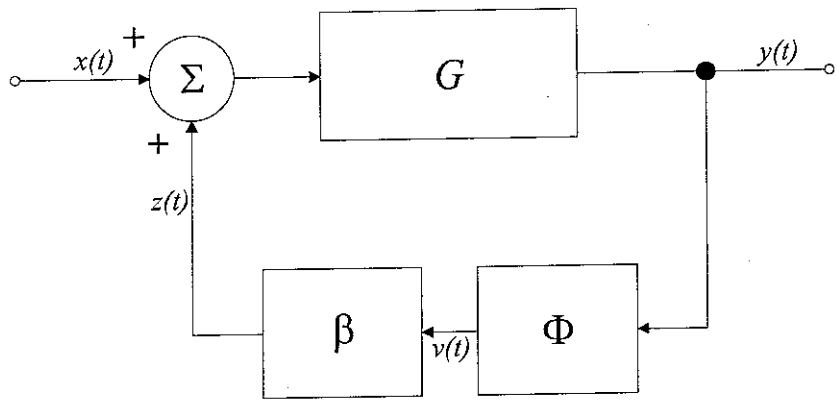

Figure 85: A block diagram of the feedforward loop as proposed by Yates [28]. The parameter $x(t)$ represents the input, whereas the $y(t)$, the output of the loop. The G denotes the plant while the Φ and β the nonlinear network and frequency-selective network, respectively.

From the analogy between the cochlea and the proposed model, the input of the feedback loop refers to the pressure difference in the cochlear fluids and the plant, G, to the BM with its motion. The nonlinear network Φ, as suggested by Yates, is of a form of a simple Boltzmann function (check [28] for details), while the frequency-selective network, β, can account for the changes in the cochlear displacement-sensitivity as in the case of damage to the OHCs [28].

As assumed by Yates, the nonlinear feedback network, Φ, is a saturating function with an input/output characteristic given by

$$v(t) = \frac{Ay(t)}{A + y(t)}, \tag{124}$$

where $y(t)$ represents the input of Φ, whereas $v(t)$, its output. The parameter A is an arbitrary threshold amplitude set to 10^4 in [27].

Following from the Eq.124., the instantaneous gain, Φ, is explicitly expressed by

$$\Phi(t) = \frac{A}{A + y(t)}. \tag{125}$$

With such input/output characteristic, the nonlinear element, Φ, will be ≈ 1 and so $v(t) \approx y(t)$, thus behaving linearly when subject to a low-amplitude

input, i.e. $|y(t)| < A$. However, at high amplitudes, $|y(t)| > A$, the gain. Φ. will approximate to $A/y(t)$, therefore reaching the threshold A and saturating i.e. $v(t) \approx A$ [8].

In the frequency domain the overall gain, G_{closed} (ratio of the complex output, Y, to the complex input, X), of the nonlinear feedback system depicted in Fig.85., is formulated by

$$G_{closed} = \frac{G}{1 - \beta\Phi_D G}. \tag{126}$$

where G and β are linear constants, chosen to give a product of βG slightly less than unity (typically $\beta = 0.999$), while Φ_D (index D denotes the describing function) is a real number that reflects the average value of $\Phi(t)$, which depends on the output signal amplitude [27, 8].

The feedback system described above, can be defined by a describing function being the Eq.125. itself as $y(t) = Y$ [8]. Additionally, since it was assumed by Yates that $|G| = 1$ and $\angle G = 0$, the complex input and output signals, X, Y, V, respectively, can be taken as real numbers, so that the gain of the feedback path will take form

$$\Phi_D = \frac{|V|}{|Y|}, \tag{127}$$

and

$$\beta\Phi_D = \frac{\beta A}{A + |Y|}. \tag{128}$$

10.2 The Model of Neely and Kim

For the derivation of the nonlinear NK generalised model the plant, G, and controller, H, have to be first defined as the positive feedback components. Furthermore, the output of the feedback loop referred to $y(t)$ in Fig.85., is now assumed to be the CP velocity, $\dot{v}_1$ in contrast to Section 9.2. A block diagram, showing the analogy of the NK generalised model feedback loop to the positive feedback loop proposed by Yates (Fig.85.), is depicted in Fig.86.

Similarly, as in Sec.9.2, differentiating

$$v_3(x) = v_1(x) - v_2(x), \tag{129}$$

with respect to time gives the formulation of the relative velocity $\dot{v}_3(x)$

$$\dot{v}_3(x) = \dot{v}_1(x) - \dot{v}_2(x), \tag{130}$$

and

$$\dot{v}_1(x) = \dot{v}_3(x) + \dot{v}_2(x). \tag{131}$$

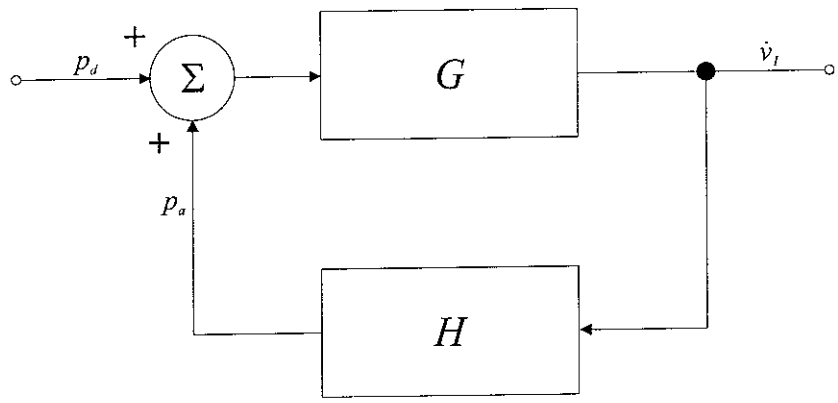

Figure 86: A block diagram of the feedforward loop for the Neely&Kim generalised model. The acoustic pressure p_d represents the input, whereas the velocity, $\dot{v}_1$, the output of the loop. The G and H terms denote the plant and the controller, respectively.

While

$$Z_2\dot{v}_2(x) = Z_3\dot{v}_3(x), \tag{132}$$

after rearrangement, $\dot{v}_2(x)$ takes form

$$\dot{v}_2(x) = \frac{Z_3}{Z_2}\dot{v}_3(x). \tag{133}$$

Substituting Eq.133. to Eq.131., the velocity $\dot{v}_1(x)$ equals

$$\dot{v}_1(x) = \left(1 + \frac{Z_3}{Z_2}\right)\dot{v}_3(x), \tag{134}$$

thus

$$\dot{v}_3(x) = \frac{Z_2}{Z_2 + Z_3}\dot{v}_1(x). \tag{135}$$

The equation of motion (EOM) in the frequency domain is formulated by

$$p_d(x) - p_a(x) = Z_1\dot{v}_1(x) + Z_3\dot{v}_3(x). \tag{136}$$

Subsequently, substituting the expression for p_a

$$p_a(x) = -gZ_4\dot{v}_3(x), \tag{137}$$

to Eq.136., the EOM takes form

$$p_d(x) - (-gZ_4)\dot{v}_3(x) = Z_1\dot{v}_1(x) + Z_3\dot{v}_3(x). \tag{138}$$

Equivalently

$$p_d(x) + \left(\frac{gZ_2Z_4}{Z_2 + Z_3}\right)\dot{v}_1(x) = Z_1\dot{v}_1(x) + \left(\frac{Z_2Z_3}{Z_2 + Z_3}\right)\dot{v}_1(x). \tag{139}$$

or

$$p_d(x) + \left(\frac{gZ_2Z_4}{Z_2+Z_3}\right)\dot{v}_1(x) = \left[\frac{Z_1(Z_2+Z_3)+Z_2Z_3}{Z_2+Z_3}\right]\dot{v}_1(x). \tag{140}$$

Dividing Eq.140. by the bracketed term of its right-hand side gives

$$\underbrace{\frac{Z_2+Z_3}{[Z_1(Z_2+Z_3)+Z_2Z_3]}}_{G} p_d(x) + \underbrace{\frac{Z_2+Z_3}{[Z_1(Z_2+Z_3)+Z_2Z_3]}}_{G}\underbrace{\left(\frac{gZ_2Z_4}{Z_2+Z_3}\right)}_{H}\dot{v}_1(x) = \dot{v}_1(x). \tag{141}$$

where G denotes the plant and H, the controller of the closed feedback loop.

Equation 141. expressed by means of G and H amounts to

$$Gp_d(x) + GH\dot{v}_1(x) = \dot{v}_1(x), \tag{142}$$

therefore

$$\dot{v}_1(x) = \frac{G}{1-GH}p_d(x), \tag{143}$$

which appears in the form of a classical positive-feedback system with the G and H components formulated in Eq.141.

The gain of the feedback path in the nonlinear, positive feedback loop now takes form of the one presented in Eq.128. and it will replace the gain, g in the formulation of the generalised NK positive feedback loop introducing the nonlinear element to the model. Taking the maximum of the absolute value of the CP velocity, $max(|\dot{v}_1|)$, corresponding to the maximum of the absolute value of the output signal $|Y|$ in Eq.128., $max(|Y|)$, the β term can be omitted and the controller H defined in Eq.141. will be now formulated as

$$H = \underbrace{\left(\frac{A}{A+|\dot{v}_1|_{max}}\right)}_{\Phi_D=g}\frac{Z_2Z_4}{Z_2+Z_3} \tag{144}$$

Finally, with the formulation in Eq.144., the entire system can be represented as a positive feedback loop with the input of the pressure difference, p_d, the plant, G, and the controller, H, which is adapted instantaneously by the nonlinear network, Φ_D (through the instantaneous change of the gain, g), scheduled on the output, the CP velocity, $\dot{v}_1$. The components of the aforementioned system, will be described by the Eqs.141. and 144. and is depicted in Fig.87.

10.3 The Stability of the Positive Feedback System

The formulation of the positive feedback loop components, the gain of the plant, G and gain of the loop, H (controller), enables us to check the stability of the system by means of the Nyquist criterion (Note that the formulation of

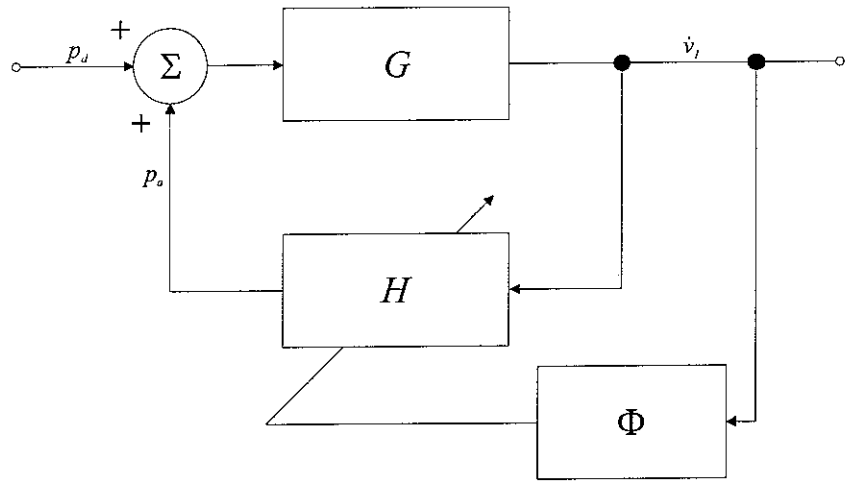

Figure 87: A block diagram of the feedforward loop for the Neely&Kim generalised model with the nonlinear network Φ scheduled on the output $\dot{v}_1$ and adapting the controller H.

stability differs from that presented in Sec.9.2., since it was determined for a negative feedback and not a positive feedback system as in this case). Figures 88-91. show the stability of the positive feedback system described in previous section for different values of the position x i.e. 0.0085, 0.0135, 0.0185, 0.0235 m with the gain, g set to one, and for different values of the gain, g i.e. 0.7, 1 and 1.1, with the position, x set to 0.0085 (basal site), 0.0185 (point on the CP corresponding to the maximum displacement, v_1 for 1 kHz) and 0.0235 m (apical region) for every case.

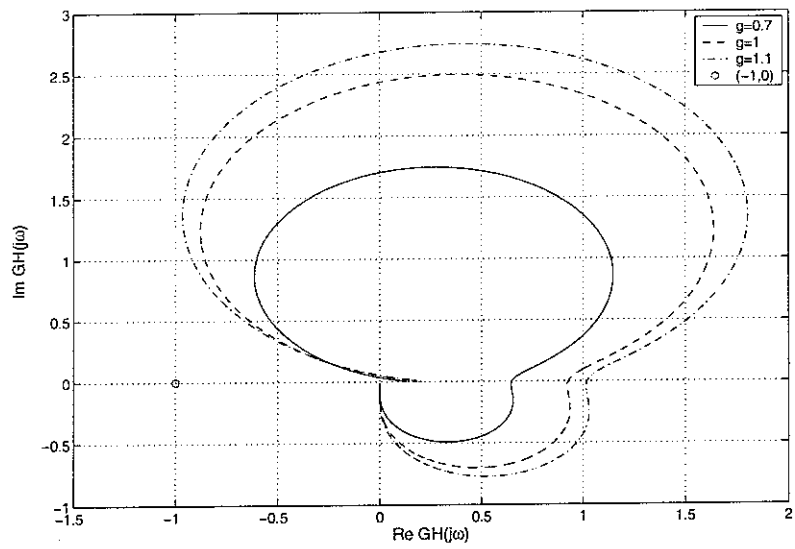

Figure 88: Nyquist plots of the positive feedback loop for $x = 0.0085\,m$ (basal site), derived for the Neely&Kim generalised model with the solid, dashed and dash-dotted lines referring to the values of gain, g, equal to 0.7, 1 and 1.1, respectively. The circle indicates the point (-1,0).

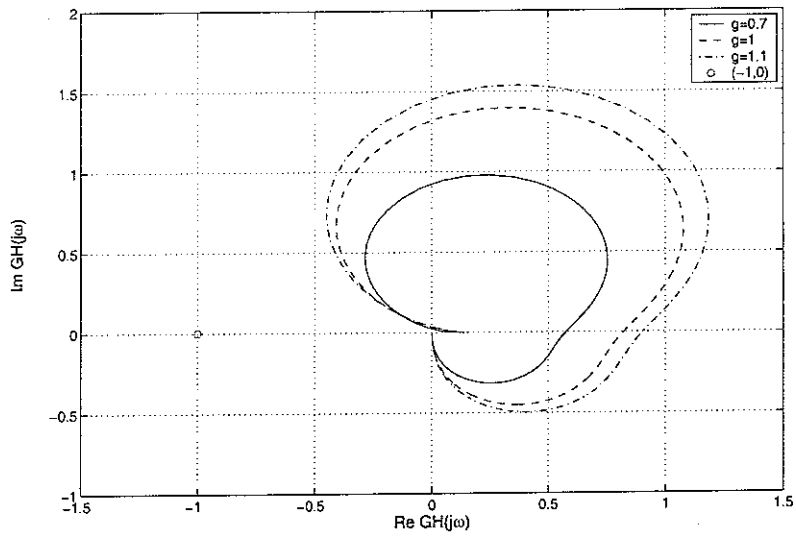

Figure 89: Nyquist plots of the positive feedback loop for $x = 0.0185\,m$ (site of the maximum displacement of the CP for $f = 1kHz$), derived for the Neely&Kim generalised model with the solid, dashed and dash-dotted lines referring to the values of gain, g, equal to 0.7, 1 and 1.1, respectively. The circle indicates the point (-1,0).

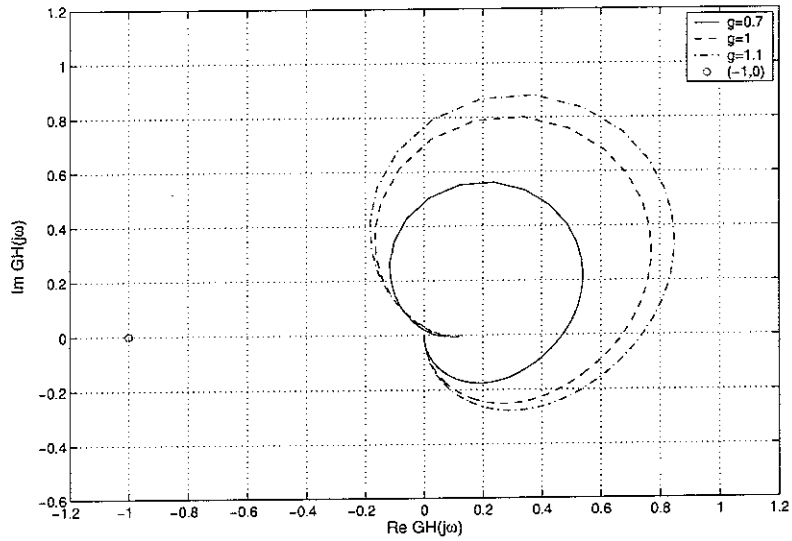

Figure 90: Nyquist plots of the positive feedback loop for $x = 0.0235\,m$ (apical site), derived for the Neely&Kim generalised model with the solid, dashed and dash-dotted lines referring to the values of gain, g, equal to 0.7, 1 and 1.1, respectively. The circle indicates the point (-1,0).

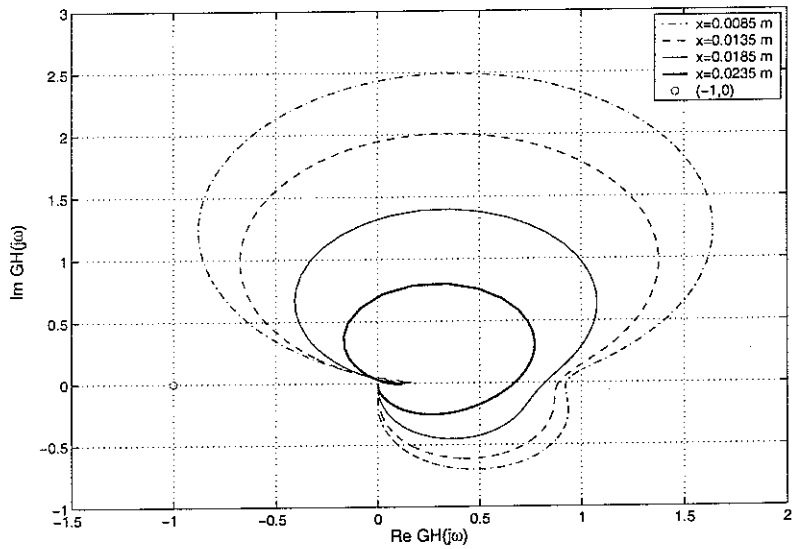

Figure 91: Nyquist plots of the positive feedback loop for $g = 1$ (active model), derived for the Neely&Kim generalised model with the dash-dotted, dashed, solid and bold lines referring to the values of position on the CP, x, equal to 0.0085, 0.0135, 0.0185 and 0.0235 m, respectively. The circle indicates the point (-1,0).

10.4 The Results

As in the previous sections, the nonlinear model was also solved in a *Matlab* (see Appendix C). The generalised NK model script used for computation of the CP response (macromechanical model solved in Sec.7.4), was modified to include the nonlinear component. The gain, g, was set to one ('fully' active model) to calculate the initial CP velocity, $\dot{v}_1$, (for the frequencies from 10 to 10000 Hz) and altered, according to Eq.144., iteratively in a loop sequence, recalculating the response (output), $\dot{v}_1$. The whole sequence was calculated in six steps (including the first value of $g = 1$) for the gain, g, to stabilise. Additionally, the gain component in Eq.144. was multiplied by the factor of 5/6 to advance the saturation (stabilisation in the whole range of frequencies or for every position on the cochlea) of the gain, g, as it was found to oscillate for some values of the input level (transition region observed for 60 dB SPL input level).

The input level was changed through the changes of the stapes velocity, u_{st} (see the source vector, q, in the formulation of the finite difference approximation of the wave equation in Eq.98.), to give a certain value of the response level in terms of the pressure difference, p_d, (in dB SPL) for the linear model with g set to unity. This gives a value of stapes velocity, $u_{st} = 2.5016 \cdot 10^{-10}\, m/s$ to reach the 20 dB SPL stimulus level (linear, active model; $g = 1$), and every increase of one order to increase the level by 20 dB SPL.

The threshold amplitude, A (check Eq.144.), was estimated through trial and error method and set to $1.54 \cdot 10^{-5}$ (amounts approximately to the half and one order decreased maximum of the absolute value of the CP velocity $|\dot{v}_1|$, calculated for $g = 1$ and u_{st} corresponding to 20 dB SPL level of the input stimulus i.e. 20 dB SPL pressure difference, p_d, in the cochlear fluid.

Next, dividing the results for the CP velocity $\dot{v}_1$ by the factor of $j\omega$, the response in terms of the CP displacement was calculated. The plots for both, the CP velocity in function of position, x, and the CP displacement in function of frequency, f, are presented for five different stimulus levels i.e. 20, 40, 60, 80 and 100 dB SPL (the lowest and highest value of the stimulus level, namely 20 and 100 dB SPL, correspond to the estimated limits of the compression region in the BM response. Check Sec.2.3.2).

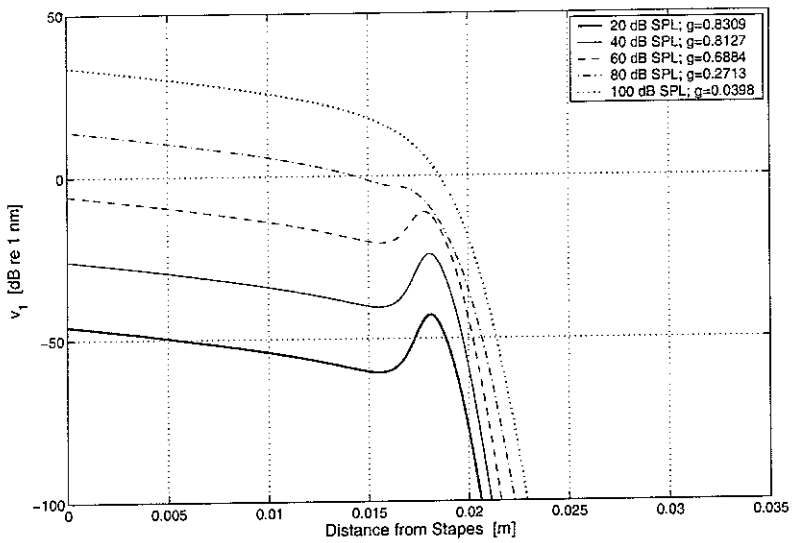

Figure 92: The CP displacement v_1 as a function of position, x, for the NK generalised nonlinear model for five stimulus levels (frequency $f = 1\ kHz$, the values of gain, g, calculated for the applied stimulus levels are also indicated on the plots).

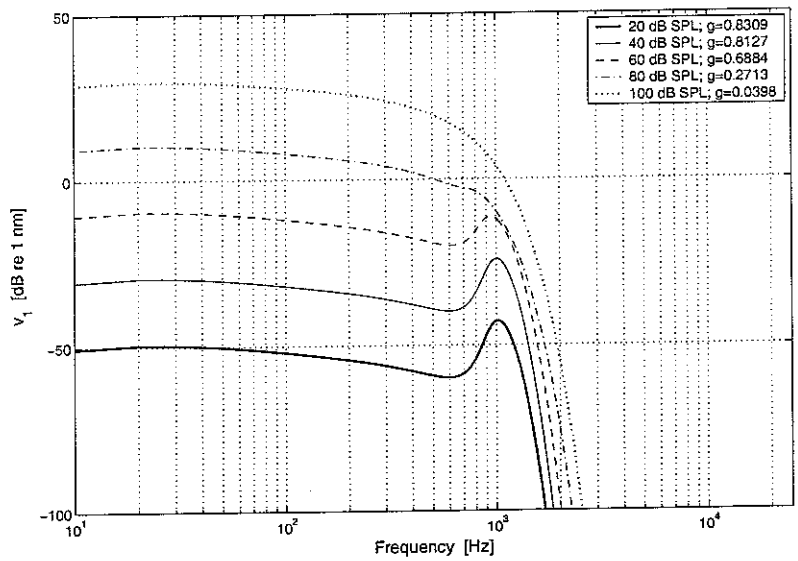

Figure 93: The CP displacement v_1 in function of frequency, f, for the NK generalised nonlinear model for five stimulus levels (position $x = 0.0185\ m$, the values of gain, g, calculated for the applied stimulus levels are also indicated on the plots).

10.5 Discussion

This nonlinear model does provide compression. The nonlinearities modelled on the basis of cochlear amplifier's gain, g, thus through the activity of the OHCs, produce a physically realistic response. The response curves (the CP displacement v_1) in Fig.92. and 93. have the main features of the function of a healthy cochlea. An increase of the stimulus level causes a decrease in the gain of the cochlear amplifier, g, so that the response becomes less active to finally resembles the one of a passive cochlea i.e. for the stimulus level of 100 dB SPL (compare Fig.10.). Furthermore, the magnitude of the CP displacement decreases at the position of the characteristic place (Fig.92.) and characteristic frequency (Fig.93.) i.e. for $x = 0.0181m$ and $f = 1020Hz$, respectively. Also the characteristic shift of the maximum of the modelled responses towards basal sites of the cochlea models the behaviour of the responses recorded in the real cochlea. Parallel curves below and above the characteristic place (CF in Fig.92.) indicate that the response remains linear outside these loci, which is also consistent with the results of physiological experiments.

The gain, g, decreases with an increase of the stimulus level, however, it reveals a very strong dependence on the frequency of the stimulus. The factor of 5/6, chosen to accelerate the saturation of gain, is rather satisfactory in the presented range of frequencies (up to 25 kHz), however, for the high frequencies, e.g. 25 kHz, the gain oscillates at 80 dB SPL stimulus level. Thus the number of steps in the loop sequence (see Sec.10.4.), used to recalculate the output, determines which of two oscillating values of gain will define the output for the given stimulus level. Therefore, it may occur that the curves calculated for 60 and 80 dB SPL intersect, thus designate the transition region, which was closer analysed for estimation of the multiplication factor of 5/6. Furthermore, as the gain, g, is strongly frequency-dependent, it saturates slower for lower frequencies than for the ones from the end of the 25 kHz range, hence the curves in Fig.93. do not demonstrate a roll-off for the below CF frequencies.

The threshold amplitude A remained constant for all computations, however, it showed a big influence on the stabilisation of gain while being estimated. First, the estimation of the threshold amplitude A should be performed on the basis of physiological data. Secondly, using a distribution of value of A on the frequency, since the threshold of saturation changes with the frequency of the stimulus (Note also that in previous sections a negative feedback was used, which might widened the bandpass of frequencies for which the parameters of the whole system were constant), seems more appropriate for the calculation of the gain (see Eq.144.) and may eliminate the need of advancing the saturation (multiplication factor 5/6).

Finally, the Nyquist plots show that the positive feedback system is stable for any position on the CP (becoming more stable while moving towards the apical sites of the cochlea). Likewise, a change in gain (from 0.7 to 1.1) does not cause

the instability of the system on the contrary to the negative feedback system becoming unstable for gain of 1.1 (system set close to instability at the basal sites of the cochlea as examined for the gain of 1, check Sec.9.4.).

11 General Discussion and Conclusions

The presented results show that the mechanical analysis enabled a generalisation of the two models of cochlear mechanics, the classical models of Neely&Kim [21] and Geisler [11]. A reduction in number of variables and constants led to a more clear representation of each of the models, however, a check of the models' response revealed the elimination of the characteristics of cochlear activity in the response of the G generalised model. No significant discrepancies between the 'original' and generalised NK model were observed (compare [16]). At every stage of investigation, both models showed a need for a physical (mathematical) clarity, simplicity and consistency e.g. the lack of uniform representation of the mechanical parameters (noticed also across the literature of the topic, compare [20]), which, along with the mathematical complexity of the Geisler model, impeded the comparison of the models.

Investigation of the modes of vibration derived for the NK model, presented in Sec.4, determined the mechanical properties of the lumped component model. Existence of two modes of vibration and the in- and anti-phase vibrations of the BM/TM complex is consistent with the theory of vibrations as well as with the results in [19, 4]. However, the peculiarities of the presented mechanical analysis, state the necessity of comprehensive study of the vibrations in the cochlea.

The stability check states that the NK model defined as a negative feedback system is set very close to instability, particularly for the basal positions in the cochlea, so that a small change in the gain may cause the system unstable. The model of G is stable for any of the values of gain examined and every position on the CP. In conclusion, every model built in the frequency domain, should be checked in terms of stability by means of an appropriate stability test in order to justify the assumption of the steady output of the system (see Sec.9.6). In case of the positive feedback system evaluated for the NK generalised model the Nyquist plots indicate the system is stable at every position on the CP (each single component) as well as for every value of gain examined.

Additionally, all the assumptions concerning either the mechanical (physical) or physiological properties of the model should be supported by a relevant analysis to avoid false conjectures and/or conclusions like in [15] or [24].

Finally, the response of the quasi-linear model of the cochlea, evaluated for the NK generalised model, resembles the main features of the real cochlea responses recorded for different stimulus levels. Therefore, the level-dependent model of the nonlinearity scheduled on the output of the positive feedback system, with notes presented in Sec.10.5, is satisfactory for the modelling of the compressive characteristic of the cochlear response.

12 Recommendations for Future Work

It is recommended that for the future research concerning the modelling of the cochlea a thorough review of the literature be undertaken to estimate a comprehensive set of mechanical parameters corresponding to the physiological and anatomical data from the real cochlea. The parameters and physical properties should correspond to one extracted from the cochlea of a single selected species. Furthermore, the values of all variables and constants should be made realistic e.g. the models should be calculated for the u_{st} corresponding to the stimulus level of 20 dB SPL (maximum activity) for the comparison with the physiological data.

Next, the main features of the modelled response such as maximum sensitivity for the CP/BM velocity and displacement along with the phase examinations, the Q_{10} factor, should be checked and compared with the physiological results of experiments made on the same species.

Finally, the vibrations of the lumped component models should be examined to determine the modes of vibration of the system and the mutual influence of the system's components i.e. BM/TM complex.

13 Appendix A

The CF, related with the position x along the BM (referred also as the cochlear frequency-place map), proposed by Greenwood is formulated as

$$CF = A\left(10^{ax/L} - K\right), \tag{145}$$

where:

CF characteristic frequency
A constant controlling the high frequency properties of the map [Hz]
a constant controlling the slope of the map
x distance from the apex [mm]
L length of the BM [mm]
K constant controlling the low frequency properties of the map [Hz]

There has been a number of experiments done on the cochleae of different species to estimate the parameters given in Eq.145. Table 2. presents the parameters for the human and cat cochleae evaluated by [12] and [17], respectively.

SPECIES	A	a	L	K
Human	165	2.1	35	1.0
Domestic cat	456	2.1	25	0.8

Table 2: List of parameters referring to the cochlear frequency-place map function evaluated for the human [12] and domestic cat [17] cochleae.

According to Table 2., the constants given above differ, with exception of a, for the human and cat cochlea. Denoting

A_H constant A for a human cochlea [Hz]
A_C constant A for a cat cochlea [Hz]
a constant controlling the slope of the map
x_H x in a human cochlea [mm]
x_C x in a cat cochlea [mm]
L_H L in a human cochlea [mm]
L_C L in a cat cochlea [mm]
K_H K in human cochlea [Hz]
K_C K in cat cochlea [Hz]

the human CF function is expressed as

$$CF_H = A_H \left(10^{ax_H/L_H} - K_H\right), \tag{146}$$

and for the cat's cochlea

$$CF_C = A_C \left(10^{ax_C/L_C} - K_C\right). \tag{147}$$

Equating Eqs.146. and 147., after simple arithematical development, the relationship between the x_H and x_C can be evaluated

$$A_H \left(10^{ax_H/L_H} - K_H\right) = A_C \left(10^{ax_C/L_C} - K_C\right), \tag{148}$$

$$A_H 10^{ax_H/L_H} - A_H K_H = A_C 10^{ax_C/L_C} - A_C K_C, \tag{149}$$

$$A_H 10^{ax_H/L_H} - A_C 10^{ax_C/L_C} = A_H K_H - A_C K_C, \tag{150}$$

$$log\left(A_H 10^{ax_H/L_H}\right) - log\left(A_C 10^{ax_C/L_C}\right) = log(A_H K_H) - log(A_C K_C), \tag{151}$$

$$log(A_H) + log\left(10^{ax_H/L_H}\right) - log(A_C) + log\left(10^{ax_C/L_C}\right) = log\left(\frac{A_H K_H}{A_C K_C}\right), \tag{152}$$

$$log\left(10^{ax_H/L_H}\right) - log\left(10^{ax_C/L_C}\right) = log\left(\frac{A_H K_H}{A_C K_C}\right) - log\left(\frac{A_H}{A_C}\right), \tag{153}$$

$$\left(\frac{ax_H}{L_H}\right) log(10) - \left(\frac{ax_C}{L_C}\right) log(10) = log\left(\frac{A_H K_H}{A_C K_C} \cdot \frac{A_C}{A_H}\right), \tag{154}$$

$$a\left(\frac{x_H}{L_H} - \frac{x_C}{L_C}\right) = log\left(\frac{K_H}{K_C}\right), \tag{155}$$

$$L_C x_H - L_H x_C = \frac{L_C L_H}{a} log\left(\frac{K_H}{K_C}\right), \tag{156}$$

$$x_H = \frac{L_H}{L_C} x_C + \frac{L_H}{a} log\left(\frac{K_H}{K_C}\right). \tag{157}$$

After numerical evaluation, using the values given in Table 2., the relationship in Eq.157. amounts to

$$x_H \cong 1.4 x_C + 1.62, \tag{158}$$

and depicted in Fig.94.

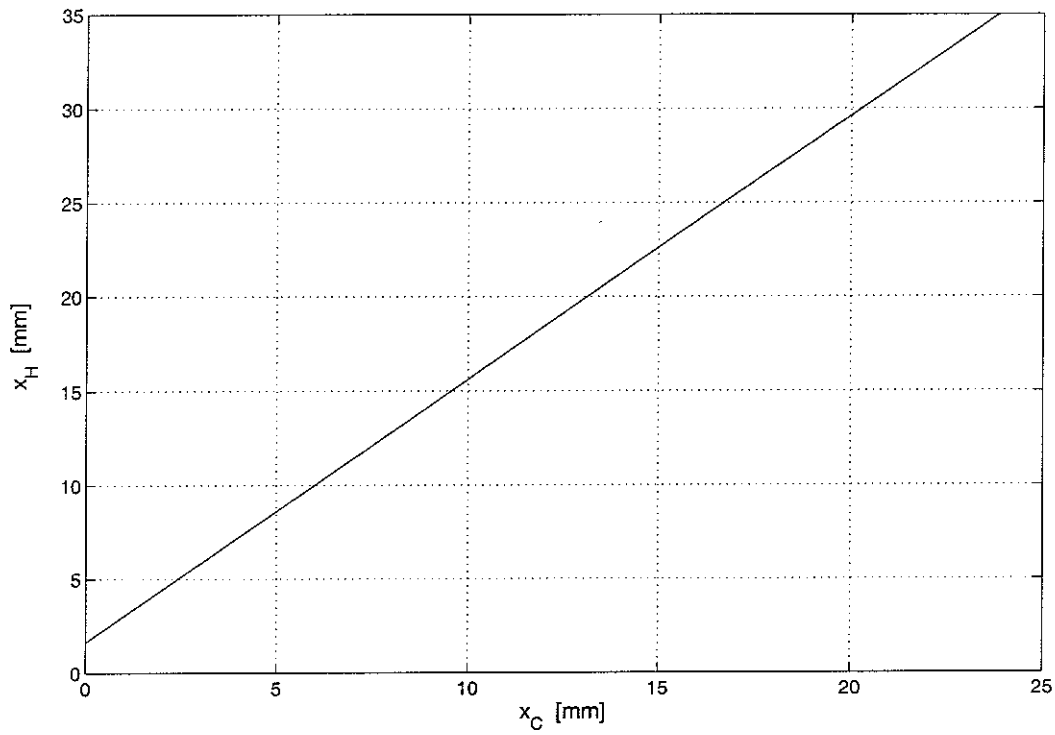

Figure 94: Graphical representation of the relationship between the distance from the apex evaluated for a human and cat cochlea, x_H and x_C, respectively.

14 Appendix B

Considering the cochlea as an opened channel, filled with fluid, in which the CP would stand for the fluid surface and the otic capsule for the channel boundaries, the travelling wave will start as a propagating, nondispersive wave with u_f independent of the wavelength λ (long-wave), and a dispersive wave at the CF site (short-wave).

In consequence, in the vicinity of the CF place, the pressure, p_d, is less uniform, being concentrated close to the CP (compare with [25]). However, while the cochlear fluids are assumed to be inviscid and incompressible, the travelling wave remains determined by the CP physical properties [3, 18] so that the BM (CP) stiffness changes along the length of the cochlea, decreasing from the base to the apex (see Section 2.3.1), cause the CP velocity and the wavelength, λ, decrease with the position x, for a given frequency, f.

Since at the CF place the travelling wave is a dispersive short-wave, the decrease of the λ, causes a decrease of the group velocity, thus a slowing of the energy and propagation until its stopping at the CF site. While the fluid is assumed to be inviscid , the CP impedance resistive component takes part in the dissipation of the wave's energy, which reveals in an increase of the CP displacement amplitude at the CF.

15 Appendix C

15.1 The Neely&Kim Generalised Model

15.1.1 Mobility

Matlab script[1] for calculation of the CP mobility for the NK generalised model for chosen stimulus frequency, f.

File: 'nkyf.m'

```
% Cochlear partition mobility of the generalised
% Neely&Kim model for chosen frequency 'f'

% Parameters
L=0.025;                                % Length of the BM
N=1024;                                 % Number of points
delta=L/(N-1);                          % Length of the element
x=[0:delta:L];                          % Position on the BM
fc=input('Choose frequency [Hz] f=');   % Stimulus frequency
f=fc;
a=num2str(fc/1000);

% Parameters for Z1
m1=0.03;                        % Mass of the BM
k1=1.1*1e10*exp(-400*x);        % Stiffness of the BM
c1=200+15e3*exp(-200*x);        % Damping of the BM
% Parameters for Z2
m2=0.005*exp(x);                % Mass of the TM
k2=7*1e7*exp(-440*x);           % Stiffness of the TM
c2=100*exp(-220*x);             % Damping of the TM
% Parameters for Z3
k3=1e8*exp(-400*x);             % Stiffness of the OC/TM coupling
c3=20*exp(-80*x);               % Damping of the OC/TM coupling
% Parameters for Z4
k4=6.15*1e9*exp(-400*x);        % Stiffness of the active source
c4=10400*exp(-200*x);           % Damping of the active source
g=1;                            % OHC force-generation gain

% Impedances
Z1=c1-i*((k1./(2*pi*f))-(2*pi*f*m1));
Z2=c2-i*((k2./(2*pi*f))-(2*pi*f*m2));
```

[1]All scripts written by Robert Pierzycki

```
Z3=c3-i*(k3./(2*pi*f));
Z4=c4-i*(k4./(2*pi*f));

% Partition impedance/mobility
Zp=Z1+((Z2.*(Z3-g*Z4))./(Z2+Z3));
Yp=1./Zp;

% Plots of magnitude/phase
% of partition mobility in function of position 'x'
figure(1)
subplot(2,1,1)
plot(x,abs(Yp)),grid on
title(['Partition Mobility for Neely&Kim Active Model for f=', ...
        a,'kHz'],'FontSize',14);
xlabel('Distance from Stapes  [m]','FontSize',14)
ylabel('|Y_p|  [m^3/Ns]','FontSize',14);

subplot(2,1,2)
plot(x,unwrap(angle(Yp))/(2*pi)),grid on
xlabel('Distance from Stapes  [m]','FontSize',14)
ylabel('\angle Y_p  [cycles]','FontSize',14);

% Plots of real/imaginary parts
% of partition mobility in function of position 'x'
figure(2)
subplot(2,1,1)
plot(x,real(Yp)),grid on
title(['Partition Mobility for Neely&Kim Active Model for f=', ...
        a,'kHz'],'FontSize',14);
xlabel('Distance from Stapes  [m]','FontSize',14)
ylabel('Re Y_p  [m^3/Ns]','FontSize',14);

subplot(2,1,2)
plot(x,imag(Yp)),grid on
xlabel('Distance from Stapes  [m]','FontSize',14)
ylabel('Im Y_p  [m^3/Ns]','FontSize',14);

=====================================
```

Matlab script for calculation of the CP mobility for the NK generalised model for chosen position on the BM, x.

File: 'nkyx.m'

```
% Cochlear partition mobility of the generalised
% Neely&Kim model for chosen position 'x'

% Parameters
xc=input('Choose the BM site [m] x=');  % Position on the BM
x=xc;
f=[10:10:25000];                        % Stimulus frequency
a=num2str(xc);

% Parameters for Z1
m1=0.03;% Mass of the BM
k1=1.1*1e10*exp(-400*x);        % Stiffness of the BM
c1=200+15e3*exp(-200*x);        % Damping of the BM
% Parameters for Z2
m2=0.005*exp(x);                % Mass of the TM
k2=7*1e7*exp(-440*x);           % Stiffness of the TM
c2=100*exp(-220*x);             % Damping of the TM
% Parameters for Z3
k3=1e8*exp(-400*x);             % Stiffness of the OC/TM coupling
c3=20*exp(-80*x);               % Damping of the OC/TM coupling
% Parameters for Z4
k4=6.15*1e9*exp(-400*x);        % Stiffness of the active source
c4=10400*exp(-200*x);           % Damping of the active source
g=1;                            % OHC force-generation gain

% Impedances
Z1=c1-i*((k1./(2*pi*f))-(2*pi*f*m1));
Z2=c2-i*((k2./(2*pi*f))-(2*pi*f*m2));
Z3=c3-i*(k3./(2*pi*f));
Z4=c4-i*(k4./(2*pi*f));

% Partition impedance/mobility
Zp=Z1+(Z2.*(Z3-g*Z4))./(Z2+Z3);
Yp=1./Zp;

% Plots of magnitude/phase
% of partition mobility in function of frequency 'f'
figure(1)
subplot(2,1,1)
semilogx(f,abs(Yp)),grid on
title(['Partition Mobility for Neely&Kim Active Model for x=', ...
        a,'m'],'FontSize',14);
xlabel('Frequency  [Hz]','FontSize',14)
```

```
ylabel('|Y_p|  [m^3/Ns]','FontSize',14);

subplot(2,1,2)
semilogx(f,unwrap(angle(Yp))/(2*pi)),grid on
xlabel('Frequency  [Hz]','FontSize',14)
ylabel('\angle Y_p  [cycles]','FontSize',14);

% Plots of real/imaginary parts
% of partition mobility in function of frequency 'f'
figure(2)
subplot(2,1,1)
semilogx(f,real(Yp)),grid on
title(['Partition Mobility for Neely&Kim Active Model for x=', ...
       a,'m'],'FontSize',12);
xlabel('Frequency  [Hz]','FontSize',14)
ylabel('Re Y_p  [m^3/Ns]','FontSize',14);

subplot(2,1,2)
semilogx(f,imag(Yp)),grid on
xlabel('Frequency  [Hz]','FontSize',14)
ylabel('Im Y_p  [m^3/Ns]','FontSize',14)
```

15.1.2 Modes

Matlab script for calculation of the resonance frequencies and modes of vibration for the NK undamped, free vibration model.

File: 'nkmodes.m'

```
% Modes and resonance frequencies for
% free undamped system of the Neely&Kim model

% Parameters
N=1024;              % Number of points
L=0.035;             % Length of the cochlea
del=L/(N-1);         % Length of the division
x=[0:del:L];         % Position on the cochlea
t=0:pi/50:2*pi;      % Time

% First degree of freedom
m1=0.03;
k1=1.1e10*exp(-400*x);
% Second degree of freedom
```

```
m2=0.005*exp(x);
k2=7e7*exp(-440*x);
% OHCs/cilia stiffness
k3=1e8*exp(-400*x);

% Constants of the quadratic
% equation for omega^2
a=1;
b=-(((k1+k3)/m1)+((k2+k3)/m2));
c=((k1.*k2)+(k1.*k3)+(k2.*k3))./(m1*m2);
delta=(b.^2)-(4*a*c);

% Roots squarerooted
% (radial frequencies)
w1=sqrt((-b+sqrt(delta))/(2*a));
w2=sqrt((-b-sqrt(delta))/(2*a));

% Resonance frequencies
% Characteristic frequency
f1=w1/(2*pi);
f2=w2/(2*pi);
fc=sqrt(k1/m1)/(2*pi);

% Ratio of frequencies
ratio=f2./f1;

% Relative amplitudes (A11=A12=1)
% (Mode shapes)
A21=(k1+k3-(m1*w1.^2))./k3;
A22=(k1+k3-(m1*w2.^2))./k3;

% Solution constants
B=A22./(A22-A21);
D=A21./(A21-A22);

% Displacements
% Corresponding at 0.0185 m site
xib=B(542)*cos(w1(542)*t)+D(542)*cos(w2(542)*t);
xit=(A21(542)*B(542))*cos(w1(542)*t) ...
    +(A22(542)*D(542))*cos(w2(542)*t);

T1=1/f1(542);   % Period for f1
T2=1/f2(542);   % Period for f2
```

```
t1=0:pi/5e6:2*T1;      % Time scale for first mode
t2=0:pi/5e6:2*T2;      % Time scale for second mode

% Motions at the first mode
xib1=cos(w1(542)*t1);
xit1=A21(542)*cos(w1(542)*t1);

% Motions at the second mode
xib2=cos(w2(542)*t2);
xit2=A22(542)*cos(w2(542)*t2);

% Plots of resonance frequencies
% characteristic frequency
% and the ratio f2/f1
% in function of position 'x'
figure(1)
semilogy(x,f1,x,f2,'r--',x,fc,'k-.')
grid on
xlabel('Distance from Stapes  [m]','FontSize',14)
ylabel('f_{1,2}  [Hz]','FontSize',14);

figure(2)
plot(x,ratio)
grid on
xlabel('Distance from Stapes  [m]','FontSize',14)
ylabel('f_{2}/f_{1}','FontSize',14);

% Plots of relative amplitudes
% in function of position 'x'
figure(3)
subplot(2,1,1)
plot(x,A21)
grid on
xlabel('Distance from Stapes  [m]','FontSize',14)
ylabel('A_{21}','FontSize',14);

subplot(2,1,2)
plot(x,A22)
grid on
xlabel('Distance from Stapes  [m]','FontSize',14)
ylabel('A_{22}','FontSize',14);
```

```
% Plots of motion at first mode
% at 0.0185 m site
figure(4)
subplot(2,1,1)
plot(t1,xib1)
grid on
xlabel('Time  [s]','FontSize',14)
ylabel('\xi_{b1}','FontSize',14);

subplot(2,1,2)
plot(t1,xit1)
grid on
xlabel('Time  [s]','FontSize',14)
ylabel('\xi_{t1}','FontSize',14);

% Plots of motion at second mode
% at 0.0185 m site
figure(5)
subplot(2,1,1)
plot(t2,xib2)
grid on
xlabel('Time  [s]','FontSize',14)
ylabel('\xi_{b2}','FontSize',14);

subplot(2,1,2)
plot(t2,xit2)
grid on
xlabel('Time  [s]','FontSize',14)
ylabel('\xi_{t2}','FontSize',14);
```

15.1.3 Coupling

Matlab script for calculation of the pressure difference in the CP fluid for the NK generalised model for chosen position on the BM, x and stimulus frequency, f.

File: 'nkpd.m'

```
% Pressure difference in the cochlear fluid
% of the generalised Neely&Kim model for chosen:
% 1) position 'x' (rows of the 'pd' matrix)
% 2) frequency 'f' (columns of the 'pd' matrix)
% The micromechanical model
```

```
% with the coupling via cochlear fluid

% Parameters
L=0.035;                        % Length of the BM
H=0.001;                        % Heigth of the SV
ro=1000;                        % Fluid density
ust=1;                          % Stapes velocity
N=1024;                         % Number of points
delta=L/(N-1);                  % Length of the element
x=[0:delta:L];                  % Position on the BM

% Coupling matrix
C=zeros(N);
C(N+2:N+1:end-1)=-2;
C(2*N+2:N+1:end)=1;
C(end-(2*N+1):-(N+1):2)=1;
C(1)=-delta;
C(N+1)=delta;
C(N,N)=delta.^2;
C=sparse(C);

% Parameters for Z1
m1=0.03;                        % Mass of the BM
k1=1.1e10*exp(-400*x);          % Stiffness of the BM
c1=200+15e3*exp(-200*x);        % Damping of the BM
% Parameters for Z2
m2=0.005*exp(x);                % Mass of the TM
k2=7e7*exp(-440*x);             % Stiffness of the TM
c2=100*exp(-220*x);             % Damping of the TM
% Parameters for Z3
k3=1e8*exp(-400*x);             % Stiffness of the OC/TM coupling
c3=20*exp(-80*x);               % Damping of the OC/TM coupling
% Parameters for Z4
k4=6.15e9*exp(-400*x);          % Stiffness of the active source
c4=10400*exp(-200*x);           % Damping of the active source
g=1;                            % OHC force-generation gain

freq=[10:10:25000];             % Stimulus frequency
for n=1:length(freq);
f=freq(n);

% Impedances
Z1=c1-i*((k1./(2*pi*f))-(2*pi*f*m1));
```

```
Z2=c2-i*((k2./(2*pi*f))-(2*pi*f*m2));
Z3=c3-i*(k3./(2*pi*f));
Z4=c4-i*(k4./(2*pi*f));

% Partition impedance/mobility
Zp=Z1+(Z2.*(Z3-g*Z4))./(Z2+Z3);
Yp1=1./Zp;

% Mobility matrix
Yp=zeros(N);
Yp=diag(Yp1);
    M=zeros(N);
M(N+2:N+1:end-1)=1;
M=M*Yp;
    M=sparse(M);

% Total matrix
T=[((1./(delta.^2))*C)-(((4*j*pi*f*ro)./H).*M)];

% Source vector
S(1)=-4*j*pi*f*ro*ust;
S(2:N)=0;

% Pressure difference
pd=(inv(T))*S';
pref=2e-5;              % Pressure reference
end
```

==========

Matlab script for calculation of the CP velocity for the NK generalised model for chosen position on the BM, x and stimulus frequency, f.

File: 'nkv1dot.m'

```
% Cochlear partition velocity of the generalised
% Neely&Kim model for chosen:
% 1) position 'x' (rows of the 'v1dot' matrix)
% 2) frequency 'f' (columns of the 'v1dot' matrix)
% The micromechanical model
% with the coupling via cochlear fluid

% Parameters
L=0.035;                    % Length of the BM
```

```
H=0.001;                        % Heigth of the SV
ro=1000;                        % Fluid density
ust=1;                          % Stapes velocity
N=1024;                         % Number of points
delta=L/(N-1);                  % Length of the element
x=[0:delta:L];                  % Position on the BM

% Coupling matrix
C=zeros(N);
C(N+2:N+1:end-1)=-2;
C(2*N+2:N+1:end)=1;
C(end-(2*N+1):-(N+1):2)=1;
C(1)=-delta;
C(N+1)=delta;
C(N,N)=delta.^2;
C=sparse(C);

% Parameters for Z1
m1=0.03;                        % Mass of the BM
k1=1.1e10*exp(-400*x);          % Stiffness of the BM
c1=200+15e3*exp(-200*x);        % Damping of the BM
% Parameters for Z2
m2=0.005*exp(x);                % Mass of the TM
k2=7e7*exp(-440*x);             % Stiffness of the TM
c2=100*exp(-220*x);             % Damping of the TM
% Parameters for Z3
k3=1e8*exp(-400*x);             % Stiffness of the OC/TM coupling
c3=20*exp(-80*x);               % Damping of the OC/TM coupling
% Parameters for Z4
k4=6.15e9*exp(-400*x);          % Stiffness of the active source
c4=10400*exp(-200*x);           % Damping of the active source
g=1;                            % OHC force-generation gain

freq=[10:10:25000];             % Stimulus frequency
for n=1:length(freq);
f=freq(n);

% Impedances
Z1=c1-i*((k1./(2*pi*f))-(2*pi*f*m1));
Z2=c2-i*((k2./(2*pi*f))-(2*pi*f*m2));
Z3=c3-i*(k3./(2*pi*f));
Z4=c4-i*(k4./(2*pi*f));
```

```
% Partition impedance/mobility
Zp=Z1+(Z2.*(Z3-g*Z4))./(Z2+Z3);
Yp1=1./Zp;

% Mobility matrix
Yp=zeros(N);
Yp=diag(Yp1);
    M=zeros(N);
M(N+2:N+1:end-1)=1;
M=M*Yp;
    M=sparse(M);

% Total matrix
T=[((1./(delta.^2))*C)-(((4*j*pi*f*ro)./H).*M)];

% Source vector
S(1)=-4*j*pi*f*ro*ust;
S(2:N)=0;

% Pressure difference
pd=(inv(T))*S';

    % Partition velocity
    v1dot(:,n)=Yp*(-2*pd);
    vdotref=2e-4;                  % Velocity reference
end
```

==========

Matlab script for calculation of the CP displacement for the NK generalised model for chosen position on the BM, x and stimulus frequency, f.

File: 'nkv1.m'

```
% Cochlear partition displacement of the generalised
% Neely&Kim model for chosen:
% 1) position 'x' (rows of the 'v1' matrix)
% 2) frequency 'f' (columns of the 'v1' matrix)
% The micromechanical model
% with the coupling via cochlear fluid

% Parameters
L=0.035;                       % Length of the BM
H=0.001;                       % Heigth of the SV
```

```
ro=1000;                          % Fluid density
ust=1;                            % Stapes velocity
N=1024;                           % Number of points
delta=L/(N-1);                    % Length of the element
x=[0:delta:L];                    % Position on the BM

% Coupling matrix
C=zeros(N);
C(N+2:N+1:end-1)=-2;
C(2*N+2:N+1:end)=1;
C(end-(2*N+1):-(N+1):2)=1;
C(1)=-delta;
C(N+1)=delta;
C(N,N)=delta.^2;
C=sparse(C);

% Parameters for Z1
m1=0.03;                          % Mass of the BM
k1=1.1e10*exp(-400*x);            % Stiffness of the BM
c1=200+15e3*exp(-200*x);          % Damping of the BM
% Parameters for Z2
m2=0.005*exp(x);                  % Mass of the TM
k2=7e7*exp(-440*x);               % Stiffness of the TM
c2=100*exp(-220*x);               % Damping of the TM
% Parameters for Z3
k3=1e8*exp(-400*x);               % Stiffness of the OC/TM coupling
c3=20*exp(-80*x);                 % Damping of the OC/TM coupling
% Parameters for Z4
k4=6.15e9*exp(-400*x);            % Stiffness of the active source
c4=10400*exp(-200*x);             % Damping of the active source
g=1;                              % OHC force-generation gain

freq=[10:10:25000];               % Stimulus frequency
for n=1:length(freq);
f=freq(n);

% Impedances
Z1=c1-i*((k1./(2*pi*f))-(2*pi*f*m1));
Z2=c2-i*((k2./(2*pi*f))-(2*pi*f*m2));
Z3=c3-i*(k3./(2*pi*f));
Z4=c4-i*(k4./(2*pi*f));

% Partition impedance/mobility
```

```
Zp=Z1+(Z2.*(Z3-g*Z4))./(Z2+Z3);
Yp1=1./Zp;

% Mobility matrix
Yp=zeros(N);
Yp=diag(Yp1);
    M=zeros(N);
M(N+2:N+1:end-1)=1;
M=M*Yp;
    M=sparse(M);

% Total matrix
T=[((1./(delta.^2))*C)-(((4*j*pi*f*ro)./H).*M)];

% Source vector
S(1)=-4*j*pi*f*ro*ust;
S(2:N)=0;

% Pressure difference
pd=(inv(T))*S';

    % Partition displacement
    v1dot=Yp*(-2*pd);
    v1=v1dot./(i*2*pi*f);
    vref=1e-9;                  % Displacement reference
end
```

15.1.4 Stability

Matlab script for calculation of the *Nyquist plots* for a negative feedback system (derived from the NK generalised model) for chosen position on the BM, x and the cochlear amplifier's gain, g.

File: 'nknegv3dot.m'

```
% Stability of negative feedback system
% of the generalised Neely&Kim model
% for specific position/gain 'x'/'g'
% Velocity v3dot-output of the loop

% Parameters
xc=input('Choose the BM site [m] x=');  % Position on the BM
x=xc;
```

```
f=0:10:1e6;                              % Frequency band

% Parameters for Z1
m1=0.03;                                 % Mass of the BM
k1=1.1*1e10*exp(-400*x);                 % Stiffness of the BM
c1=200+15e3*exp(-200*x);                 % Damping of the BM
% Parameters for Z2
m2=0.005*exp(x);                         % Mass of the TM
k2=7*1e7*exp(-440*x);                    % Stiffness of the TM
c2=100*exp(-220*x);                      % Damping of the TM
% Parameters for Z3
k3=1e8*exp(-400*x);                      % Stiffness of the OC/TM coupling
c3=20*exp(-80*x);                        % Damping of the OC/TM coupling
% Parameters for Z4
k4=6.15*1e9*exp(-400*x);                 % Stiffness of the active source
c4=10400*exp(-200*x);                    % Damping of the active source

% OHC force-generation gain
gc=input('Choose cochlear amplifier''s gain g=');
g=gc;

% Impedances
Z1=c1-i*((k1./(2*pi*f))-(2*pi*f*m1));
Z2=c2-i*((k2./(2*pi*f))-(2*pi*f*m2));
Z3=c3-i*(k3./(2*pi*f));
Z4=c4-i*(k4./(2*pi*f));

% Feedback components
G=1./(Z1+((Z1.*Z3)./Z2)+Z3);             % Plant
H=-g*Z4;                                 % Controller

% Nyquist plots of imaginary vs real
% of negative feedback system for
% specific position/gain 'x'/'g'
plot(real(G.*H),imag(G.*H)),grid on
xlabel('Re GH(j\omega)','FontSize',14)
ylabel('Im GH(j\omega)','FontSize',14)
hold on
plot(-1,0,'ro')
```

15.1.5 Nonlinearity

Matlab script for calculation of the CP nonlinearity for the NK generalised model for chosen position on the BM, x and stimulus frequency, f.

File: 'nknonlinearity.m'

```
% Cochlear partition nonlinearity
% of the generalised Neely&Kim model

% Parameters
L=0.035;                    % Length of the BM
He=0.001;                   % Heigth of the SV
ro=1000;                    % Fluid density
ust=2.5016e-10;             % Stapes velocity
N=1024;                     % Number of points
delta=L/(N-1);              % Length of the element
x=[0:delta:L];              % Position on the BM

% Coupling matrix
C=zeros(N);
C(N+2:N+1:end-1)=-2;
C(2*N+2:N+1:end)=1;
C(end-(2*N+1):-(N+1):2)=1;
C(1)=-delta;
C(N+1)=delta;
C(N,N)=delta.^2;
C=sparse(C);

% Parameters for Z1
m1=0.03;                    % Mass of the BM
k1=1.1e10*exp(-400*x);      % Stiffness of the BM
c1=200+15e3*exp(-200*x);    % Damping of the BM
% Parameters for Z2
m2=0.005*exp(x);            % Mass of the TM
k2=7e7*exp(-440*x);         % Stiffness of the TM
c2=100*exp(-220*x);         % Damping of the TM
% Parameters for Z3
k3=1e8*exp(-400*x);         % Stiffness of the OC/TM coupling
c3=20*exp(-80*x);           % Damping of the OC/TM coupling
% Parameters for Z4
k4=6.15e9*exp(-400*x);      % Stiffness of the active source
c4=10400*exp(-200*x);       % Damping of the active source
```

```
g(1)=1;                          % OHC force-generation gain

freq=[10:10:25000];              % Stimulus frequency
for l=1:length(freq);
f=freq(l);

    % Evaluation of partition velocity
    % to define a feedback system output

% Impedances
Z1=c1-i*((k1./(2*pi*f))-(2*pi*f*m1));
    Z2=c2-i*((k2./(2*pi*f))-(2*pi*f*m2));
    Z3=c3-i*(k3./(2*pi*f));
    Z4=c4-i*(k4./(2*pi*f));

    % Feedback components
G=(Z2+Z3)./(Z1.*Z2+Z1.*Z3+Z2.*Z3);  % Plant
H=(-g(1)*Z2.*Z4)./(Z2+Z3);          % Controller

% Partition impedance/mobility
Zp=Z1+(Z2.*(Z3-g(1)*Z4))./(Z2+Z3);
Yp1=1./Zp;

% Mobility matrix
Yp=zeros(N);
Yp=diag(Yp1);
    M=zeros(N);
M(N+2:N+1:end-1)=1;
M=M*Yp;
M=sparse(M);

% Total matrix
T=[((1./(delta.^2))*C)-(((4*j*pi*f*ro)./He).*M)];

    % Source vector
S(1)=-4*j*pi*f*ro*ust;
S(2:N)=0;

% Pressure difference
pd=(inv(T))*S';

    % Partition velocity
v1dot=(G/(1-G.*H))*pd;
```

```
    % Recalculation of partition velocity
    % to saturate OHC force-generation gain
for n=2:6;
        g(1)=1;
g(n)=(5*1.54e-5)/(6*(1.54e-5+max(abs(v1dot))));

        % Partition impedance/mobility
        Zp=Z1+(Z2.*(Z3-g(n)*Z4))./(Z2+Z3);
Yp1=1./Zp;
        H=(g(n)*Z2.*Z4)./(Z2+Z3);

        % Mobility matrix
        Yp=zeros(N);
        Yp=diag(Yp1);
        M=zeros(N);
        M(N+2:N+1:end-1)=1;
M=M*Yp;
M=sparse(M);

% Total matrix
T=[((1./(delta.^2))*C)-(((4*j*pi*f*ro)./He).*M)];

% Pressure difference
pd=(inv(T))*S';

        % Partition velocity
v1dot=(G/(1-G.*H))*pd;

        % Partition displacement
        v1(:,1)=v1dot/(i*2*pi*f);
        vref=1e-9;                      % Displacement reference
end
end
```

15.2 Investigation of Ren and Kolston Models

Matlab script for investigation of the Ren model on the basis of NK generalised model.

File: 'ren.m'

```
% Pressure difference in the cochlear fluid
```

```
% of the generalised Neely&Kim model for chosen
% position 'x'
% The micromechanical model
% with the coupling via cochlear fluid
% and two positions of stimulus

% Parameters
L=0.035;                        % Length of the BM
H=0.001;                        % Heigth of the SV
ro=1000;                        % Fluid density
ust=1;                          % Stapes velocity
N=1024;                         % Number of points
delta=L/(N-1);                  % Length of the element
x=[0:delta:L];                  % Position on the BM

% Coupling matrix
C=zeros(N);
C(N+2:N+1:end-1)=-2;
C(2*N+2:N+1:end)=1;
C(end-(2*N+1):-(N+1):2)=1;
C(1)=-delta;
C(N+1)=delta;
C(N,N)=delta.^2;
C=sparse(C);

% Parameters for Z1
m1=0.03;                        % Mass of the BM
k1=1.1e10*exp(-400*x);          % Stiffness of the BM
c1=200+15e3*exp(-200*x);        % Damping of the BM
% Parameters for Z2
m2=0.005*exp(x);                % Mass of the TM
k2=7e7*exp(-440*x);             % Stiffness of the TM
c2=100*exp(-220*x);             % Damping of the TM
% Parameters for Z3
k3=1e8*exp(-400*x);             % Stiffness of the OC/TM coupling
c3=20*exp(-80*x);               % Damping of the OC/TM coupling
% Parameters for Z4
k4=6.15e9*exp(-400*x);          % Stiffness of the active source
c4=10400*exp(-200*x);           % Damping of the active source
g=1;                            % OHC force-generation gain

f=1000;          % Stimulus frequency
```

```
% Impedances
Z1=c1-i*((k1./(2*pi*f))-(2*pi*f*m1));
Z2=c2-i*((k2./(2*pi*f))-(2*pi*f*m2));
Z3=c3-i*(k3./(2*pi*f));
Z4=c4-i*(k4./(2*pi*f));

% Partition impedance/mobility
Zp=Z1+(Z2.*(Z3-g*Z4))./(Z2+Z3);
Yp1=1./Zp;

% Mobility matrix
Yp=zeros(N);
Yp=diag(Yp1);
M=zeros(N);
M(N+2:N+1:end-1)=1;
M=M*Yp;
M=sparse(M);

% Total matrix
T=[((1./(delta.^2))*C)-(((4*j*pi*f*ro)./H).*M)];

% Source vector
% Source at stapes
S1(1)=-4*j*pi*f*ro*ust;
S1(2:N)=0;

% Source vector
% Source at 0.0185m site
S2(1:N)=0;
S2(542)=-4*j*pi*f*ro*ust;

% Pressure difference
% (Source at the stapes)
pd1=(inv(T))*S1';
pref=2e-5;              % Pressure reference

% Pressure difference
% (Source at 0.0185m site)
pd2=(inv(T))*S2';
==========================================
```

Matlab script for investigation of the Kolston model on the basis of NK gen-

eralised model.

File: 'kolston.m'

```
% Cochlear partition maximum velocity of the generalised
% Neely&Kim model for chosen:
% 1) position 'x' (rows of the 'v1dot' matrix)
% 2) gain 'g' (columns of the 'v1dot' matrix)
% The micromechanical model
% with the coupling via cochlear fluid
% and

% Parameters
L=0.035;                    % Length of the BM
H=0.001;                    % Heigth of the SV
ro=1000;                    % Fluid density
ust=1;                      % Stapes velocity
N=1024;                     % Number of points
delta=L/(N-1);              % Length of the element
x=[0:delta:L];              % Position on the BM

% Coupling matrix
C=zeros(N);
C(N+2:N+1:end-1)=-2;
C(2*N+2:N+1:end)=1;
C(end-(2*N+1):-(N+1):2)=1;
C(1)=-delta;
C(N+1)=delta;
C(N,N)=delta.^2;
C=sparse(C);

% Parameters for Z1
m1=0.03;                    % Mass of the BM
k1=1.1e10*exp(-400*x);      % Stiffness of the BM
c1=200+15e3*exp(-200*x);    % Damping of the BM
% Parameters for Z2
m2=0.005*exp(x);            % Mass of the TM
k2=7e7*exp(-440*x);         % Stiffness of the TM
c2=100*exp(-220*x);         % Damping of the TM
% Parameters for Z3
k3=1e8*exp(-400*x);         % Stiffness of the OC/TM coupling
c3=20*exp(-80*x);           % Damping of the OC/TM coupling
% Parameters for Z4
k4=6.15e9*exp(-400*x);      % Stiffness of the active source
```

```
c4=10400*exp(-200*x);          % Damping of the active source
gain=[0:0.05:2];               % OHC force-generation gain

f=1000;          % Stimulus frequency
for n=1:length(gain);
g=gain(n);

% Impedances
Z1=c1-i*((k1./(2*pi*f))-(2*pi*f*m1));
Z2=c2-i*((k2./(2*pi*f))-(2*pi*f*m2));
Z3=c3-i*(k3./(2*pi*f));
Z4=c4-i*(k4./(2*pi*f));

% Partition impedance/mobility
Zp=Z1+(Z2.*(Z3-g*Z4))./(Z2+Z3);
Yp1=1./Zp;

% Mobility matrix
Yp=zeros(N);
Yp=diag(Yp1);
    M=zeros(N);
M(N+2:N+1:end-1)=1;
M=M*Yp;
    M=sparse(M);

% Total matrix
T=[((1./(delta.^2))*C)-(((4*j*pi*f*ro)./H).*M)];

% Source vector
S(1)=-4*j*pi*f*ro*ust;
S(2:N)=0;

% Pressure difference
pd=(inv(T))*S';

    % Partition velocity
    v1dot=Yp*(-2*pd);
    v1dotmax(:,n)=max(abs(v1dot));  % Velocity maximum
    vdotref=2e-4;                   % Velocity reference
end
```

15.3 The Geisler Generalised Model

15.3.1 Mobility

Matlab script for calculation of the CP mobility for the G generalised model for chosen stimulus frequency, f.

File: 'gyf.m'

```
% Cochlear partition mobility of the generalised
% Geisler model for chosen frequency 'f'

% Parameters
L=0.035;                                  % Length of the BM
N=1024;                                   % Number of points
delta=L/(N-1);                            % Length of the element
x=[0:delta:L];                            % Position on the BM
fc=input('Choose frequency [Hz] f=');     % Stimulus frequency
f=fc;
a=num2str(fc/1000);

% Parameters for Z1
m1=0.5;                          % Mass of the BM
k1=6.4*1e10*exp(-368*x);         % Stiffness of the BM
c1=1.8*1e5*exp(-184*x);          % Damping of the BM
% Parameters for Z2
k2=3.8*1e10*exp(-368*x);         % Stiffness of the TM
% Parameters for Z3
k3=7.5*1e10*exp(-368*x);         % Stiffness of the coupling
% Parameters for Z4
wo=2*pi*57e3*exp(-184*x);        % Characteristic frequency
T=2*pi./wo;                      % Time delay
g=1;                             % OHC force-generation gain

% Impedances
Z1=c1-i*((k1./(2*pi*f))-(2*pi*f*m1));
Z2=-i*(k2./(2*pi*f));
Z3=-i*(k3./(2*pi*f));
Z4=(-i*k1./(2*pi*f)).*(((wo/20)-i*2*pi*f)./ ...
    ((wo/20)+i*2*pi*f)).*(exp(-i*2*pi*f*T));

% Partition impedance/mobility
Zp=Z1+((Z2.*Z3)./(Z2+Z3+g*Z4));
```

```
Yp=1./Zp;

% Plots of magnitude/phase
% of partition mobility in function of position 'x'
figure(1)
subplot(2,1,1)
plot(x,abs(Yp)),grid on
title(['Partition Mobility for Geisler Active Model for f=', ...
        a,'kHz'],'FontSize',14);
xlabel('Distance from Stapes  [m]','FontSize',14)
ylabel('|Y_p|  [m^3/Ns]','FontSize',14);

subplot(2,1,2)
plot(x,unwrap(angle(Yp))/(2*pi)),grid on
xlabel('Distance from Stapes  [m]','FontSize',14)
ylabel('\angle Y_p  [cycles]','FontSize',14);

% Plots of real/imaginary parts
% of partition mobility in function of position 'x'
figure(2)
subplot(2,1,1)
plot(x,real(Yp)),grid on
title(['Partition Mobility for Geisler Active Model for f=', ...
        a,'kHz'],'FontSize',14);
xlabel('Distance from Stapes  [m]','FontSize',14)
ylabel('Re Y_p  [m^3/Ns]','FontSize',14);

subplot(2,1,2)
plot(x,imag(Yp)),grid on
xlabel('Distance from Stapes  [m]','FontSize',14)
ylabel('Im Y_p  [m^3/Ns]','FontSize',14);

==========================================
```

Matlab script for calculation of the CP mobility for the G generalised model for chosen stimulus frequency, f, and delay factor, n equal to 0.4 (optimum value estimated in G model).

File: 'gynf.m'

```
% Cochlear partition mobility of the generalised
% Geisler model for chosen frequency 'f'
% with the delay factor n=0.4
```

```
% Parameters
L=0.035;                                    % Length of the BM
N=1024;                                     % Number of points
delta=L/(N-1);                              % Length of the element
x=[0:delta:L];                              % Position on the BM
fc=input('Choose frequency [Hz] f=');       % Frequency of the signal
f=fc;
a=num2str(fc/1000);

% Parameters for Z1
m1=0.5;                                 % Mass of the BM
k1=6.4*1e10*exp(-368*x);                % Stiffness of the BM
c1=1.8*1e5*exp(-184*x);                 % Damping of the BM
% Parameters for Z2
k2=3.8*1e10*exp(-368*x);                % Stiffness of the TM
% Parameters for Z3
k3=7.5*1e10*exp(-368*x);                % Stiffness of the coupling
% Parameters for Z4
wo=2*pi*57e3*exp(-184*x);               % Characteristic frequency
T=0.4*pi./wo;                           % Time delay
g=1;                                    % OHC force-generation gain

% Impedances
Z1=c1-i*((k1./(2*pi*f))-(2*pi*f*m1));
Z2=-i*(k2./(2*pi*f));
Z3=-i*(k3./(2*pi*f));
Z4=(-i*k1./(2*pi*f)).*(((wo/20)-i*2*pi*f)./ ...
    ((wo/20)+i*2*pi*f)).*(exp(-i*2*pi*f*T));

% Partition impedance/mobility
Zp=Z1+((Z2.*Z3)./(Z2+Z3+g*Z4));
Yp=1./Zp;

% Plots of magnitude/phase
% of partition mobility in function of position 'x'
figure(1)
subplot(2,1,1)
plot(x,abs(Yp)),grid on
title(['Partition Mobility for Geisler Active Model for f=', ...
       a,'kHz'],'FontSize',14);
xlabel('Distance from Stapes  [m]','FontSize',14)
ylabel('|Y_p|  [m^3/Ns]','FontSize',14);
```

```
subplot(2,1,2)
plot(x,unwrap(angle(Yp))/(2*pi)),grid on
xlabel('Distance from Stapes  [m]','FontSize',14)
ylabel('\angle Y_p  [cycles]','FontSize',14);

% Plots of real/imaginary parts
% of partition mobility in function of position 'x'
figure(2)
subplot(2,1,1)
plot(x,real(Yp)),grid on
title(['Partition Mobility for Geisler Active Model for f=', ...
        a,'kHz'],'FontSize',14);
xlabel('Distance from Stapes  [m]','FontSize',14)
ylabel('Re Y_p  [m^3/Ns]','FontSize',14);

subplot(2,1,2)
plot(x,imag(Yp)),grid on
xlabel('Distance from Stapes  [m]','FontSize',14)
ylabel('Im Y_p  [m^3/Ns]','FontSize',14);

==========================================
```

Matlab script for calculation of the CP mobility for the G generalised model for chosen position on the BM, x.

File: 'gyx.m'

```
% Cochlear partition mobility of the generalised
% Geisler model for chosen position 'x'

% Parameters
xc=input('Choose the BM site [m] x=');  % Position on the BM
x=xc;
f=[10:10:25000];                        % Stimulus frequency
a=num2str(xc);

% Parameters for Z1
m1=0.5;                         % Mass of the BM
k1=6.4*1e10*exp(-368*x);        % Stiffness of the BM
c1=1.8*1e5*exp(-184*x);         % Damping of the BM
% Parameters for Z2
k2=3.8*1e10*exp(-368*x);        % Stiffness of the TM
% Parameters for Z3
k3=7.5*1e10*exp(-368*x);        % Stiffness of the coupling
```

```
% Parameters for Z4
wo=2*pi*57e3*exp(-184*x);       % Characteristic frequency
T=2*pi./wo;                     % Time delay
g=1;                            % OHC force-generation gain

% Impedances
Z1=c1-i*((k1./(2*pi*f))-(2*pi*f*m1));
Z2=-i*(k2./(2*pi*f));
Z3=-i*(k3./(2*pi*f));
Z4=(-i*k1./(2*pi*f)).*(((wo/20)-i*2*pi*f)./ ...
    ((wo/20)+i*2*pi*f)).*(exp(-i*2*pi*f*T));

% Partition impedance/mobility
Zp=Z1+((Z2.*Z3)./(Z2+Z3+g*Z4));
Yp=1./Zp;

% Plots of magnitude/phase
% of partition mobility in function of frequency 'f'
figure(1)
subplot(2,1,1)
semilogx(f,abs(Yp)),grid on
title(['Partition Mobility for Geisler Active Model for x=', ...
        a,'m'],'FontSize',14);
xlabel('Frequency  [Hz]','FontSize',14)
ylabel('|Y_p|  [m^3/Ns]','FontSize',14);

subplot(2,1,2)
semilogx(f,unwrap(angle(Yp))/(2*pi)),grid on
xlabel('Frequency  [Hz]','FontSize',14)
ylabel('\angle Y_p  [cycles]','FontSize',14);

% Plots of real/imaginary parts
% of partition mobility in function of frequency 'f'
figure(2)
subplot(2,1,1)
semilogx(f,real(Yp)),grid on
title(['Partition Mobility for Geisler Active Model for x=', ...
        a,'m'],'FontSize',14);
xlabel('Frequency  [Hz]','FontSize',14)
ylabel('Re Y_p  [m^3/Ns]','FontSize',14);

subplot(2,1,2)
semilogx(f,imag(Yp)),grid on
```

```
xlabel('Frequency  [Hz]','FontSize',14)
ylabel('Im Y_p  [m^3/Ns]','FontSize',14);
```

==========

Matlab script for calculation of the CP mobility for the G generalised model for chosen position on the BM, x, and delay factor, n equal to 0.4 (optimum value estimated in G model).

File: 'gynx.m'

```
% Cochlear partition mobility of the generalised
% Geisler model for chosen position 'x'
% with the delay factor n=0.4

% Parameters
xc=input('Choose the BM site [m] x=');  % Position on the BM
x=xc;
a=num2str(xc);
f=[10:10:25000];                        % Stimulus frequency

% Parameters for Z1
m1=0.5;                          % Mass of the BM
k1=6.4*1e10*exp(-368*x);         % Stiffness of the BM
c1=1.8*1e5*exp(-184*x);          % Damping of the BM
% Parameters for Z2
k2=3.8*1e10*exp(-368*x);         % Stiffness of the TM
% Parameters for Z3
k3=7.5*1e10*exp(-368*x);         % Stiffness of the coupling
% Parameters for Z4
wo=2*pi*57e3*exp(-184*x);        % Characteristic frequency
T=0.4*pi./wo;                    % Time delay
g=1;                             % OHC force-generation gain

% Impedances
Z1=c1-i*((k1./(2*pi*f))-(2*pi*f*m1));
Z2=-i*(k2./(2*pi*f));
Z3=-i*(k3./(2*pi*f));
Z4=(-i*k1./(2*pi*f)).*(((wo/20)-i*2*pi*f)./ ...
    ((wo/20)+i*2*pi*f)).*(exp(-i*2*pi*f*T));

% Partition impedance/mobility
Zp=Z1+((Z2.*Z3)./(Z2+Z3+g*Z4));
Yp=1./Zp;
```

```
% Plots of magnitude/phase
% of partition mobility in function of frequency 'f'
figure(1)
subplot(2,1,1)
semilogx(f,abs(Yp)),grid on
title(['Partition Mobility for Geisler Active Model for x=', ...
        a,'m'],'FontSize',14);
xlabel('Frequency  [Hz]','FontSize',14)
ylabel('|Y_p|  [m^3/Ns]','FontSize',14);

subplot(2,1,2)
semilogx(f,unwrap(angle(Yp))/(2*pi)),grid on
xlabel('Frequency  [Hz]','FontSize',14)
ylabel('\angle Y_p  [cycles]','FontSize',14);

% Plots of real/imaginary parts
% of partition mobility in function of frequency 'f'
figure(2)
subplot(2,1,1)
semilogx(f,real(Yp)),grid on
title(['Partition Mobility for Geisler Active Model for x=', ...
        a,'m'],'FontSize',14);
xlabel('Frequency  [Hz]','FontSize',14)
ylabel('Re Y_p  [m^3/Ns]','FontSize',14);

subplot(2,1,2)
semilogx(f,imag(Yp)),grid on
xlabel('Frequency  [Hz]','FontSize',14)
ylabel('Im Y_p  [m^3/Ns]','FontSize',14);
```

15.3.2 Coupling

Matlab script for calculation of the pressure difference in the CP fluid for the G generalised model for chosen for chosen position on the BM, x and stimulus frequency, f.

File: 'gpd.m'

```
% Pressure difference in the cochlear fluid
% of the generalised Geisler model for chosen:
% 1) position 'x' (rows of the 'pd' matrix)
% 2) frequency 'f' (columns of the 'pd' matrix)
```

```
% The micromechanical model
% with the coupling via cochlear fluid

% Parameters
L=0.035;                        % Length of the BM
H=0.001;                        % Heigth of the SV
ro=1000;                        % Fluid density
ust=1;                          % Stapes velocity
N=1024;                         % Number of points
delta=L/(N-1);                  % Length of the element
x=[0:delta:L];                  % Position on the BM

% Coupling matrix
C=zeros(N);
C(N+2:N+1:end-1)=-2;
C(2*N+2:N+1:end)=1;
C(end-(2*N+1):-(N+1):2)=1;
C(1)=-delta;
C(N+1)=delta;
C(N,N)=delta.^2;
C=sparse(C);

% Parameters for Z1
m1=0.5;                             % Mass of the BM
k1=6.4*1e10*exp(-368*x);            % Stiffness of the BM
c1=1.8*1e5*exp(-184*x);             % Damping of the BM
% Parameters for Z2
k2=3.8*1e10*exp(-368*x);            % Stiffness of the TM
% Parameters for Z3
k3=7.5*1e10*exp(-368*x);            % Stiffness of the coupling
% Parameters for Z4
wo=2*pi*57e3*exp(-184*x);           % Characteristic frequency
Td=2*pi./wo;                        % Time delay
g=1;                                % OHC force-generation gain

freq=[10:10:25000];                 % Stimulus frequency
for n=1:length(freq);
f=freq(n);

% Impedances
Z1=c1-i*((k1./(2*pi*f))-(2*pi*f*m1));
Z2=-i*(k2./(2*pi*f));
Z3=-i*(k3./(2*pi*f));
```

```
Z4=(-i*k1./(2*pi*f)).*(((wo/20)-i*2*pi*f)./ ...
        ((wo/20)+i*2*pi*f)).*(exp(-i*2*pi*f*Td));

% Partition impedance/mobility
Zp=Z1+((Z2.*Z3)./(Z2+Z3+g*Z4));
Yp1=1./Zp;

% Mobility matrix
Yp=zeros(N);
Yp=diag(Yp1);
    M=zeros(N);
M(N+2:N+1:end-1)=1;
M=M*Yp;
    M=sparse(M);

% Total matrix
T=[((1./(delta.^2))*C)-(((4*j*pi*f*ro)./H).*M)];

% Source vector
S(1)=-4*j*pi*f*ro*ust;
S(2:N)=0;

% Pressure difference
pd=(inv(T))*S';
pref=2e-5;                    % Pressure reference
end
```

==========

Matlab script for calculation of the pressure difference in the CP fluid for the G generalised model for chosen position on the BM, x and stimulus frequency, f, with the delay factor, n equal to 0.4 (optimum value estimated in G model).

File: 'gnpd.m'

```
% Pressure difference in the cochlear fluid
% of the generalised Geisler model for chosen:
% 1) position 'x' (rows of the 'pd' matrix)
% 2) frequency 'f' (columns of the 'pd' matrix)
% The micromechanical model
% with the coupling via cochlear fluid
% The delay factor n=0.4

% Parameters
```

```
L=0.035;                        % Length of the BM
H=0.001;                        % Heigth of the SV
ro=1000;                        % Fluid density
ust=1;                          % Stapes velocity
N=1024;                         % Number of points
delta=L/(N-1);                  % Length of the element
x=[0:delta:L];                  % Position on the BM

% Coupling matrix
C=zeros(N);
C(N+2:N+1:end-1)=-2;
C(2*N+2:N+1:end)=1;
C(end-(2*N+1):-(N+1):2)=1;
C(1)=-delta;
C(N+1)=delta;
C(N,N)=delta.^2;
C=sparse(C);

% Parameters for Z1
m1=0.5;                                 % Mass of the BM
k1=6.4*1e10*exp(-368*x);                % Stiffness of the BM
c1=1.8*1e5*exp(-184*x);                 % Damping of the BM
% Parameters for Z2
k2=3.8*1e10*exp(-368*x);                % Stiffness of the TM
% Parameters for Z3
k3=7.5*1e10*exp(-368*x);                % Stiffness of the coupling
% Parameters for Z4
wo=2*pi*57e3*exp(-184*x);               % Characteristic frequency
Td=0.4*pi./wo;                          % Time delay
g=1;                                    % OHC force-generation gain

freq=[10:10:25000];                     % Stimulus frequency
for n=1:length(freq);
f=freq(n);

% Impedances
Z1=c1-i*((k1./(2*pi*f))-(2*pi*f*m1));
Z2=-i*(k2./(2*pi*f));
Z3=-i*(k3./(2*pi*f));
Z4=(-i*k1./(2*pi*f)).*(((wo/20)-i*2*pi*f)./ ...
        ((wo/20)+i*2*pi*f)).*(exp(-i*2*pi*f*Td));

% Partition impedance/mobility
```

```
Zp=Z1+((Z2.*Z3)./(Z2+Z3+g*Z4));
Yp1=1./Zp;

% Mobility matrix
Yp=zeros(N);
Yp=diag(Yp1);
    M=zeros(N);
M(N+2:N+1:end-1)=1;
M=M*Yp;
    M=sparse(M);

% Total matrix
T=[((1./(delta.^2))*C)-(((4*j*pi*f*ro)./H).*M)];

% Source vector
S(1)=-4*j*pi*f*ro*ust;
S(2:N)=0;

% Pressure difference
pd=(inv(T))*S';
pref=2e-5;                    % Pressure reference
end
```

==========

Matlab script for calculation of the CP velocity for the G generalised model for chosen position on the BM, x and stimulus frequency, f.

File: 'gv1dot.m'

```
% Cochlear partition velocity of the generalised
% Geisler model for chosen:
% 1) position 'x' (rows of the 'v1dot' matrix)
% 2) frequency 'f' (columns of the 'v1dot' matrix)
% The micromechanical model
% with the coupling via cochlear fluid

% Parameters
L=0.035;                      % Length of the BM
H=0.001;                      % Heigth of the SV
ro=1000;                      % Fluid density
ust=1;                        % Stapes velocity
N=1024;                       % Number of points
delta=L/(N-1);                % Length of the element
```

```
x=[0:delta:L];              % Position on the BM

% Coupling matrix
C=zeros(N);
C(N+2:N+1:end-1)=-2;
C(2*N+2:N+1:end)=1;
C(end-(2*N+1):-(N+1):2)=1;
C(1)=-delta;
C(N+1)=delta;
C(N,N)=delta.^2;
C=sparse(C);

% Parameters for Z1
m1=0.5;                         % Mass of the BM
k1=6.4*1e10*exp(-368*x);        % Stiffness of the BM
c1=1.8*1e5*exp(-184*x);         % Damping of the BM
% Parameters for Z2
k2=3.8*1e10*exp(-368*x);        % Stiffness of the TM
% Parameters for Z3
k3=7.5*1e10*exp(-368*x);        % Stiffness of the coupling
% Parameters for Z4
wo=2*pi*57e3*exp(-184*x);       % Characteristic frequency
Td=2*pi./wo;                    % Time delay
g=1;                            % OHC force-generation gain

freq=[10:10:25000];             % Stimulus frequency
for n=1:length(freq);
f=freq(n);

% Impedances
Z1=c1-i*((k1./(2*pi*f))-(2*pi*f*m1));
Z2=-i*(k2./(2*pi*f));
Z3=-i*(k3./(2*pi*f));
Z4=(-i*k1./(2*pi*f)).*(((wo/20)-i*2*pi*f)./ ...
        ((wo/20)+i*2*pi*f)).*(exp(-i*2*pi*f*Td));

% Partition impedance/mobility
Zp=Z1+((Z2.*Z3)./(Z2+Z3+g*Z4));
Yp1=1./Zp;

% Mobility matrix
Yp=zeros(N);
Yp=diag(Yp1);
```

```
    M=zeros(N);
M(N+2:N+1:end-1)=1;
M=M*Yp;
    M=sparse(M);

% Total matrix
T=[((1./(delta.^2))*C)-(((4*j*pi*f*ro)./H).*M)];

% Source vector
S(1)=-4*j*pi*f*ro*ust;
S(2:N)=0;

% Pressure difference
pd=(inv(T))*S';

    % Partition velocity
    v1dot(:,n)=Yp*(-2*pd);
    vdotref=2e-4;              % Velocity reference
end
```

==========

Matlab script for calculation of the CP velocity for the G generalised model for chosen position on the BM, x and stimulus frequency, f, with the delay factor, n equal to 0.4 (optimum value estimated in G model).

File: 'gnv1dot.m'

```
% Cochlear partition velocity of the generalised
% Geisler model for chosen:
% 1) position 'x' (rows of the 'v1dot' matrix)
% 2) frequency 'f' (columns of the 'v1dot' matrix)
% The micromechanical model
% with the coupling via cochlear fluid
% The delay factor n=0.4

% Parameters
L=0.035;                   % Length of the BM
H=0.001;                   % Heigth of the SV
ro=1000;                   % Fluid density
ust=1;                     % Stapes velocity
N=1024;                    % Number of points
delta=L/(N-1);             % Length of the element
x=[0:delta:L];             % Position on the BM
```

```
% Coupling matrix
C=zeros(N);
C(N+2:N+1:end-1)=-2;
C(2*N+2:N+1:end)=1;
C(end-(2*N+1):-(N+1):2)=1;
C(1)=-delta;
C(N+1)=delta;
C(N,N)=delta.^2;
C=sparse(C);

% Parameters for Z1
m1=0.5;                          % Mass of the BM
k1=6.4*1e10*exp(-368*x);         % Stiffness of the BM
c1=1.8*1e5*exp(-184*x);          % Damping of the BM
% Parameters for Z2
k2=3.8*1e10*exp(-368*x);         % Stiffness of the TM
% Parameters for Z3
k3=7.5*1e10*exp(-368*x);         % Stiffness of the coupling
% Parameters for Z4
wo=2*pi*57e3*exp(-184*x);        % Characteristic frequency
Td=0.4*pi./wo;                   % Time delay
g=1;                             % OHC force-generation gain

freq=[10:10:25000];              % Stimulus frequency
for n=1:length(freq);
f=freq(n);

% Impedances
Z1=c1-i*((k1./(2*pi*f))-(2*pi*f*m1));
Z2=-i*(k2./(2*pi*f));
Z3=-i*(k3./(2*pi*f));
Z4=(-i*k1./(2*pi*f)).*(((wo/20)-i*2*pi*f)./ ...
        ((wo/20)+i*2*pi*f)).*(exp(-i*2*pi*f*Td));

% Partition impedance/mobility
Zp=Z1+((Z2.*Z3)./(Z2+Z3+g*Z4));
Yp1=1./Zp;

% Mobility matrix
Yp=zeros(N);
Yp=diag(Yp1);
    M=zeros(N);
```

```
M(N+2:N+1:end-1)=1;
M=M*Yp;
    M=sparse(M);

% Total matrix
T=[((1./(delta.^2))*C)-(((4*j*pi*f*ro)./H).*M)];

% Source vector
S(1)=-4*j*pi*f*ro*ust;
S(2:N)=0;

% Pressure difference
pd=(inv(T))*S';

    % Partition velocity
    v1dot(:,n)=Yp*(-2*pd);
    vdotref=2e-4;                % Velocity reference
end
```

==========

Matlab script for calculation of the CP displacement for the G generalised model for chosen position on the BM, x and stimulus frequency, f.

File: 'gv1.m'

```
% Cochlear partition displacement of the generalised
% Geisler model for chosen:
% 1) position 'x' (rows of the 'v1' matrix)
% 2) frequency 'f' (columns of the 'v1' matrix)
% The micromechanical model
% with the coupling via cochlear fluid

% Parameters
L=0.035;                     % Length of the BM
H=0.001;                     % Heigth of the SV
ro=1000;                     % Fluid density
ust=1;                       % Stapes velocity
N=1024;                      % Number of points
delta=L/(N-1);               % Length of the element
x=[0:delta:L];               % Position on the BM

% Coupling matrix
C=zeros(N);
```

```
C(N+2:N+1:end-1)=-2;
C(2*N+2:N+1:end)=1;
C(end-(2*N+1):-(N+1):2)=1;
C(1)=-delta;
C(N+1)=delta;
C(N,N)=delta.^2;
C=sparse(C);

% Parameters for Z1
m1=0.5;                          % Mass of the BM
k1=6.4*1e10*exp(-368*x);         % Stiffness of the BM
c1=1.8*1e5*exp(-184*x);          % Damping of the BM
% Parameters for Z2
k2=3.8*1e10*exp(-368*x);         % Stiffness of the TM
% Parameters for Z3
k3=7.5*1e10*exp(-368*x);         % Stiffness of the coupling
% Parameters for Z4
wo=2*pi*57e3*exp(-184*x);        % Characteristic frequency
Td=2*pi./wo;                     % Time delay
g=1;                             % OHC force-generation gain

freq=[10:10:25000];              % Stimulus frequency
for n=1:length(freq);
f=freq(n);

% Impedances
Z1=c1-i*((k1./(2*pi*f))-(2*pi*f*m1));
Z2=-i*(k2./(2*pi*f));
Z3=-i*(k3./(2*pi*f));
Z4=(-i*k1./(2*pi*f)).*(((wo/20)-i*2*pi*f)./ ...
        ((wo/20)+i*2*pi*f)).*(exp(-i*2*pi*f*Td));

% Partition impedance/mobility
Zp=Z1+((Z2.*Z3)./(Z2+Z3+g*Z4));
Yp1=1./Zp;

% Mobility matrix
Yp=zeros(N);
Yp=diag(Yp1);
    M=zeros(N);
M(N+2:N+1:end-1)=1;
M=M*Yp;
    M=sparse(M);
```

```
% Total matrix
T=[((1./(delta.^2))*C)-(((4*j*pi*f*ro)./H).*M)];

% Source vector
S(1)=-4*j*pi*f*ro*ust;
S(2:N)=0;

% Pressure difference
pd=(inv(T))*S';

    % Partition displacement
    v1dot=Yp*(-2*pd);
    v1(:,n)=v1dot./(i*2*pi*f);
    vref=1e-9;                  % Displacement reference
end
```

==========

Matlab script for calculation of the CP displacement for the G generalised model for chosen position on the BM, x and stimulus frequency, f, with the delay factor, n equal to 0.4 (optimum value estimated in G model).

File: 'gnv1.m'

```
% Cochlear partition displacement of the generalised
% Geisler model for chosen:
% 1) position 'x' (rows of the 'v1' matrix)
% 2) frequency 'f' (columns of the 'v1' matrix)
% The micromechanical model
% with the coupling via cochlear fluid
% The delay factor n=0.4

% Parameters
L=0.035;                    % Length of the BM
H=0.001;                    % Heigth of the SV
ro=1000;                    % Fluid density
ust=1;                      % Stapes velocity
N=1024;                     % Number of points
delta=L/(N-1);              % Length of the element
x=[0:delta:L];              % Position on the BM

% Coupling matrix
C=zeros(N);
```

```
C(N+2:N+1:end-1)=-2;
C(2*N+2:N+1:end)=1;
C(end-(2*N+1):-(N+1):2)=1;
C(1)=-delta;
C(N+1)=delta;
C(N,N)=delta.^2;
C=sparse(C);

% Parameters for Z1
m1=0.5;                          % Mass of the BM
k1=6.4*1e10*exp(-368*x);         % Stiffness of the BM
c1=1.8*1e5*exp(-184*x);          % Damping of the BM
% Parameters for Z2
k2=3.8*1e10*exp(-368*x);         % Stiffness of the TM
% Parameters for Z3
k3=7.5*1e10*exp(-368*x);         % Stiffness of the coupling
% Parameters for Z4
wo=2*pi*57e3*exp(-184*x);        % Characteristic frequency
Td=0.4*pi./wo;                   % Time delay
g=1;                             % OHC force-generation gain

freq=[10:10:25000];              % Stimulus frequency
for n=1:length(freq);
f=freq(n);

% Impedances
Z1=c1-i*((k1./(2*pi*f))-(2*pi*f*m1));
Z2=-i*(k2./(2*pi*f));
Z3=-i*(k3./(2*pi*f));
Z4=(-i*k1./(2*pi*f)).*(((wo/20)-i*2*pi*f)./ ...
        ((wo/20)+i*2*pi*f)).*(exp(-i*2*pi*f*Td));

% Partition impedance/mobility
Zp=Z1+((Z2.*Z3)./(Z2+Z3+g*Z4));
Yp1=1./Zp;

% Mobility matrix
Yp=zeros(N);
Yp=diag(Yp1);
    M=zeros(N);
M(N+2:N+1:end-1)=1;
M=M*Yp;
    M=sparse(M);
```

```
% Total matrix
T=[((1./(delta.^2))*C)-(((4*j*pi*f*ro)./H).*M)];

% Source vector
S(1)=-4*j*pi*f*ro*ust;
S(2:N)=0;

% Pressure difference
pd=(inv(T))*S';

    % Partition displacement
    v1dot=Yp*(-2*pd);
    v1(:,n)=v1dot./(i*2*pi*f);
    vref=1e-9;                  % Displacement reference
end
```

15.3.3 Stability

Matlab script for calculation of the *Nyquist plots* for a negative feedback system (derived from the Geisler generalised model) for chosen position on the BM, x and the cochlear amplifier's gain, g.

File: 'gnegv3dot.m'

```
% Stability of negative feedback system
% of the generalised Geisler model
% for specific position/gain 'x'/'g'
% Velocity v3dot-output of the loop

% Parameters
xc=input('Choose the BM site [m] x='); % Position on the BM
x=xc;
f=0:10:1e6;                            % Frequency band

% Parameters for Z1
m1=0.5;                        % Mass of the BM
k1=6.4*1e10*exp(-368*x);       % Stiffness of the BM
c1=1.8*1e5*exp(-184*x);        % Damping of the BM
% Parameters for Z2
k2=3.8*1e10*exp(-368*x);       % Stiffness of the TM
% Parameters for Z3
k3=7.5*1e10*exp(-368*x);       % Stiffness of the coupling
```

```
% Parameters for Z4
wo=2*pi*57e3*exp(-184*x);        % Characteristic frequency
T=2*pi./wo;                      % Time delay

% OHC force-generation gain
gc=input('Choose cochlear amplifier''s gain g=');
g=gc;

% Impedances
Z1=c1-i*((k1./(2*pi*f))-(2*pi*f*m1));
Z2=-i*(k2./(2*pi*f));
Z3=-i*(k3./(2*pi*f));
Z4=(-i*k1./(2*pi*f)).*(((wo/20)-i*2*pi*f)./ ...
    ((wo/20)+i*2*pi*f)).*(exp(-i*2*pi*f*T));

% Feedback components
G=1./(Z1+((Z1.*Z3)./Z2)+Z3);     % Plant
H=g*(((Z4.*Z1)./Z2)-Z4);         % Controller

% Nyquist plots of imaginary vs real
% of negative feedback system for
% specific position/gain 'x'/'g'
plot(real(G.*H),imag(G.*H)),grid on
xlabel('Re GH(j\omega)','FontSize',14)
ylabel('Im GH(j\omega)','FontSize',14);
hold on
plot(-1,0,'ro')
```

16 Appendix D

The attached CD contains the scripts presented in Appendix C, along with the calculated data and presented figures (see list of figures). Additionally, a *pdf* copy of the text is also included.

References

[1] Allen, J. (**2001**). "Nonlinear cochlear signal processing," in *Physiology of the Ear*, Second Edition, edited by F.J. Anthony, J. Santos-Sacchi, (Singular Thompson), 393-442.

[2] Allen, J. B., Neely, S. T. (**1992**). "Micromechanical models of the cochlea," Phys. Today **45**(7), 40-47.

[3] Dallos, P., Popper, A. N., Fay, R. R. (**1996**). The Cochlea (Springer, New York).

[4] Chadwick, R. S., Dimitriadis, E.K., Iwasa, K.H. (**1996**). "Active control of waves in a cochlear model with subpartitions," Proc. Natl. Acad. Sci. USA **93**, 2564-2569.

[5] de Boer, E. (**1991**). "Auditory Physics. Physical principles in hearing theory. III," Phys. Rep. **203**, 127-229.

[6] de Boer, E. (**1995**). "On equivalence of locally active models of the cochlea," J. Acoust. Soc. Am. **98**, 1400-1409.

[7] de Boer, E. (**1997**). "Cochlear models and minimum phase," J. Acoust. Soc. Am. **102**, 1400-1409.

[8] Elliott, S. J., Harte, J. M. (**2003**). "Models for compressive nonlinearities in the cochlea," Technical memorandum, Institute of Sound and Vibration Research, University of Southampton, UK.

[9] Franklin, G. F., Powell, J. D., Emami-Naeini, A. (**1991**). Feedback Control of Dynamic Systems. Theory and Applications, Second Edition (Addison-Wesley Publishing Company).

[10] Geisler, D. C. (**1991**). "A cochlear model using feedback from motile outer hair cells," Hear. Res. **54**, 105-117.

[11] Geisler, D. C. (**1993**). "A realizable cochlear model using feedback from motile outer hair cells," Hear. Res. **68**, 253-262.

[12] Greenwood, D. D. (**1990**). "A cochlear frequency-position function for several species-29 years later," J. Acoust. Soc. Am. **87**, 2592-2605.

[13] Kanis, L. J. (**1995**). "Cochlear nonlinearity. A computational model of the cochlea solved in the frequency domain." Ph.D. thesis, University of Amsterdam, The Netherlands.

[14] Khoo, M. C. (**2000**). Physiological Control Systems. Analysis, Simulation, and Estimation (IEEE Press, New York).

[15] Kolston, P. J. (**1999**). "Comparing *in vitro*, *in situ*, and *in vivo* experimental data in a three-dimensional model of mammalian cochlear mechanics," Proc. Natl. Acad. Sci. USA **96**, 3676-3681.

[16] Le Henaff, B., Elliott, S. J., Maury, C. (**2003**). "Modelling wave propagation in the cochlea." Technical memorandum, Institute of Sound and Vibration Research, University of Southampton, UK.

[17] Liberman, M. C. (**1982**). "The cochlear frequency map for the cat: labeling auditory nerve fibers of known characteristic frequency," J. Acoust. Soc. Am. **72**, 1441-1449.

[18] Lineton, B. (**2001**). "Testing a model of stimulus frequency otoacoustic emissions in humans." Ph.D. thesis, Institute of Sound and Vibration Research, University of Southampton, UK.

[19] Lukashkin, A. N., Russel, I. J. (**2003**). "A second, low-frequency mode of vibration in the intact mammalian cochlea," J. Acoust. Soc. Am. **113**, 1544-1550.

[20] Neely, S. T. (**1993**). "A model of cochlear mechanics with outer hair cell motility," J. Acoust. Soc. Am. **94**, 137-146.

[21] Neely, S. T., Kim, D. O. (**1986**). "A model for active elements in cochlear biomechanics," J. Acoust. Soc. Am. **79**, 1472-1480.

[22] Nobili, R., Mammano, F., Ashmore, J. (**1998**). "How well do we understand the cochlea?" Trends Neurosc. **21**, 159-167.

[23] Pickles, J. O. (**1982**). An Introduction to the Physiology of Hearing (Academic, London).

[24] Ren, T. (**2004**). "Reversed propagation of sound in the gerbil cochlea," Nature Neurosc. **7**, 333-334.

[25] Robles, L., Ruggero, M. A. (**2001**). "Mechanics of the mammalian cochlea," Phys. Rev. **81**, 1305-1352.

[26] Tse, F. S., Morse, I. E., Hinkle, R. T. (**2001**). Mechanical Vibrations. Theory and Applications, Second Edition (Allyn and Bacon, Inc.).

[27] Yates, G. K. (**1990**). "Basilar membrane nonlinearity and its influence on auditory nerve rate-intensity functions," Hear. Res. **50**, 145-162.

[28] Yates, G. K. (**1990**). "The basilar membrane nonlinear input-output function," in *Mechanics and Biophysics of Hearing*, edited by P. Dallos, C. D. Geisler, J. W. Matthews, M. A. Ruggero and C. Steele (Springer Verlag, New York), pp.106-113.